AD-A109 676 DAYTON UNIV OH RESEARCH INST F/G 11/6
IMPACT DAMAGE ON VARIOUS METAL LEADING EDGES FROM SMALL HARD OB--ETC(U)
AUG 81 R S BERTKE F33615-76-C-5124
UNCLASSIFIED UDR-TR-81-06 AFWAL-TR-81-4066 NL

1 OF 2
AD A
109676

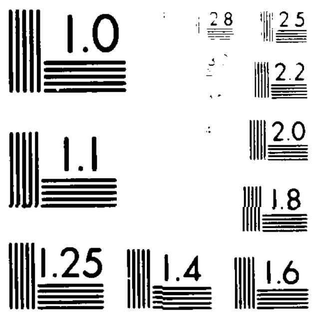

MICROCOPY RESOLUTION TEST CHART

AD A109676

LEVEL II

(12)

AFWAL-TR-81-4066

IMPACT DAMAGE ON VARIOUS METAL LEADING EDGES FROM SMALL HARD OBJECTS

ROBERT S. BERTKE
UNIVERSITY OF DAYTON RESEARCH INSTITUTE
300 COLLEGE PARK AVE.
DAYTON, OHIO 45469

AUGUST 1981

TECHNICAL REPORT
FINAL REPORT FOR PERIOD MARCH 1979 - NOVEMBER 1979

MATERIALS LABORATORY
AIR FORCE WRIGHT AERONAUTICAL LABORATORIES
AIR FORCE SYSTEMS COMMAND
WRIGHT-PATTERSON AIR FORCE BASE, OHIO 45433

NOTICE

When Government drawings, specifications, or other data are used for any purpose other than in connection with a definitely related Government procurement operation, the United States Government thereby incurs no responsibility nor any obligation whatsoever; and the fact that the government may have formulated, furnished, or in any way supplied the said drawings, specifications, or other data, is not to be regarded by implication or otherwise as in any manner licensing the holder or any other person or corporation, or conveying any rights or permission to manufacture, use, or sell any patented invention that may in any way be related thereto.

This report has been reviewed by the Office of Public Affairs (ASD/PA) and is releasable to the National Technical Information Services (NTIS). At NTIS, it will be available to the general public, including foreign nations.

This technical report has been reviewed and is approved for publication.

Theodore Nicholas

THEODORE NICHOLAS
Project Engineer

FOR THE COMMANDER

John P. Henderson

J. P. HENDERSON
Branch Chief/AFWAL/MLLN

"If your address has changed, if you wish to be removed from our mailing list, or if the addressee is no longer employed by your organization please notify AFWAL/TST-ML, Wright-Patterson Air Force Base, Ohio 45433 to help us maintain a current mailing list".

Copies of this report should not be returned unless return is required by security considerations, contractual obligations, or notice on a specific document.

AIR FORCE/56780/31 December 1981 — 350

UNCLASSIFIED

SECURITY CLASSIFICATION OF THIS PAGE (When Data Entered)

REPORT DOCUMENTATION PAGE		READ INSTRUCTIONS BEFORE COMPLETING FORM
1. REPORT NUMBER AFWAL-TR-81-4066	2. GOVT ACCESSION NO. AD-A109	3. RECIPIENT'S CATALOG NUMBER 676
4. TITLE (and Subtitle) Impact Damage on Various Metal Leading Edges From Small Hard Objects		5. TYPE OF REPORT & PERIOD COVERED Technical Report Mar. 1979 - Nov. 1979
		6. ~~PERFORMING ORG. REPORT~~ NUMBER UDR-TR-81-06
7. AUTHOR(s) Robert S. Bertke		8. CONTRACT OR GRANT NUMBER(s) F33615-76-C-5124
9. PERFORMING ORGANIZATION NAME AND ADDRESS University of Dayton Research Institute 300 College Park Ave. Dayton, Ohio 45469		10. PROGRAM ELEMENT, PROJECT, TASK AREA & WORK UNIT NUMBERS 7351 06 B5
11. CONTROLLING OFFICE NAME AND ADDRESS Materials Laboratory (AFWAL/MLLN) Air Force Wright Aeronautical Laboratories Wright-Patterson Air Force Base, OH 45433		12. REPORT DATE August 1981
		13. NUMBER OF PAGES 121
14. MONITORING AGENCY NAME & ADDRESS(if different from Controlling Office)		15. SECURITY CLASS. (of this report) Unclassified
		15a. DECLASSIFICATION/DOWNGRADING SCHEDULE
16. DISTRIBUTION STATEMENT (of this Report) Approved for public release; distribution unlimited.		
17. DISTRIBUTION STATEMENT (of the abstract entered in Block 20, if different from Report)		
18. SUPPLEMENTARY NOTES		
19. KEY WORDS (Continue on reverse side if necessary and identify by block number) Titanium, steel, aluminum, Foreign Object Damage, Leading Edge Impact Damage, fatigue tests, scaling, shot peening.		
20. ABSTRACT (Continue on reverse side if necessary and identify by block number) Impact damage on various metal leading edge configurations was studied by performing a series of hard particle impact tests and characterizing the damage. Fatigue tests were used to assess the damage and the concept of an equivalent elastic stress concentration factor was used to characterize severity of damage. Notch fatigue specimens were also fatigue tested in tension to provide baseline data for each material investigated. The materials investigated included 8Al-1Mo-1V titanium, 4130 steel		

DD FORM 1 JAN 73 1473 EDITION OF 1 NOV 65 IS OBSOLETE

UNCLASSIFIED

SECURITY CLASSIFICATION OF THIS PAGE (When Data Entered)

10 100

in the annealed and heat-treated conditions, and 7075-T651 aluminum. The data demonstrated good reproducibility and showed that the extent of a particular type of damage could be categorized in terms of an equivalent elastic stress concentration factor. Based on the results, the 4130 steel was superior in performance with the highest critical velocity values and being less sensitive to fatigue degradation than the other materials. No correlation could be established between the critical velocity and the target material parameters of density, modulus, or yield strength.

The concept of geometric scaling was investigated by performing a series of tests using different leading edge thicknesses and projectile sizes. Observation of the type of damage and plots of critical velocity versus particle size (in relation to leading edge thickness) appeared to validate the scaling concepts.

PREFACE

The effect reported herein was conducted by the Impact Physics Group of the Experimental and Applied Mechanics Division at the University of Dayton Research Institute (UDRI), Dayton, Ohio, under Contract No. F33615-76-C-5124, for the Air Force Wright Aeronautical Laboratories/Materials Laboratory (AFWAL/ML), Wright-Patterson Air Force Base, Ohio. Air Force administrative direction and technical support was provided by Dr. Theodore Nicholas, AFWAL/MLLN.

The work described herein was conducted in the UDRI Impact Physics Facility at the University of Dayton during the period of March to November 1979. The principal investigator was Mr. Robert S. Bertke of the University of Dayton Research Institute. Project supervision was provided by Dr. S. Bless of UDRI.

The author wishes to acknowledge the following persons of the University of Dayton Research Institute who provided direct support to this work. Mr. Charles E. Acton conducted the impact and fatigue testing, Mr. Richard Tocci conducted the photographic coverage, Mrs. Gloria Miller and Mrs. Yvonne Conner conducted the typing of this manuscript.

TABLE OF CONTENTS

TABLE OF CONTENTS (CONTINUED)

LIST OF ILLUSTRATIONS

LIST OF ILLUSTRATIONS (CONTINUED)

LIST OF ILLUSTRATIONS (CONTINUED)

LIST OF ILLUSTRATIONS (CONTINUED)

LIST OF TABLES

SECTION I
INTRODUCTION

Fan and compressor blade damage resulting from the ingestion of foreign objects into gas turbine aircraft engines has to be given serious consideration for reasons of flight safety and costs. The blades are exposed to potential impacts from a variety of objects ranging from large birds and ice to small hard particles such as sand. The threat is defined by the environment in which the engine is constrained to operate. The engine speed, blade material, blade geometry, point of impact, and type and size of the impactor all play important roles in determining the type, if any, and the severity of damage which might occur.

Impacts between blades and foreign objects will almost always cause at least localized minor damage which may be treated as maintenance problems. This blade damage may also be severe to cause instantaneous fracture or failure, or may be of the type that could lead to eventual failure through fatigue crack initiation or growth to a catastrophic size. This blade failure may result in immediate power loss of the engine and lead to destruction of the aircraft and crew. The task of the blade designer is to either design a blade which has a specified level of resistance to foreign object damage (FOD) or to evaluate a given blade and predict the extent of damage to be expected.

The overall design problem has two aspects. The first aspect is a ballistic impact problem. In this instance, a method must be developed to relate the mode and extent of damage to the threat and target parameters. The second aspect of the design problem is to relate the ballistic impact induced damage to the residual properties of the blade. It is the mechanical properties of the blade that are of the most importance or significance in the foreign object damage design problem.

Compressor blades can be especially susceptible to damage from ingested small hard particles such as sand or stones because of the large quantity of such particles in the environment and the thin leading edge of these blades. Leading edge thicknesses of 0.010 inches (0.25 mm) or less are common in the compressor stages of high performance engines currently in the field. In-service inspections of such blades occasionally reveal damage in the form of small nicks, dents, or bulges. This type of damage can lead to complete blade failure due to the propagation of fatigue cracks from the damaged area. Visual inspection of blades nicked or damaged along the leading edge does not permit accurate determination of the size and type of object that may have caused the damage.

This report describes an experimental study conducted to investigate the response of typical fan and compressor blade materials to small hard particle leading edge impacts. Numerous parameters investigated in the study include material density, material yield strength, material modulus, leading edge thickness, impact angle, and impactor size.

SECTION II
EXPERIMENTAL PROGRAM

The experimental program involved performing leading edge impact tests on flat constant thickness specimens using small hard particles in the size range of 0.063 to 0.250 inch (1.60 to 6.25 mm) diameter. The study involved determining the critical velocity region (cracks are generated with the damage) for each test condition. Previous work conducted on titanium material indicated that the extent of damage depended primarily on the type of damage and appeared to be relatively independent of size (see Reference 1). In this work, the least severe damage for impacted leading edges was a clean perforation with complete material removal. The next worst case was that where the leading edge curled back extensively or bulged. The worst case in regards to extent of damage was where the curl back or bulge initiated a rip or tear along the leading edge from which the fatigue crack could propagate. For a given projectile size and leading edge geometry, the test data of the previous work indicated that perforation occurred at the highest impact velocities, bulging at lower velocities, and a bulge with a tear as some intermediate or critical velocity which is analogous to a ballistic limit velocity in projectile-plate penetration phenomena.

The intent of the program was to determine this critical velocity for each test condition. Then, using this velocity, at least seven specimens were impacted under identical test conditions so that fatigue tests could be used to evaluate the damage. Each material investigated was characterized in terms of notch fatigue strength such that the fatigue testing of the impact damaged specimens could be compared with notch fatigue data for each test material. Thus, equivalent stress concentration factors could be evaluated for each test condition using machined notched specimens with a known (calculated) stress concentration factor as the reference. This technique to characterize impact induced fatigue strength degradation was developed in the previous work of Reference 1. In this study, the effects of leading edge thickness, impact angle, particle size, particle material, and target material were investigated for damage response.

1. MATERIALS INVESTIGATED

Three materials were investigated in the study to evaluate the effects of different material properties to resist impact damage from the hard particle leading edge impacts. The materials were 8Al-1Mo-1V (8-1-1) titanium, 7075-T651 aluminum, and 4130 steel. The titanium material was selected as the baseline materials for all tests in this program. The effect of shot-peening on the titanium material was also investigated for damage response for two intensities of 0.005 to 0.008 N and 0.010 to 0.16 N using glass beads 0.023 to 0.033 inch (0.58 to 0.84 mm) diameter. The 4130 steel material was tested in the annealed condition with a Rockwell hardness of B-84 and a heat-treated condition with Rockwell hardness of C-31.

a. Material Characterization

Notch fatigue specimens were machined from 6.0 x 1.0 inch (152.4 x 25.4 mm) blanks cut from the sheet of material to be investigated to the dimensions shown in Figure 1. The test section containing the notches was machined onto the center 1.0 inch (25.4 mm) portion of the specimen. The test section thickness was a constant 0.02 inches (0.508 mm) across the width of the specimens. The nominal thickness for the titanium and steel sheets was 0.063 inches (1.59 mm) while the nominal thickness for the aluminum sheet was 0.250 inches (6.35 mm) thick. All specimens were cut in the same direction in each material sheet to avoid any preferred orientation effects in the sheet.

At least six specimens of each notch type for each material were machined. The calculated stress concentration factors (K_T) of 1.39, 2.12, and 3.55 were determined for

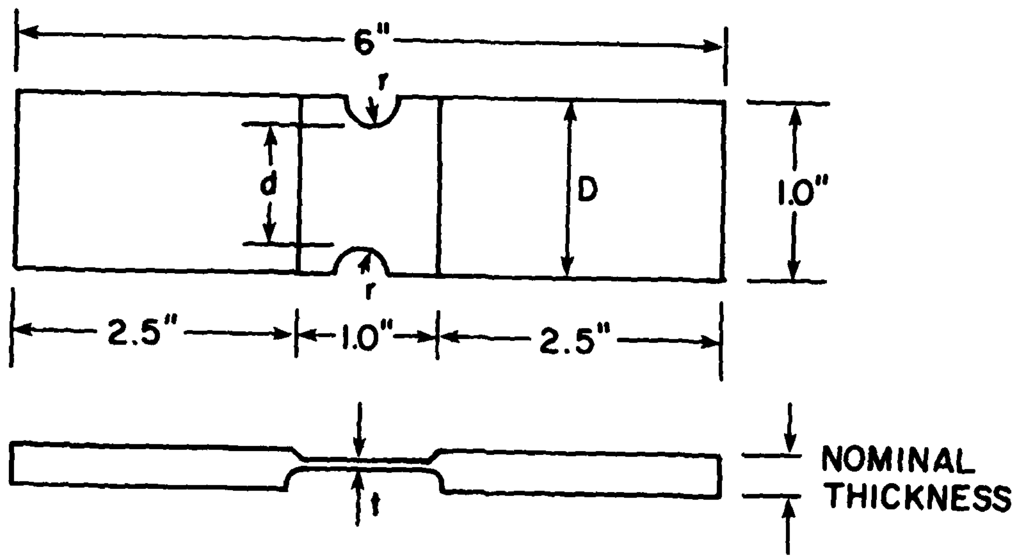

TYPE	D (INCHES)	d (INCHES)	r (INCHES)	K_T
I	1.0	0.75	0.5000	1.39
II	1.0	0.75	0.1250	2.12
III	1.0	0.75	0.0312	3.55

Figure 1. Geometry of Notch Fatigue Specimens.

each notch size (see Reference 2). The specimens were then fatigue tested in tension in a 2-ton (17.8 KN) Shenck Resonant Fatigue Testing Machine using a ratio of minimum load to maximum load (R ratio) of 0.1. The cyclic frequency of the Shenck machine is approximately 33 Hz. The number of cycles to failure (complete separation) was recorded for each specimen. No attempt was made to correct for the number of cycles necessary to propagate from the first observable crack to failure; in all cases this was small compared to the total cycles. The data for the three notch groups of specimens for each material could then be plotted as N_f (number of cycles to failure) versus maximum net section stress. For each notch group, a straight line can be drawn through the data and used as the baseline representation of the notch fatigue strength of the test material.

2. IMPACT TEST SET-UP AND PROCEDURES

The impact tests were conducted on the test range shown schematically in Figure 2.

a. <u>Test Range</u>

The range set-up consisted of a launch tube, velocity measuring system, and a target tank with a mounting fixture. The launch tube had a smooth bore of 30 cal (7.62 mm) and a length of 3.0 feet (0.91 m). In every case, the projectile particle to be fired was positioned into a recessed pocket of a lexan sabot to provide protection and support for the particle during launch. The particle was held within the pocket by an oil film during the launch. The projectile particle/sabot package was launched down the tube by utilizing either compressed gas or powder gas depending on the desired impact velocity. Compressed gas was used for impact velocities up to 1,000 ft/sec (305 m/s). Above 1,000 ft/sec (305 m/s),

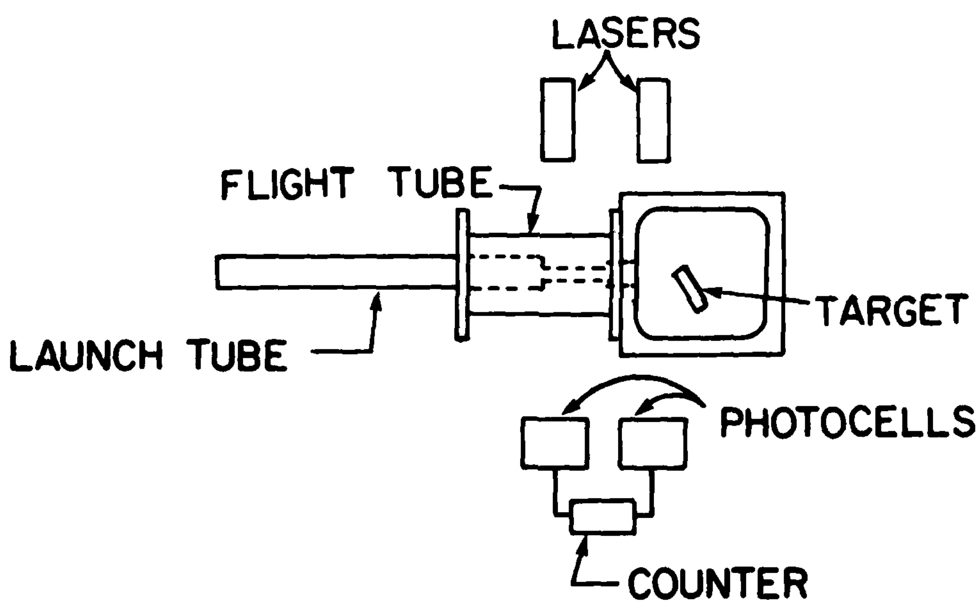

Figure 2. Schematic of Range Set-Up.

a powder gun was used. A sabot stopper device was located at the muzzle of the launch tube. The purpose of this device was to slow down and eventually stop the sabot, permitting the particle to separate from the sabot and continue on a trajectory toward the target specimen.

b. Impact Velocity Measurement

The projectile velocity was measured by utilizing a pair of HeNe laser/photomultiplier stations spaced a known distance apart. Each laser beam intersected the projectile particle trajectory normal to the trajectory and illuminated one of the photomultiplier stations. When the projectile/sabot package interrupted the first beam (first station had laser beam projecting through slots at muzzle of launch tube), the first photomultiplier station generated a voltage pulse to start a counter-timer. The counter-timer was stopped when the particle interrupted the second beam. The projectile velocity was then calculated from the travel time between the stations.

c. Target Mounting Procedure

The impact testing of the target specimens was conducted using the free-free method of mounting by taping the specimen to a mounting frame which was rigidly fixed to the base of the target tank as shown in Figure 3. Upon impact, this free-free method of mounting would permit the specimen to free flight. The mounting fixture was designed to be adjustable such that the desired impact angle could be achieved. Due to the high drag of the small projectile particles, the target specimen was located about 4.0 inches (102 mm) from the launch tube muzzle. In addition, the air within the target tank was partially evacuated for all impacts.

The majority of the impacts on the three materials were conducted at an impact angle of 30 degrees. To determine the effect of the angle of incidence on the damage generated,

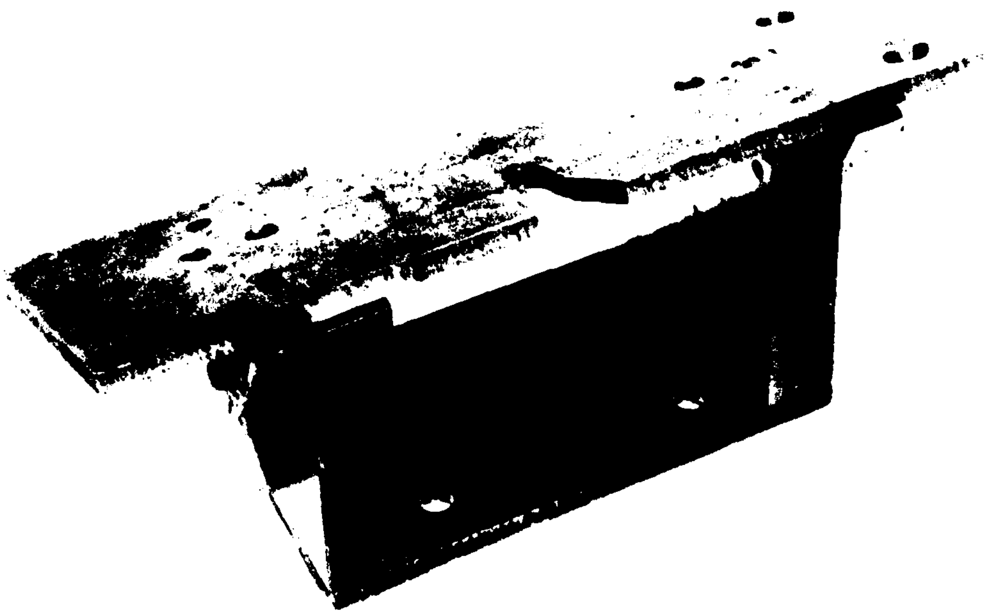

Figure 3. Free-Free Mounting Frame Utilized.
(Specimen not shown.)

additional tests were conducted on the baseline titanium material at impact angles of 7.5, 15.0 and 45.0 degrees.

d. Target Alignment

Target alignment onto the mounting fixture was achieved by projecting a laser beam through the bore of the launch tube onto the desired impact site of the target. Since all of the impacts were edge impacts, the target was positioned such that the laser beam was split by the target edge at the desired impact site.

e. Projectile Types and Sizes

Two types of projectile materials were utilized in the impact tests. The projectiles were either spheres of 2017-T4 aluminum or chrome steel. Early in the program, the aluminum spheres were observed to be deforming substantially during the impact event; therefore, the chrome steel spheres were used in the remainder of the program. This switch was made to avoid the uncertainty surrounding the effect of projectile deformation upon the damage inflicted on the test specimens.

The nominal particle sphere sizes used in the study were 0.063 (1.60), 0.125 (3.18), and 0.250 inch (6.35 mm) diameters. These various size sphere particles were used in the impacts to investigate the concept of geometric scaling of the damage generated on various specimen leading edge thicknesses. The majority of the impacts were conducted using the 0.063-inch (1.6 mm) diameter spheres.

f. Target Specimen Size and Leading Edge Thickness

The test specimens for the impact tests were machined from 6.0 x 1.0 inch (152.4 x 25.4 mm) blanks cut out from the sheet of material to be investigated. A flat constant thickness test section, where the edge impacts were to be conducted, was machined onto the center 1.0 inch (25.4 mm) portion of the specimen similar to that for the notch fatigue specimens. The test section thickness for the majority of the testing was 0.02 inches (0.508 mm). In addition, impact tests were also conducted on 0.01 and 0.04 inch (0.254 and 1.016 mm) thick test sections on the baseline titanium material to investigate the concept of geometric scaling. The nominal thickness for the titanium and steel sheets was 0.063 inches (1.59 mm) while the nominal thickness for the aluminum sheet was 0.250 inches (6.35 mm). Again, as for the notch fatigue specimens, the impact specimens were cut in the same direction in each material sheet to avoid any preferred orientation effects in the sheet. Sufficient specimens were prepared for each test condition to determine the critical velocity and impact at least seven specimens under identical test conditions at the critical velocity level. Single particle impacts were conducted on the test specimens in every case.

g. <u>Damage Assessment</u>

The damage assessment of the data collected was given particular consideration in the study. The critical velocity for each test condition was determined. Then, using this velocity, at least seven specimens were impacted under identical test conditions. The mode of damage was determined for each impact and the extent of damage was measured. Tests were then conducted on the selected damaged specimens to determine either the residual tensile strength or residual fatigue strength properties.

(1) Mode and Extent of Damage

The damage mode occurring on the target specimens was anticipated to be in the form of a nick with mass loss from the leading edge or substantial deformation with material loss and a crack. The damaged specimens having a nick were characterized by measurements of the depth and width of the resulting dent, crater, or perforation. The damaged specimens having a substantial deformation with material loss and a crack were characterized by determining the crack length.

In all impact experiments, the damage was measured, described, and photographed.

(2) Residual Property Measurements

Having completed the damage measurements and photographing the damaged specimens, the damage was described in terms of an equivalent stress concentration factor or residual tensile strength. To investigate the concept of an equivalent stress concentration factor, a series of fatigue tests was conducted using the various groups of specimens impacted under identical conditions. The fatigue data was then compared to that received in the baseline notch fatigue tests.

Each group of specimens with assumed identical damage was fatigue tested in the Schenck resonant tensile fatigue machine using an R ratio of 0.1. The load levels were chosen to produce failure in the range from 10^3 to 10^5 cycles, the same region in which the baseline notch fatigue data were obtained for each material. For each group of specimens, the data were plotted in the form of net section average stress against the number of cycles to failure. Corrections were made for the area removed due to the impact or the crack length across the width of the specimens.

In the case where the damage was substantial with long tears on the specimens, tensile tests were used to determine the residual tensile strength of the damaged specimens.

SECTION III
EXPERIMENTAL RESULTS

The experimental results of the edge impacts conducted to investigate the response of typical fan and compressor blade materials from small hard particles are summarized in the following paragraphs. A total of about 360 shots were fired to obtain 231 good impact data shots on the test specimens. A fairly large number of shots were test shots to determine the critical velocity region (cracks are generated with the damage), velocity determination, and alignment purposes. Tables of all the impacts giving the test conditions, damage measurements, and a description of the damage are presented in Appendix B.

1. MATERIAL CHARACTERIZATION

The physical and mechanical properties of the three materials investigated are presented in Table 1. The materials were 8-1-1 titanium, 7075-T651 aluminum, and 4130 steel. The 4130 steel material was tested in the annealed condition with a Rockwell hardness of B-84 and a heat treated condition with a Rockwell hardness of C-31.

TABLE 1

MATERIAL PHYSICAL AND MECHANICAL PROPERTIES

Material	Yield Strength ksi (MPa)	Density lb/in^3 (Kg/m^3)	Modulus of Elasticity in Tension ksi (MPa)
4130 steel (annealed)	60 (413.7)	0.283 ($7.83x10^3$)	$30x10^6$ (206.8)
4130 steel (heat-treated)	116 (799.8)	0.283 ($7.83x10^3$)	$30x10^6$ (206.8)
8-1-1 titanium	150 (1034.2)	0.158 ($4.37x10^3$)	$18x10^6$ (124.1)
7075-T651 aluminum	73 (503.3)	0.101 ($2.77x10^3$)	$10.4x10^6$ (71.7)

The results of the fatigue tests conducted on the notch fatigue specimens are presented in Figures 4 through 7. A straight line was drawn through the data and used as the baseline representation of the notch fatigue strength of the test materials. The stress concentration factor (K_T) is also given for each notch group. Figure 4 presents the baseline notch fatigue data for the 8-1-1 titanium material. Also included in Figure 4 is the baseline notch fatigue data from the same titanium sheet for 0.063-inch (1.60 mm) thick specimens. Figures 5 and 6 present the notch fatigue data for the 4130 steel material in the annealed and heat-treated condition, respectively. The notch fatigue data for the 7075-T651 aluminum is given in Figure 7.

2. RESULTS OF THE IMPACT TESTS

The testing involved conducting leading-edge impacts on flat constant thickness specimens of the three materials investigated. The study involved determining the critical velocity region where cracks or tears are generated with the damage for each test condition. Then, using this velocity, at least seven specimens were impacted under identical test conditions. Each group of specimens with assumed identical damage was then fatigue tested in tension to evaluate the damage. In several cases, residual tensile testing was substituted for the fatigue tests because of the extensive damage received from the impact. The fatigue data of the damaged specimen for each test condition was then plotted in the form of net average stress against the number of cycles to failure. Each material investigated was characterized in terms of the notch fatigue strength such that the fatigue data of the impact damaged specimens could be compared with the notch fatigue data for each test material. Equivalent stress concentration factors were then evaluated for each test condition by superimposing the curves of the notch fatigue data onto the plots of the damaged specimens. The stress concentration factors for the notch fatigue tests were K_T=1.39, 2.12,

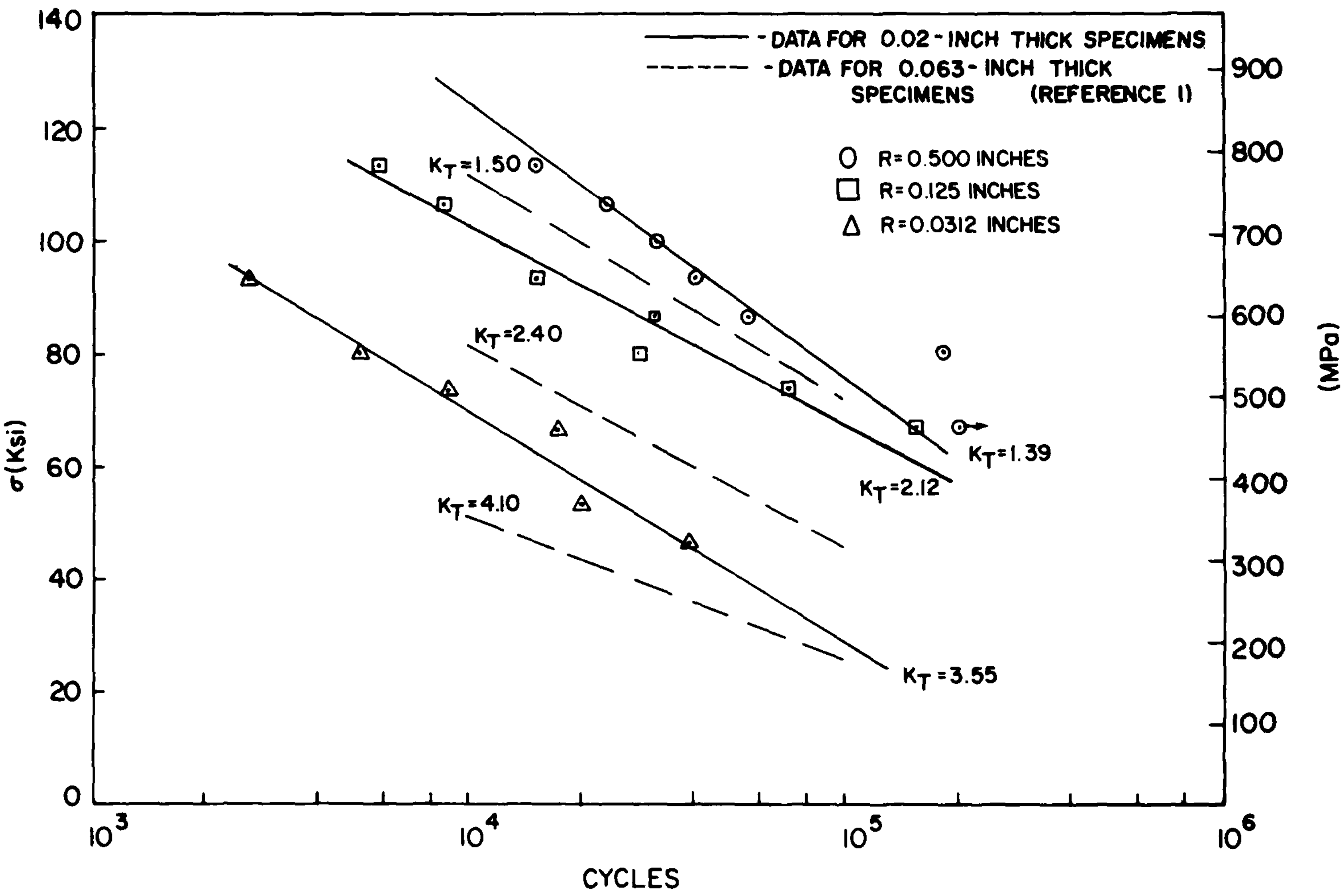

Figure 4. Baseline Notch Fatigue Data for 8-1-1 Titanium (0.508 mm Thick).

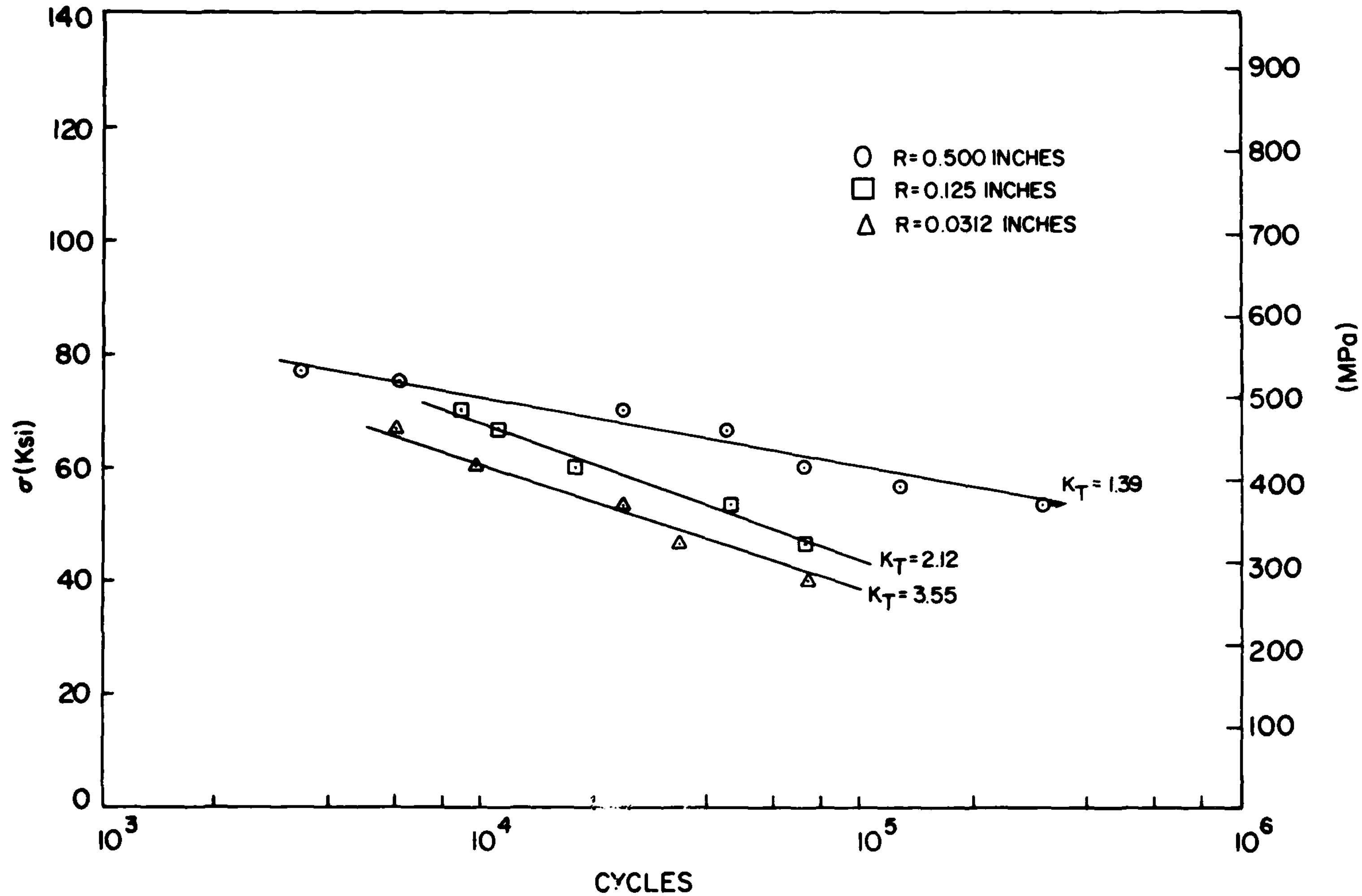

Figure 5. Baseline Notch Fatigue Data for 4130 Steel (Annealed Condition) (0.508 mm Thick).

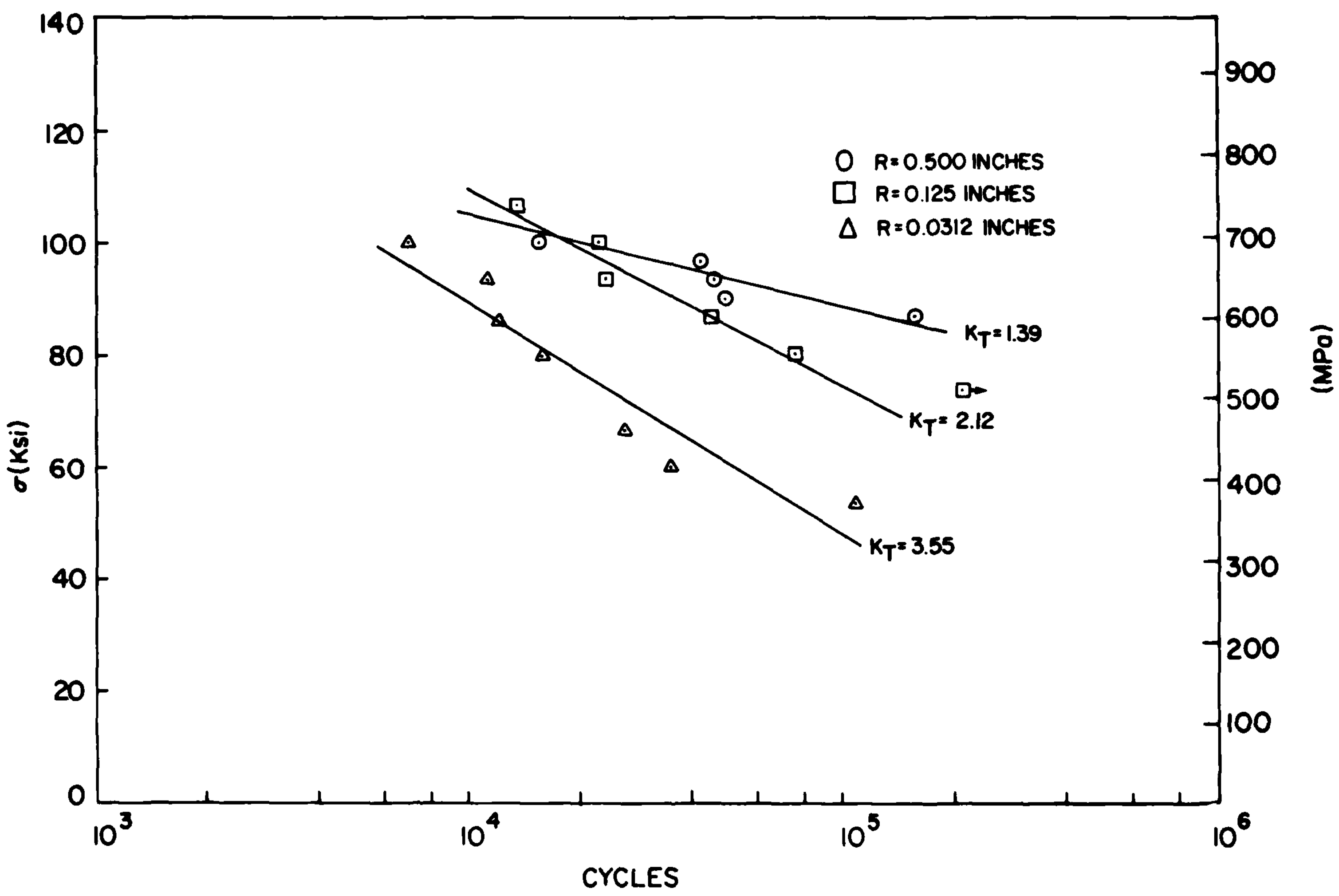

Figure 6. Baseline Notch Fatigue Data for 4130 Steel (Heat-Treated Condition) (0.508 mm Thick).

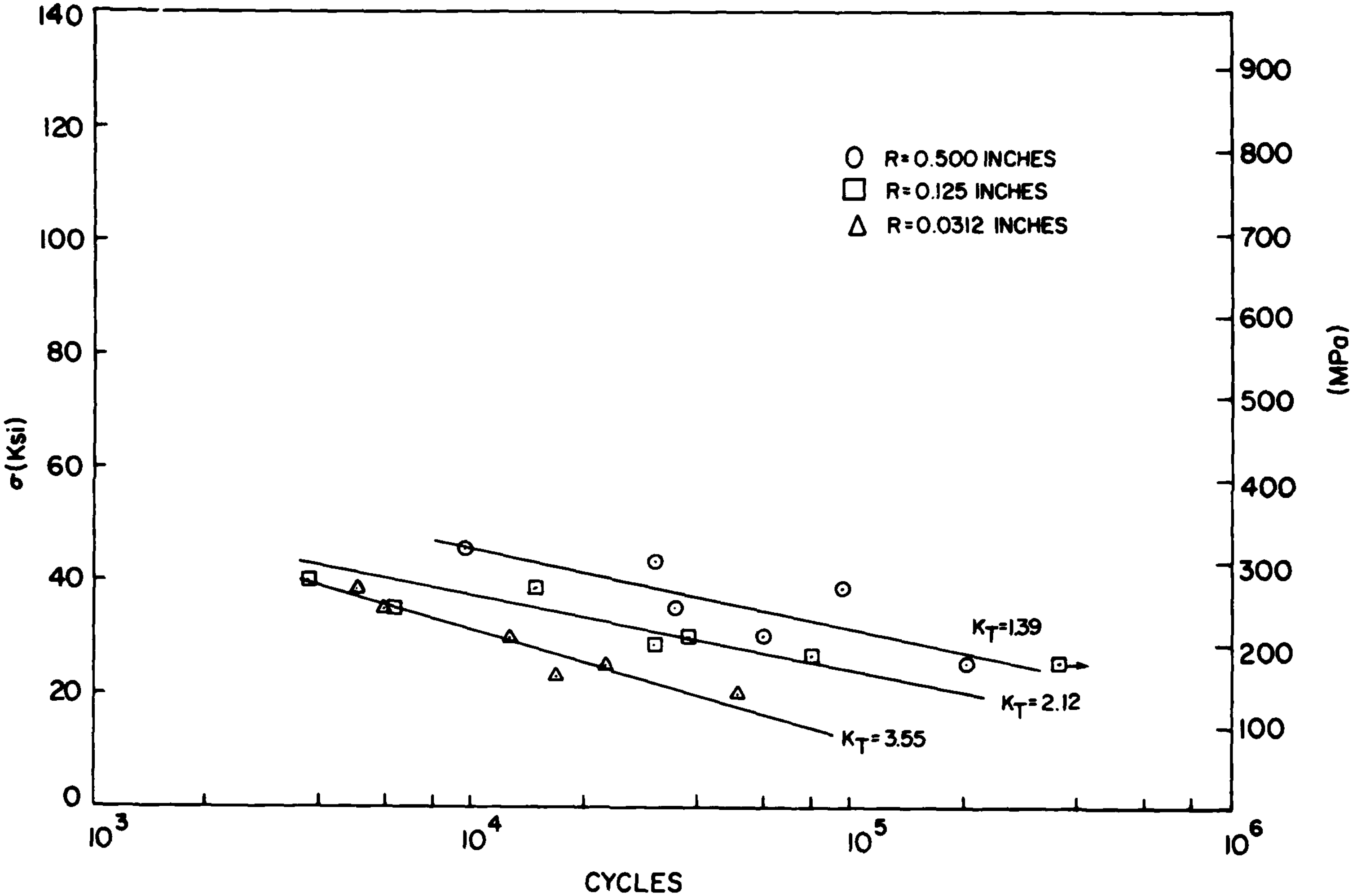

Figure 7. Baseline Notch Fatigue Data for 7075-T651 Aluminum (0.508 mm Thick).

and 3.55. Using this technique, an equivalent stress concentration factor was determined for each test condition. The effects of leading edge thickness, impact velocity, impact angle, particle size, particle material, and target material were investigated for damage response in the study.

a. Critical Velocity

The critical velocity was determined for each test condition. Table 2 presents a summary of the impact results. Impacts at similar test conditions are grouped together and averaged. The number in parenthesis in the table indicates the number of tests averaged in that group. Included in the table is the damage mode observed for each group. The equivalent stress concentration factor is also determined from the fatigue curves which are presented in a later section of this report.

The aluminum sphere impacts on the titanium material required the highest impact velocities to generate damage where tears or rips were received with bulging at the impact site. It was observed that the aluminum spheres would substantially deform plastically during the impact event; therefore, chrome steel spheres were substituted for the aluminum spheres. This switch was made to avoid the uncertainty surrounding the effect of projectile deformation upon the damage inflected on the test specimens. The impact test results for the aluminum sphere impacts are given in Tables 1 and 2 of Appendix B.

The damaged titanium specimens impacted by the 0.125 inch (3.18 mm) diameter aluminum spheres at a velocity of 1054 ft/s (321 m/s), were pulled to failure in tension to give an average residual net section strength value of 109.1 ksi (752.2 MPa). The damage for the titanium specimens impacted by the 0.063 inch (1.60 mm) diameter aluminum spheres was substantial and no tests were conducted to determine the residual tensile or fatigue strength values for this test condition. It was during these tests that it was discovered that the aluminum spheres were

TABLE 2. CRITICAL VELOCITY RESULTS FOR VARIOUS TEST CONDITIONS

Material	Leading Edge Thickness Inches (mm)	Impact Angle (°)	Projectile Material	Projectile Size Inches (mm)	Critical Velocity ft/s (m/s)	Damage Mode	Equivalent Stress Concentration Factor (K_T)	Residual Tensile Strength Ksi (MPa)
8-1-1 Ti (4)	0.01 (0.254)	30.0	2017-T4 Aluminum	0.063 (1.60)	2852 (869)	Tear	-----	-----
8-1-1 Ti (7)	0.01 (0.254)	30.0	2017-T4 Aluminum	0.125 (3.18)	1054 (321)	Tear	-----	109.1 (752.2)
8-1-1 Ti (6)	0.01 (0.254)	30.0	Chrome Steel	0.063 (1.60)	823 (251)	Tear	-----	116.6 (803.9)
8-1-1 Ti (7)	0.01 (0.254)	30.0	Chrome Steel	0.125 (3.18)	700 (213)	Tear	-----	84.4 (581.9)
8-1-1 Ti (7)	0.02 (0.508)	30.0	Chrome Steel	0.063 (1.60)	1154 (352)	Nick	3.2	-----
8-1-1 Ti (7)	0.02 (0.508)	30.0	Chrome Steel	0.125 (3.18)	760 (232)	Tear	4.2	-----
8-1-1 Ti (7)	0.02 (0.508)	30.0	Chrome Steel	0.250 (6.35)	745 (227)	Tear	4.1	-----
8-1-1 Ti (7)	0.02 (0.508)	7.5	Chrome Steel	0.125 (3.18)	895 (273)	Tear	3.6	-----
8-1-1 Ti (7)	0.02 (0.508)	15.0	Chrome Steel	0.125 (3.18)	775 (236)	Tear	3.4	-----
8-1-1 Ti (7)	0.02 (0.508)	45.0	Chrome Steel	0.125 (3.18)	847 (258)	Tear	4.1	-----
8-1-1 Ti (7)	0.04 (1.016)	30.0	Chrome Steel	0.125 (3.18)	802 (244)	Nick	3.6	-----
8-1-1 Ti (7)	0.04 (1.016)	30.0	Chrome Steel	0.250 (6.35)	836 (255)	Tear	4.9	-----
8-1-1 Ti (7) Glass Peened 5-8N	0.02 (0.508)	30.0	Chrome Steel	0.125 (3.18)	819 (250)	Tear	4.1	-----
8-1-1 Ti (7) Glass Peened 10-16 N	0.02 (0.508)	30.0	Chrome Steel	0.125 (3.18)	883 (269)	Tear	4.3	-----
4130 (7) Annealed	0.02 (0.508)	30.0	Chrome Steel	0.125 (3.18)	922 (281)	Tear	1.4	-----
4130 (7) Heat-Treated	0.02 (0.508)	30.0	Chrome Steel	0.125 (3.18)	820 (250)	Tear	2.1	-----
7075-T651 (7) Aluminum	0.02 (0.508)	30.0	Chrome Steel	0.063 (1.60)	1003 (306)	Nick	3.0	-----
7075-T651 (7) Aluminum	0.02 (0.508)	30.0	Chrome Steel	0.125 (3.18)	675 (206)	Tear	-----	77.4 (533.3)

plastically deforming during the impact event at velocities of 2852 ft/s (869 m/s). Typical damage for the 0.063 and 0.125 inch (1.60 and 3.18 mm) aluminum sphere impacts on the 0.101 inch (0.254 mm) thick titanium specimens is presented in Figures A.1 and A.2 of Appendix A, respectively.

The critical velocity data of the chrome steel impacts on the various materials, material thicknesses, and different angles of incidence are presented in Figure 8. This figure plots the critical velocity versus the material thickness. Based on this plot, the highest critical velocity value for the 0.02 inch (0.508 mm) thick specimens was for the 4130 steel material in the annealed condition. The shot peened titanium material also required higher velocity values to generate tears than for the basic titanium material. Impact results for all the sphere impacts are presented in Tables 1 through 18 of Appendix B for the various material and test conditions.

Typical photographs of the damage received from the sphere impacts for each test condition are presented in Figures A.1 through A.18 of Appendix A. The failure mode for the majority of the test conditions was bulging with a rip or tear. A nick on the leading edge with mass loss was the failure mode for the 0.063 inch (1.60 mm) diameter sphere impacts on the 0.020 inch (0.508 mm) thick titanium and aluminum materials and the 0.125 inch (3.18 mm) diameter sphere impacts on the 0.04 inch (1.016 mm) thick titanium specimens.

The effect of the various parameters on the specimen damage from the sphere impacts is discussed in detail in a later section of this report.

b. <u>Residual Tensile and Fatigue Test Results</u>

After documenting the damage on each specimen by making the damage measurements and taking photographs, the damaged specimens were either pulled to failure in tension or fatigue tests were conducted to be able to describe the damage in terms of an equivalent stress concentration factor.

The residual tensile strength was determined for the 0.01 inch (0.254 mm) thick titanium groups and the 0.020-inch (0.508 mm) thick aluminum material impacted by the 0.125-inch (3.18 mm) diameter steel spheres. Each group of specimens impacted under identical conditions were pulled to failure under tension. The impact angle for all these groups was 30 degrees. For the titanium material, the average residual tensile strength for the 0.125 inch (3.18 mm) diameter aluminum sphere impacts was 109.1 ksi (752.2 MPa). For the 0.063 inch (1.60 mm) and 0.125 inch (3.18 mm) chrome steel impacts on the 0.01 inch (0.254 mm) thick titanium, the average residual net section tensile strength was 116.6 ksi (803.9 MPa) and 84.4 ksi (581.9 MPa), respectively. The average residual tensile strength of the 0.02 inch (0.508 mm) aluminum material for 0.125 inch (3.18 mm) diameter steel spheres was 77.4 ksi (533.3 MPa).

The remaining groups of specimens damaged under identical test conditions were fatigue tested in tension. The data points for the various groups of damaged specimens are presented in Figures A19 through A31 of Appendix A in the form of plots of average net section stress (σ) against number of cycles to failure (N_f).

The fatigue data in the form of straight lines taken from Figures A19 through A28 of Appendix A for all test conditions on the titanium material are presented in Figure 9 as solid lines. The baseline notch fatigue data for K_T = 2.12 and 3.55 for the 0.02 inch (0.51 mm) thick notch specimens are superimposed on the plot as dashed lines. In addition, the baseline notch fatigue data from the same sheet of material conducted in the previous study of Reference 1 for 0.063 inch (1.60 mm) thick material is also superimposed on the plot with K_T values of 1.50, 2.40, and 4.10 as dashed lines. This simplified comparing one set of data with another by determining an equivalent stress concentration factor for each group of specimens impacted under identical test conditions. Based on these K_T values for the notch specimens, an equivalent stress

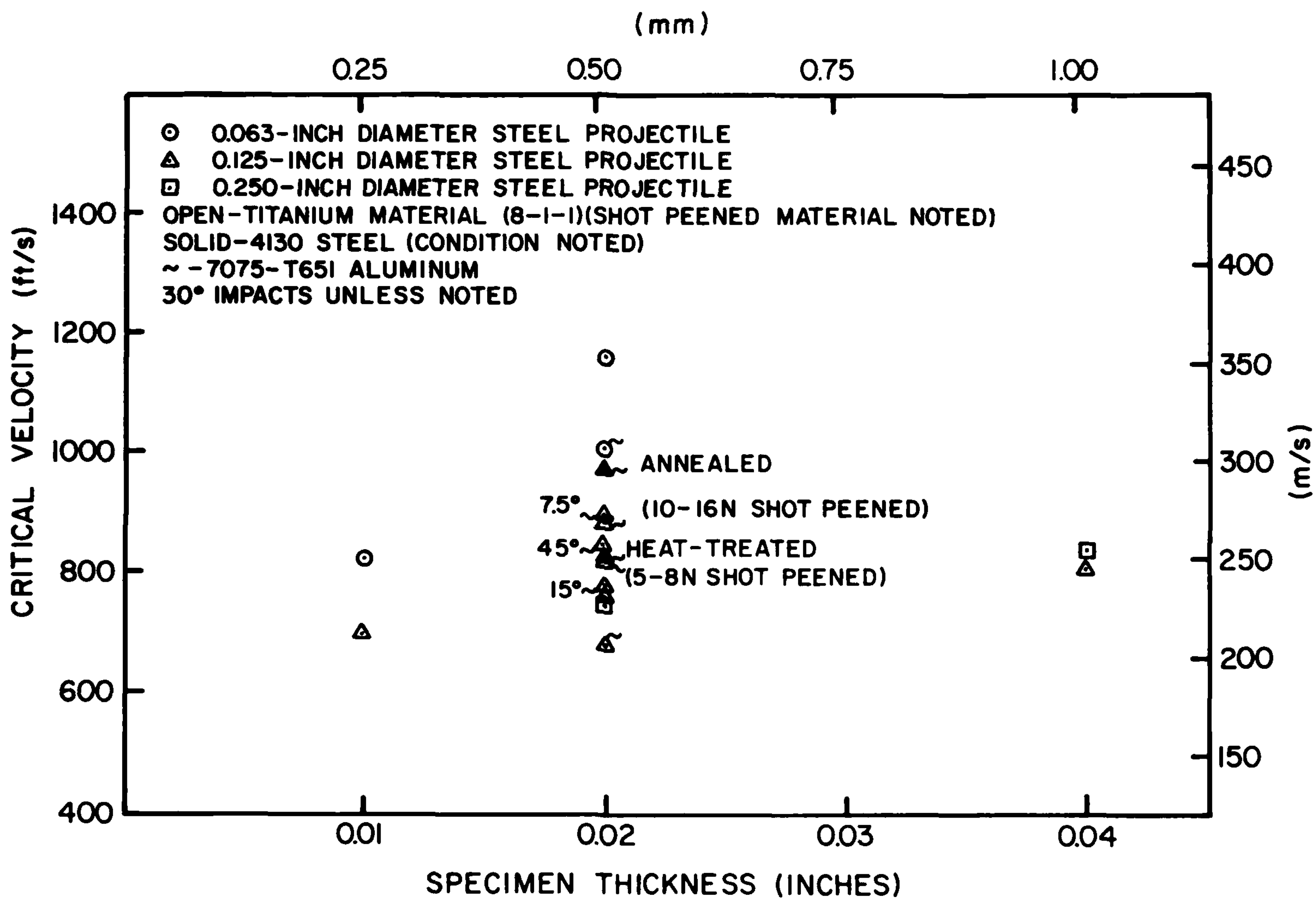

Figure 8. Critical Velocity versus Specimen Thickness Plot for all Materials.

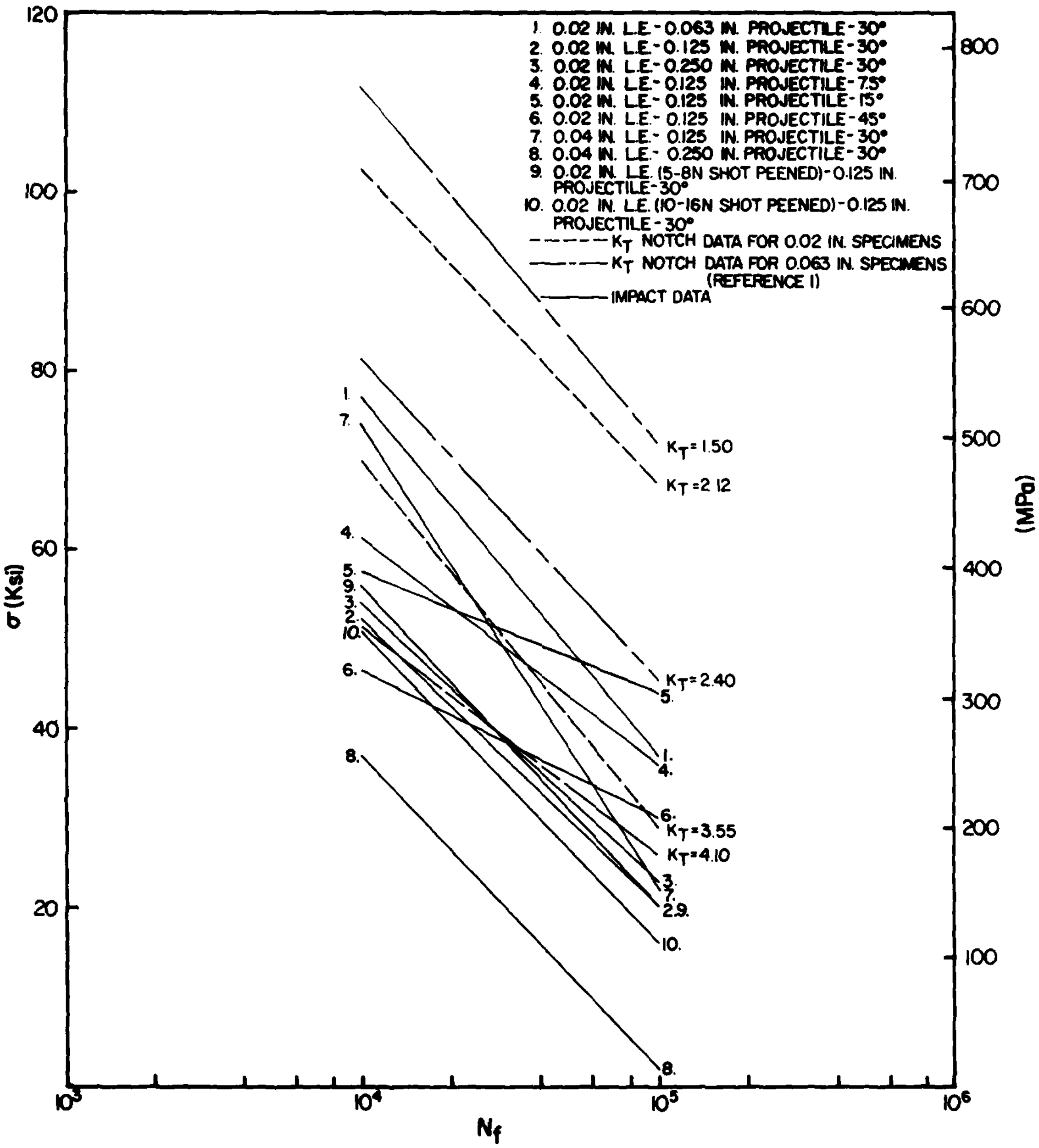

Figure 9. Fatigue Data Results for Titanium Material.

concentration factor was determined for each test condition and is given in Table 2. In several cases, extrapolation of the data was necessary to determine the equivalent stress concentration factor for the damaged specimen groups. The lowest K_T value of 3.2 was received for the 0.063 inch (1.60 mm) diameter steel sphere impacts on 0.02 inch (0.51 mm) thick titanium specimens at an impact angle of 30 degrees. The damage mode was in the form of a nick with mass removed from the leading edge at the impact site at a critical velocity of 1154 ft/s (353 m/s). The highest K_T value of 4.9 was received for 30 dgree impacts of 0.250 inch (6.35 mm) diameter steel spheres on a 0.04 inch (1.016 mm) thick titanium specimens. A velocity of 836 ft/s (255 m/s) was required to generate this damage which was in the form of bulging with tearing at the impact site. Figure 10 presents a plot of the equivalent stress concentration values (K_T) versus the critical velocity for the titanium material. Notice that the majority of the various groups of specimens had a critical velocity value between about 750 ft/s (228 m/s) and 900 ft/s (274 m/s) and a K_T value between 3.4 to 4.9. Typical damage on the titanium material due to the steel sphere impacts is shown in Figures A.3 through A.14 of Appendix A. The effects of leading edge thickness and angle of incidence on the type and extent of damage sustained due to the particle impacts were investigated and are reported in a later section of the report. In addition, the applicability of geometric scaling concepts was investigated which is also reported in a later section of this report.

The fatigue data in a form of a straight line taken from Figures A.29 and A.30 of Appendix A for the annealed and heat-treated steel are presented in Figure 11 as solid lines. The data are in the form of a plot of the average stress (σ) versus the number of cycles to failure (N_f). The baseline notch fatigue data for both material conditions are also superimposed on the plot as dashed lines. The K_T values for the notched

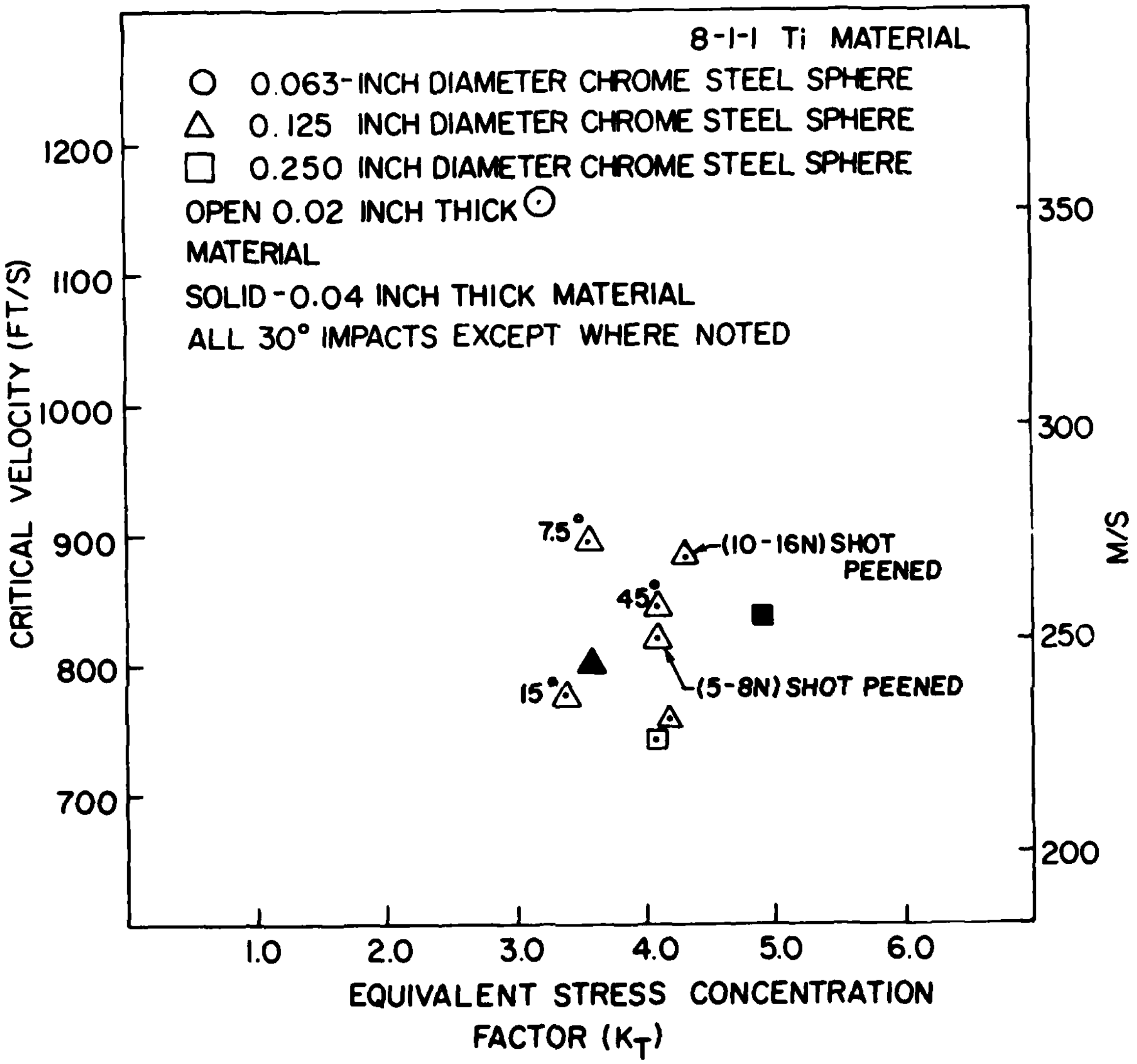

Figure 10. Critical Velocity versus Equivalent Stress Concentration Factor (K_T) Plot for Titanium Material.

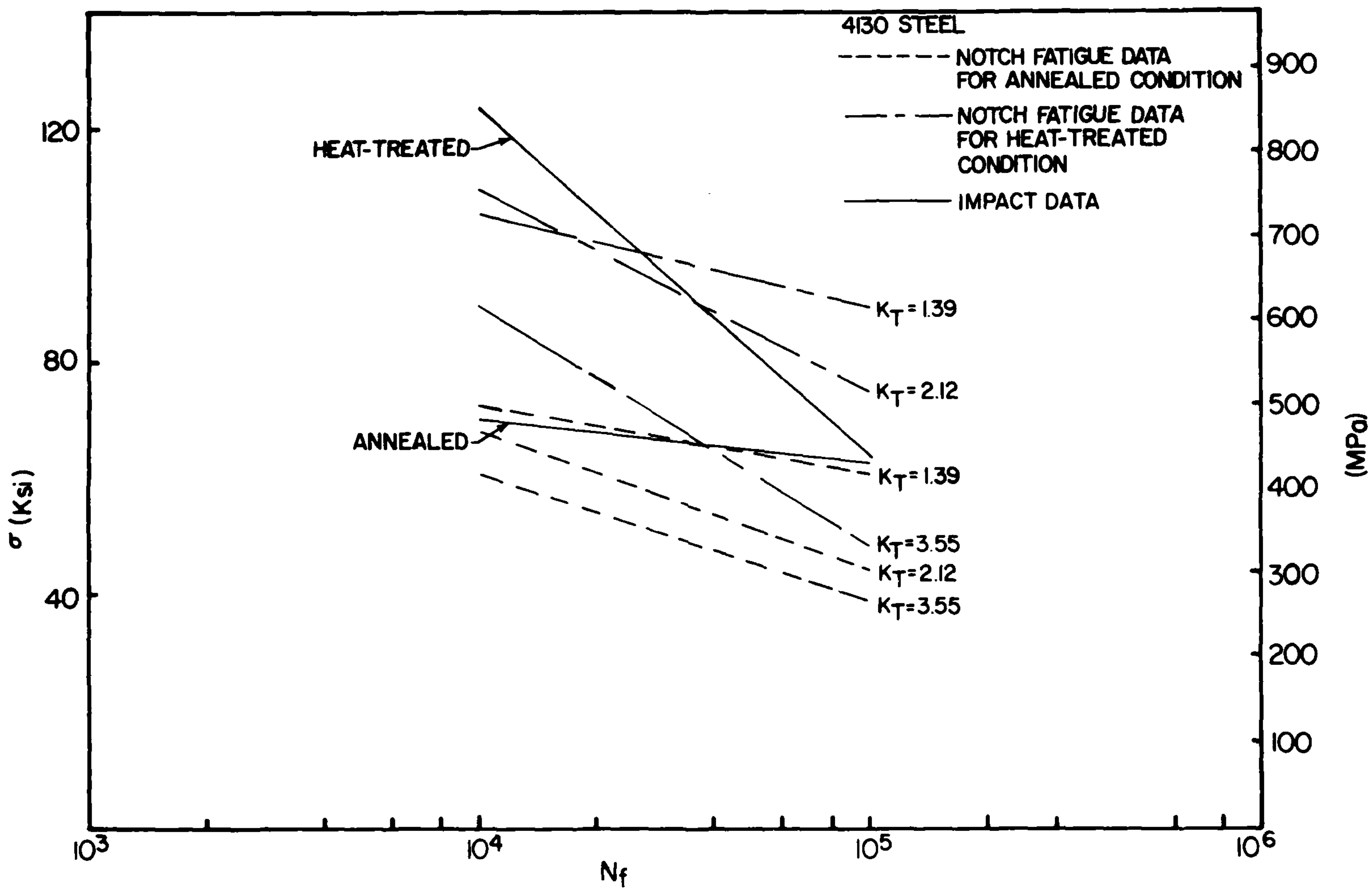

Figure 11. Fatigue Data Results for Annealed and Heat-Treated Steel Material.

specimens were 1.39, 2.12, and 3.55. Then, using the notch fatigue data, the damaged specimens of each group could be compared by describing the damage in terms of an equivalent stress concentration factor. Based on this technique to quantitatively measure the damage, the K_T values for the 0.125 inch (3.18 mm) diameter steel sphere impacts at 30 degrees on 0.02 inch (0.51 mm) thick specimens was 1.4 for the annealed group and 2.1 for the heat-treated group. Notice that the slope for the heat-treated group (both notch and damaged) is much greater than for the annealed condition group. This indicates that the heat-treated specimens are more sensitive to the loading than the annealed specimens; however, the stress is also higher for the heat-treated specimens. Both groups had a failure mode of bulging with a tear or rip at the impact site. The annealed group of specimens had the highest critical velocity level of 922 ft/s (281 m/s) for all materials at similar test conditions. The critical velocity for the heat-treated group was 820 ft/s (250 m/s). From this information, one can say that the annealed specimens were ductile enough to be able to absorb a substantial amount of energy; however, it also had the property of being very tough. Typical damage received for the steel material is given in Figures A.15 and A.16 of Appendix A.

The fatigue data curve from Figure A.31 of Appendix A for the 0.063 inch (1.60 mm) steel impacts on 0.02 inch (0.51 mm) thick 7075-T651 aluminum material is presented in Figure 12. Again, the notch fatigue curves as dashed lines are superimposed to permit determining an equivalent stress concentration factor (K_T) for the damaged group. A K_T value of 3.0 was determined for the 30 degree impacts at a critical velocity of 1003 ft/s (306 m/s). The mode of failure for the specimens was in the form of nick with mass removal at the impact site as shown in Figure A.17 of Appendix A.

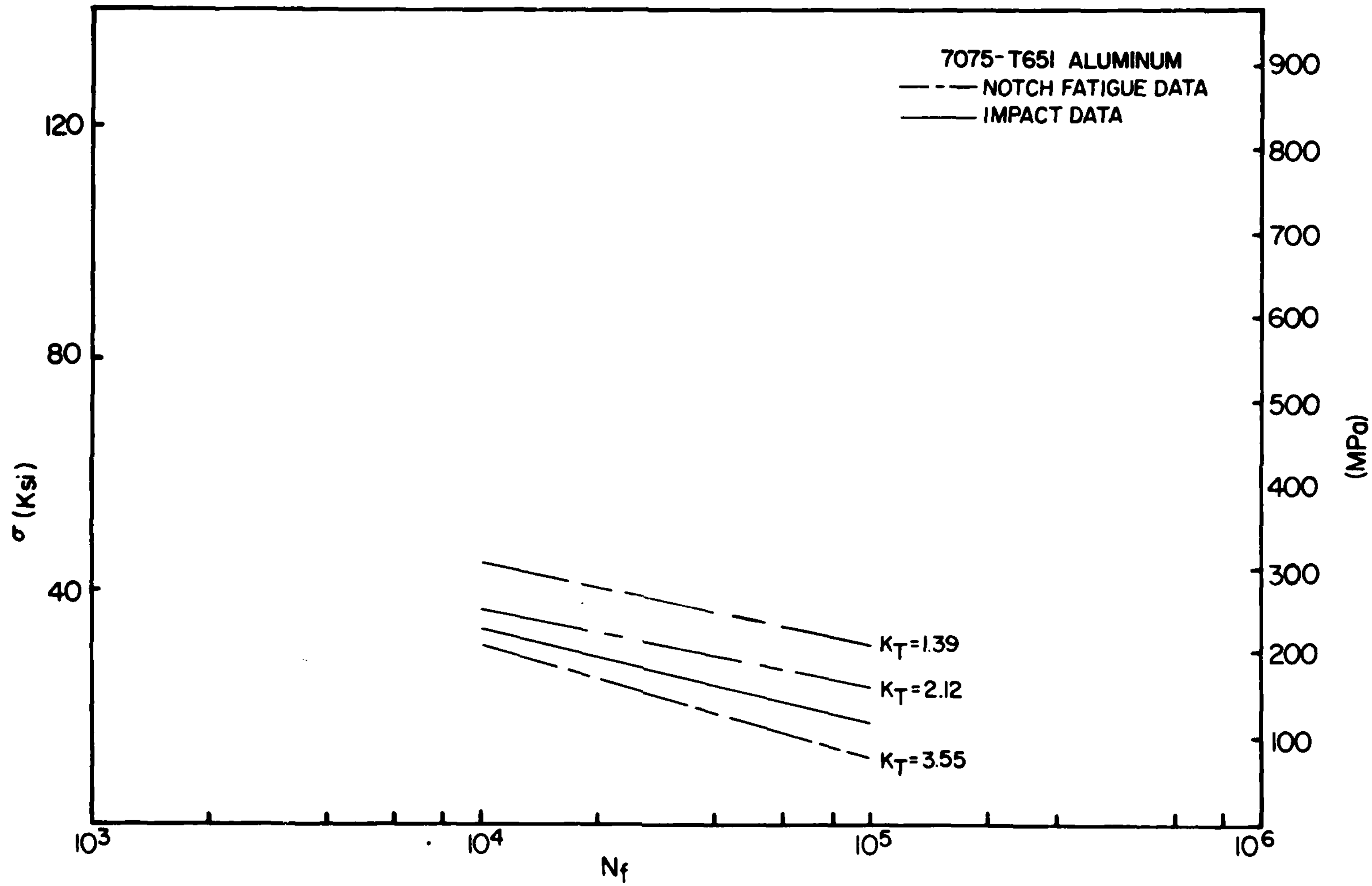

Figure 12. Fatigue Data Results for 7075-T651 Aluminum Material.

3. GEOMETRIC SCALING

One phase of the investigation was to determine the applicability, if any, of geometric scaling concepts. Geometric scaling is based on the concept of comparing responses of geometrically similar bodies. In this case, spherical projectiles of diameter (d) impacting leading edges of thickness (t) are considered. If the ratio of the projectile diameter and leading edge thickness is s for two different events, then for a given velocity (the same for both cases) the ratio of momentum or kinetic energy is s^3. It is assumed that the material density is identical in both cases. The forces that impacts exerts on the target specimen have a magnitude ratio of s^2 and a duration ratio s. The local pressure or stress depends only on the velocity and thus is independent of s. (Note that the stress due to a one-dimensional impact against a rigid target is ρCV, i.e., depends on the velocity of impact (v) for a given material having density (ρ) and wave speed (c). The resistance to bending of a target specimen or structure varies as s^3, s^2 due to the thickness, and s for the width or lateral dimensions. Resistance to shear or penetration also varies as s^3, s^2 due to the area of a shear plug, and s due to the thickness. With identical stresses in both cases, the deflections should scale linearly with the ratio s. One can expect, for example, that the damage in an 0.010 inch (0.254 mm) thick specimen due to an impact of an 0.063 inch (1.60 mm) diameter projectile would be geometrically similar to that in an 0.020 inch (0.508 mm) thick specimen impacted with an 0.125 inch (3.18 mm) diameter projectile.

The average damage results of a series of tests performed on leading edge thicknesses of 0.01, 0.02, and 0.04 inch (0.254, 0.508, and 1.016 mm) are given in Table 3. The material for all the specimens was from the same sheet of 8-1-1 titanium. The incidence angle was 30 degrees and the chrome steel projectile diameters were 0.063, 0.125 and 0.250 inch (1.60, 3.18, and 6.35 mm). Although the impact velocities are not equal for Table 3 for comparing the various groups, the results indicate

TABLE 3

DAMAGE RESULTS FOR VARIOUS GROUPS TO INVESTIGATE SCALING

Leading Edge Thickness inches (mm)	Impact Angle (°)	Projectile Size inches (mm)	Critical Velocity ft/s (m/s)	Damage Measurements			K_T Value
				Tear Length inches (mm)	Width inches (mm)	Depth inches (mm)	
0.01 (0.254)	30	0.063 (1.60)	823(251)	0.086(2.18)	---	---	---
0.02 (0.508)	30	0.125 (3.18)	760(232)	0.194(4.93)	---	---	4.2
0.02 (0.508)	30	0.063 (1.60)	1154(352)	---	0.050(1.27)	0.022(0.56)	3.2
0.04 (1.016)	30	0.125 (3.18)	802(244)	---	0.094(2.39)	0.033(1.40)	3.6
0.02 (0.508)	30	0.125 (3.18)	760(232)	0.194(4.93)	---	---	4.2
0.04 (1.016)	30	0.250 (6.35)	836(255)	0.447(11.4)	---	---	4.9

that linear scaling seemed to work as well as expected, considering the reproducibility of damage scatter from test to test because of the difficulty of hitting the leading edge in the same central location in every test. For linear scaling to be applicable, the damage measurements for the large projectile sizes impacting the thicker specimens should be twice that for the smaller projectiles impacting the thinner specimens. The equivalent stress concentration factors should be equal for each group compared. Based on this information, the tear length for the 0.125 inch (3.18 mm) projectile impacts on 0.02 inch (0.508 mm) thick specimens is 13 percent higher than would be predicted by the results of the half scale impacts for the 0.063 inch (1.60 mm) projectiles on 0.01 inch (0.254 mm) specimens. The K_T value of 4.9 for the larger projectile impacts on the thicker specimens is also about 17 percent greater than that for the K_T of 4.2 received for the smaller projectile impacts on the thinner specimens. The mode of damage for these two groups of specimens compared was similar with bulging and tearing.

The comparison of the results for the second two groups of specimens in Table 3 was for 0.063 and 0.125 inch (1.60 and 3.18 mm) projectile impacts on 0.02 and 0.04 inch (0.508 and 1.061 mm) thick specimens. The damage mode for these two groups was similar with nicks and mass removed from the leading edge. The width and depth for the larger projectile was 6 percent and 25 percent lower than for the smaller size projectile, respectively; however, the K_T value for the larger projectile was about 13 percent too high for linear scaling.

The comparison of the results for the last two groups of specimens in Table 3 for linear scaling was for 0.125 and 0.250 inch (3.18 and 6.35 mm) projectile impacts on 0.02 and 0.04 inch (0.508 and 1.016 mm) thick specimens. The damage mode for these two groups was similar with bulging with tearing at the impact site. In this case, the tear length damage for the larger projectile was 15 percent higher than predicted for linear scaling.

The K_T value for the larger projectile was also 17 percent higher than predicted for linear scaling to be applicable.

Based on the results of the three separate groups, linear scaling seemed to work as well as expected and the consistency of linear scaling data can be considered as good. The groups with tearing at the impact site were high as much as 15 percent for the tear length for linear scaling to be applicable. In the case of the damage mode being a nick, the width and depth damage was low 6 percent and 25 percent, respectively, for linear scaling. Also, the K_T values were off as much as 17 percent for linear scaling.

Another technique used to investigate the concept of geometric scaling was to plot the critical velocity versus the normalized projectile diameter as given in Figure 13. The projectile size for each of the critical damaged groups was normalized to that causing equivalent damage in an 0.02 inch (0.508 mm) thick leading edge specimen following the concept of geometric scaling outlined above. Thus, an 0.125 inch (3.18 mm) projectile impacting an 0.01 inch (0.254 mm) leading edge thickness was normalized to an 0.250 inch (6.35 mm) projectile impacting a reference 0.02 inch (0.508) leading edge. The data of Figure 13 show a general trend; namely, the critical velocity increases dramatically when the particle size gets smaller than 0.08 inches (2.0 mm) or the particle size becomes smaller than four times the leading edge thickness. A small decrease in critical velocity is observed as the projectile increases in (normalized) size above 0.08 inches (2.0 mm). Considering the scatter in the data due to the difficulty in hitting the leading edge at the same central location in every test, the consistency of the data is good.

4. EFFECT OF VARIOUS PARAMETERS ON SPECIMEN DAMAGE

Important impact, material, and geometry parameters were varied in the testing to determine the effect of the various parameters on the specimen damage.

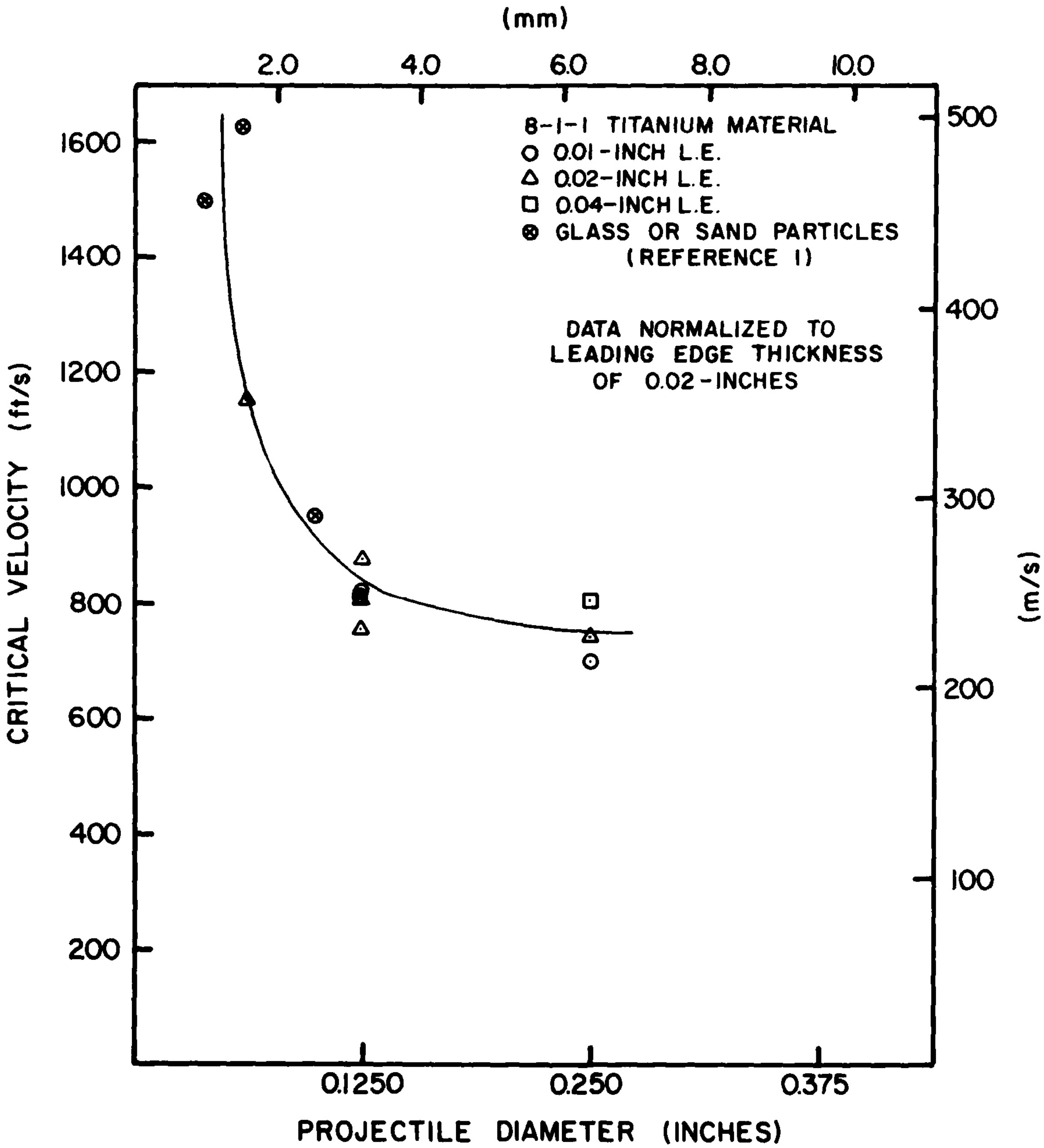

Figure 13. Plot of Critical Velocity versus Normalized Projectile Diameter for Titanium Material and 30° Impacts.

The following paragraphs discuss the trend of the specimen damage or critical velocity for the various parameters varied.

a. Projectile Parameters

The two projectile parameters investigated in the testing were projectile density and projectile size.

(1) Effect of Projectile Density on Damage

The density of the projectile material greatly affected the velocity required to obtain critical damage. The data of Table 2 shows that the critical velocity of 2017-T4 aluminum 0.125 inch (3.18 mm) diameter sphere on 0.01 inch (0.254 mm) thick titanium specimens was 1054 ft/s (321 m/s), whereas for similar test conditions using chrome steel projectiles the critical velocity was 700 ft/s (213 m/s). Thus, the aluminum spheres required a much higher velocity to obtain critical damage on the specimens. The residual tensile strength of the damaged specimens for the aluminum sphere impacts was 109.1 ksi (752.2 MPa), while the tensile strength for the same material for the steel sphere impacts was 84.4 ksi (581.9 MPa). Based on these results, the chrome steel impacts generate much greater damage at lower impact velocities.

(2) Effect of Projectile Size on Critical Velocity

The effect of projectile diameter on the critical velocity values was shown in Figure 13. The plot of the critical velocity versus an equivalent projectile diameter with the data being normalized to a leading edge thickness of 0.02 inch (0.508 mm) shows that as the projectile size decreases the critical velocity increases at a substantial rate below a projectile size of 0.08 inch (2.0 mm). Above a projectile size of 0.08 inch (2.0 mm), a small decrease in critical velocity results as the projectile increases in (normalized) size.

The effect of projectile size on generating damage on titanium specimens is shown in Figure 14.

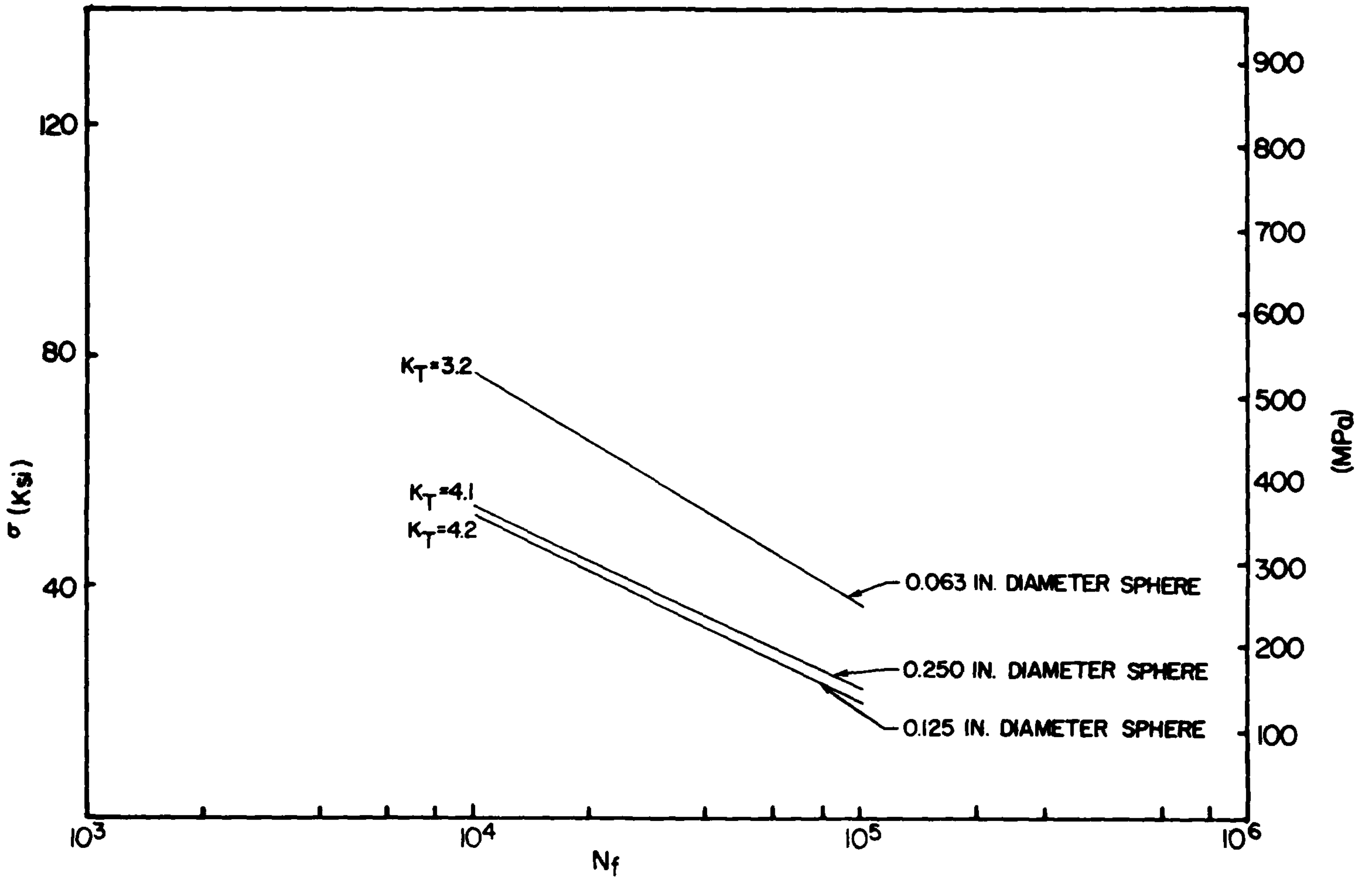

Figure 14. Fatigue Data Results for Titanium Material and Various Size Projectile Impacts.

Figure 14 presents a plot of average net-section stress (σ) against number of cycles to failure (N_f) for the impacts of the three projectile sizes used in the study. The leading edge thickness of the 8-1-1 titanium material was 0.02 inch (0.508 mm) and the angle of incidence was 30°. Notice that the K_T value or damage of the 0.063 inch (0.254 mm) diameter sphere was the lowest at 3.2. The damage mode for this size projectile was a nick with mass removal at the impact site. The K_T values for the 0.125 and 0.250 inch (0.508 and 1.016 mm) diameter spheres were similar at 4.2 and 4.1, respectively. The K_T value for the 0.125 inch (0.508 mm) diameter projectile was determined to be slightly greater than that for the 0.250 inch (1.016 mm) diameter projectile. The failure mode of these larger projectile impacts was in the form of bulging with tearing at the impact site. The critical velocity for the 0.063, 0.125, and 0.250 inch (0.254, 0.508, and 1.016 mm) diameter steel spheres was determined to be 1154, 760, and 745 ft/s (352, 232, and 227 m/s), respectively. Thus, the critical velocity decreased as the projectile size was increased.

b. Material Parameters

The three material parameters investigated in the testing were density, modulus, and yield strength.

(1) Effect of Material Density on Critical Velocity

The effect of material density on the critical velocity is presented in Figure 15. Figure 15 gives a plot of the critical velocity against the density of the 8-1-1 titanium, 4130 steel, and 7075-T651 aluminum material. Data for the shot-peened titanium is included along with the data for the steel in the annealed and heat-treated conditions. Based on the results of this plot, the critical velocity increases with a density increase; however, changing the hardness of the material or material surface also affects the critical velocity. Thus, it can be stated that using the material density is not sufficient

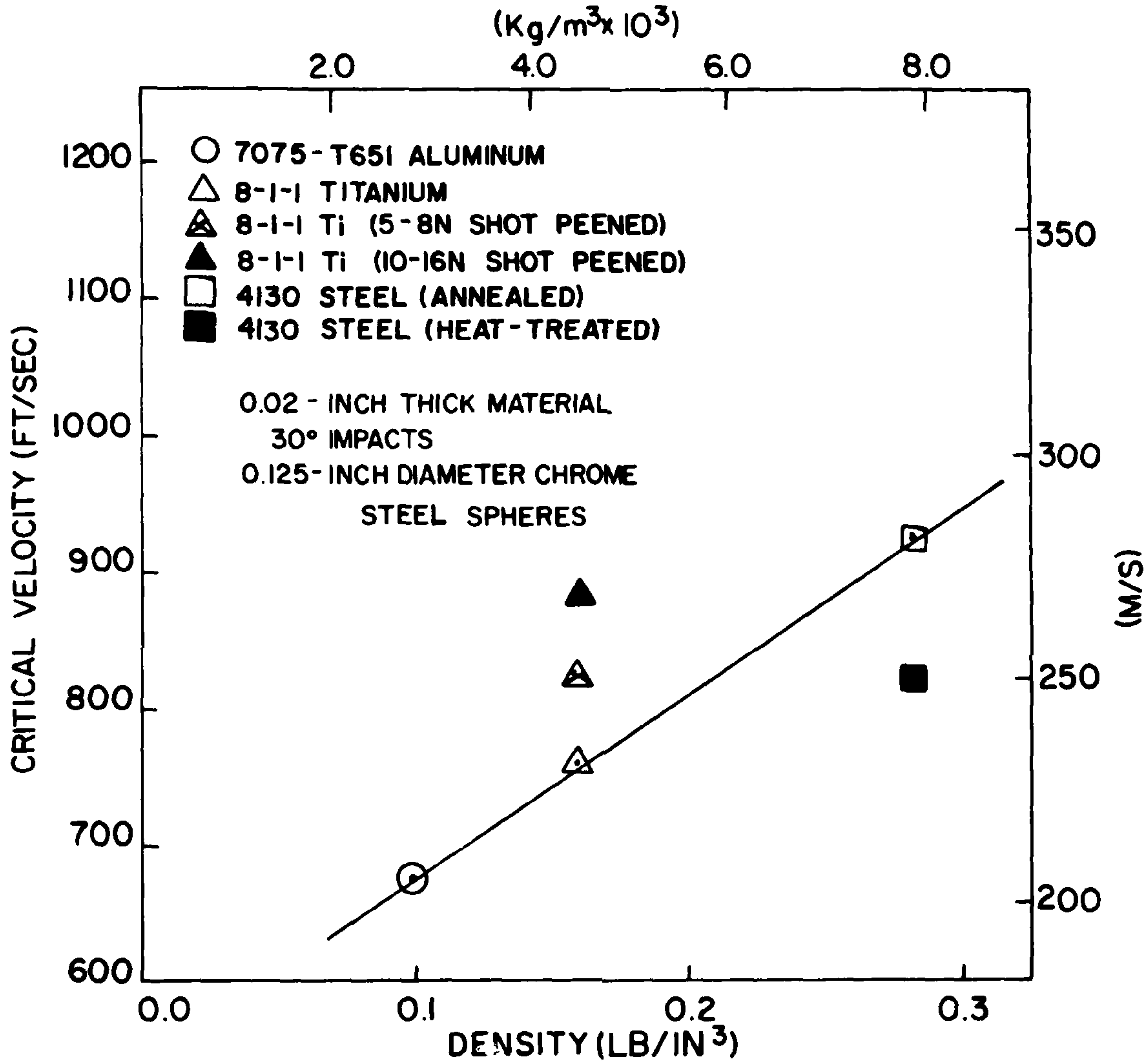

Figure 15. Critical Velocity versus Material Density Plot for all Materials.

in determining the critical velocity of a material. The material hardness or surface hardness must also be known to accurately determine the critical velocity.

The damage on the three materials is also affected as shown in Table 2 by the equivalent stress concentration factor K_T. The lowest K_T of 1.4 was received by the annealed steel followed by a K_T of 2.1 for the steel in the heat-treated condition. The K_T for the alumimum was 3.0. The K_T values for the titanium was 3.2 for the raw titanium, 4.1 for the 5-8N shot peening, and 4.3 for the 10-16N shot peened condition.

(2) Effect of Material Modulus of Elasticity on Critical Velocity

The effect of the material modulus of elasticity on the critical velocity is presented in Figure 16. Figure 16 gives a plot of the critical velocity against the material modulus for the 8-1-1 titanium, 4130 steel, and 7075-T651 aluminum. Again, data for the shot peened titanium is included along with the data for the steel in the annealed and heat-treated conditions. The plot makes it clear that specimen modulus and critical velocity are not sensibly correlated.

The damage quantified by the equivalent stress concentration factor also was affected in the same manner as for the material density.

(3) Effect of Material Yield Strength on Critical Velocity

The effect of material yield strength on critical velocity is presented in Figure 17. Figure 17 gives a plot of the critical velocity versus the yield strength for the three basic materials investigated along with that for the shot peened conditions for the titanium and the heat-treated condition of the steel material. Based on the results of this plot, no correlation can be established for the yield strength on the critical velocity.

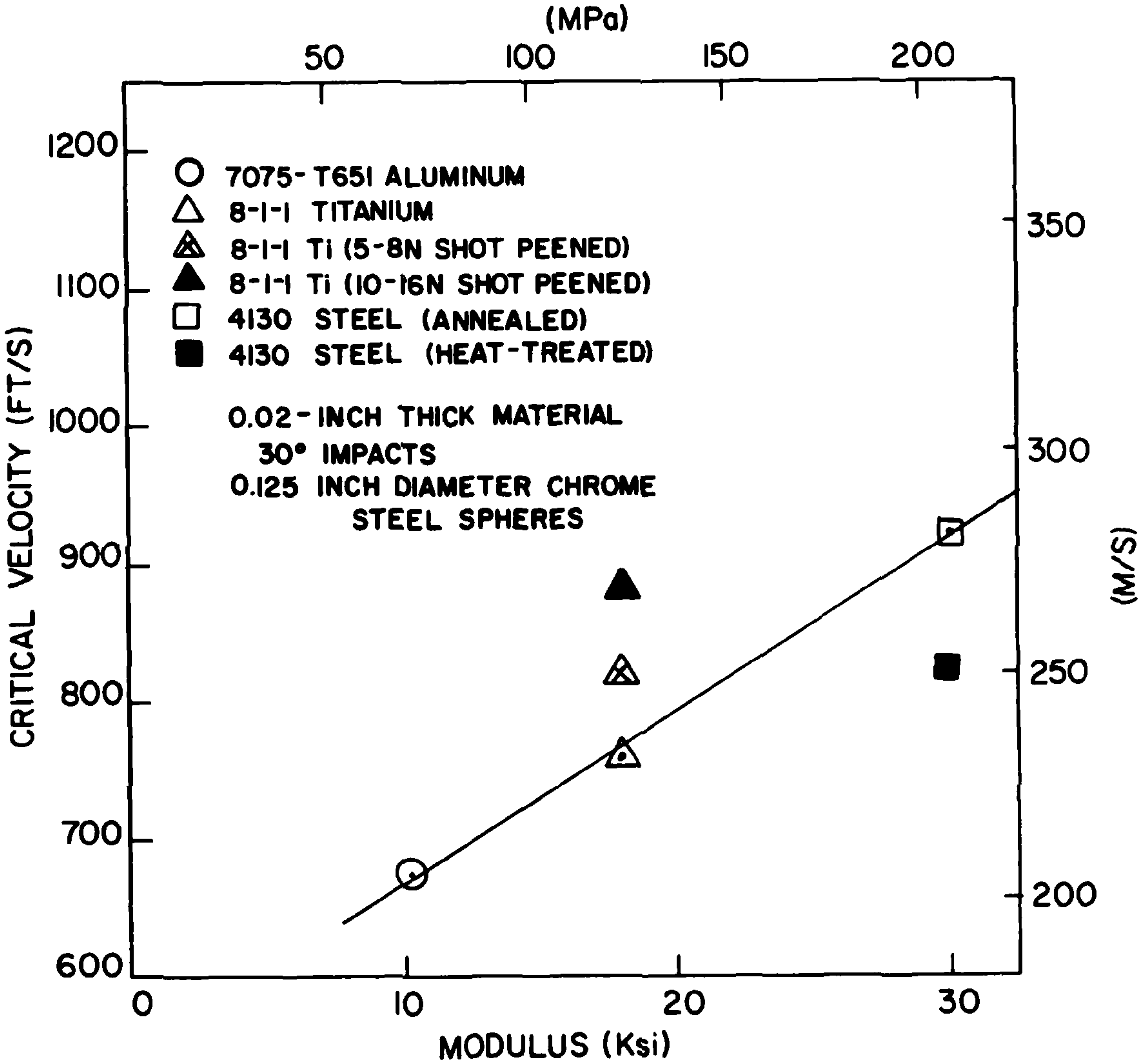

Figure 16. Critical Velocity versus Material Modulus Plot for all Materials.

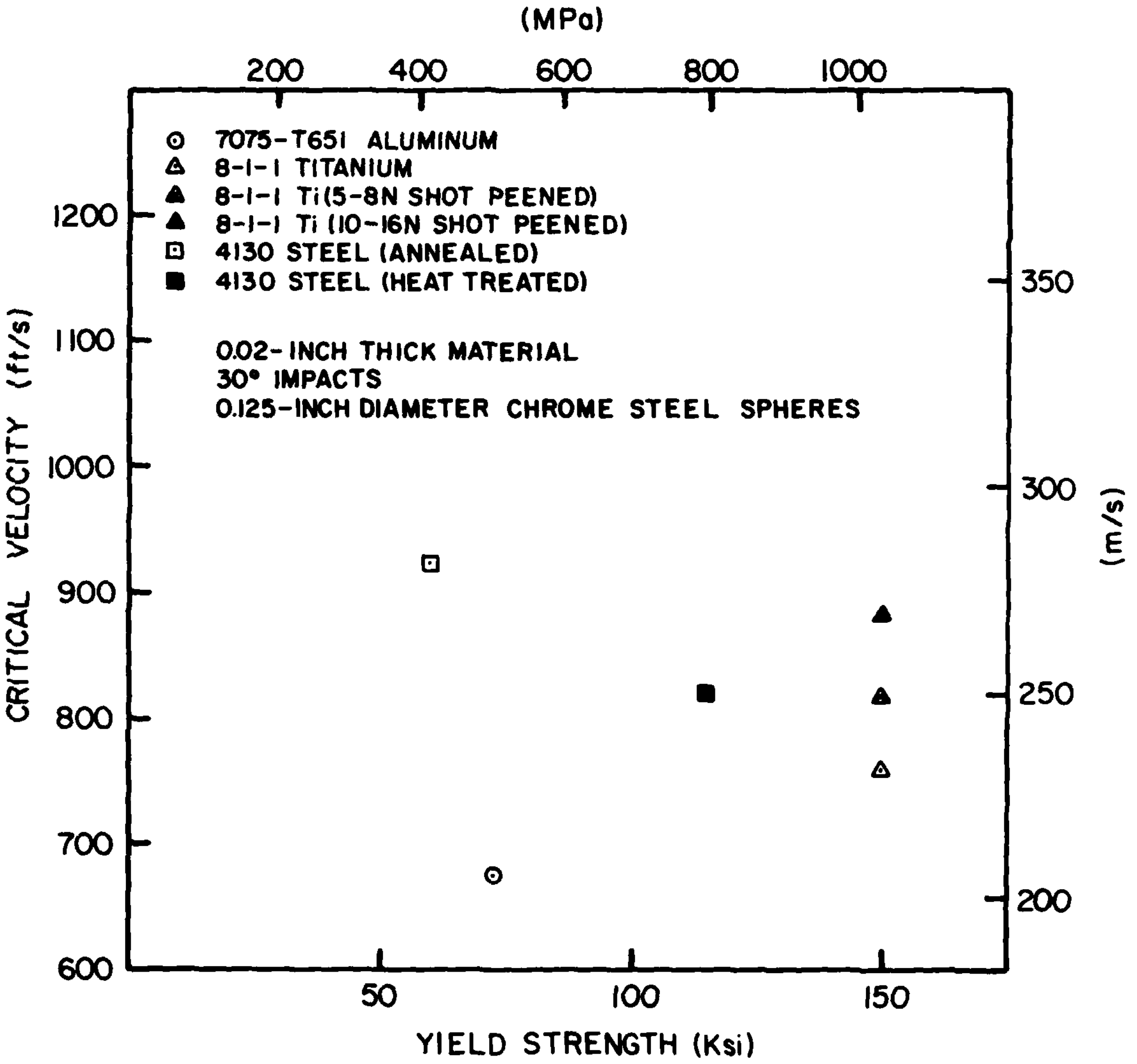

Figure 17. Critical Velocity versus Material Yield Strength Plot for all Materials.

An attempt was made to establish some correlation by plotting the critical velocity versus the yield strength divided by the density as presented in Figure 18. Again, the results of the plot shows that no correlation can be established.

(4) Effect of Shot Peening Titanium on Critical Velocity

The effect of shot peening the 8-1-1 titanium on the critical velocity can be determined from Figure 15 which is a plot of the critical velocity versus material density. Based on this plot and Table 2, the shot peening increases the critical velocity. The basic unpeened titanium material has a critical velocity of 760 ft/s (232 m/s) for the 0.125 inch (3.18 mm) diameter steel impacts on the 0.02 inch (0.508 mm) thick leading edge. Shot peening the material surface to an intensity of 0.005-0.008N increased the critical velocity to a value of 819 ft/s (250 m/s). Increasing the shot peening intensity further to 0.010-0.016N again increased the critical velocity to a value of 883 ft/s (269 m/s). Thus, the effect of shot peening can increase the critical velocity by as much as 16 percent.

The effect of shot peening on the damage is shown in Figure 19 and Table 2. Figure 19 presents a plot of the average net-section stress (σ) versus the number of cycles to failure (N_f). Notice that the curves are close to one another which indicates that shot peening has little effect on the damage received. The equivalent stress concentration factors for the 0.005-0.008N and 0.010-0.016N shot peening intensities are 4.1 and 4.3, respectively. The K_T value for the unpeened material is 4.2.

c. Impact Parameter

The impact parameter investigated in the testing was the angle of incidence.

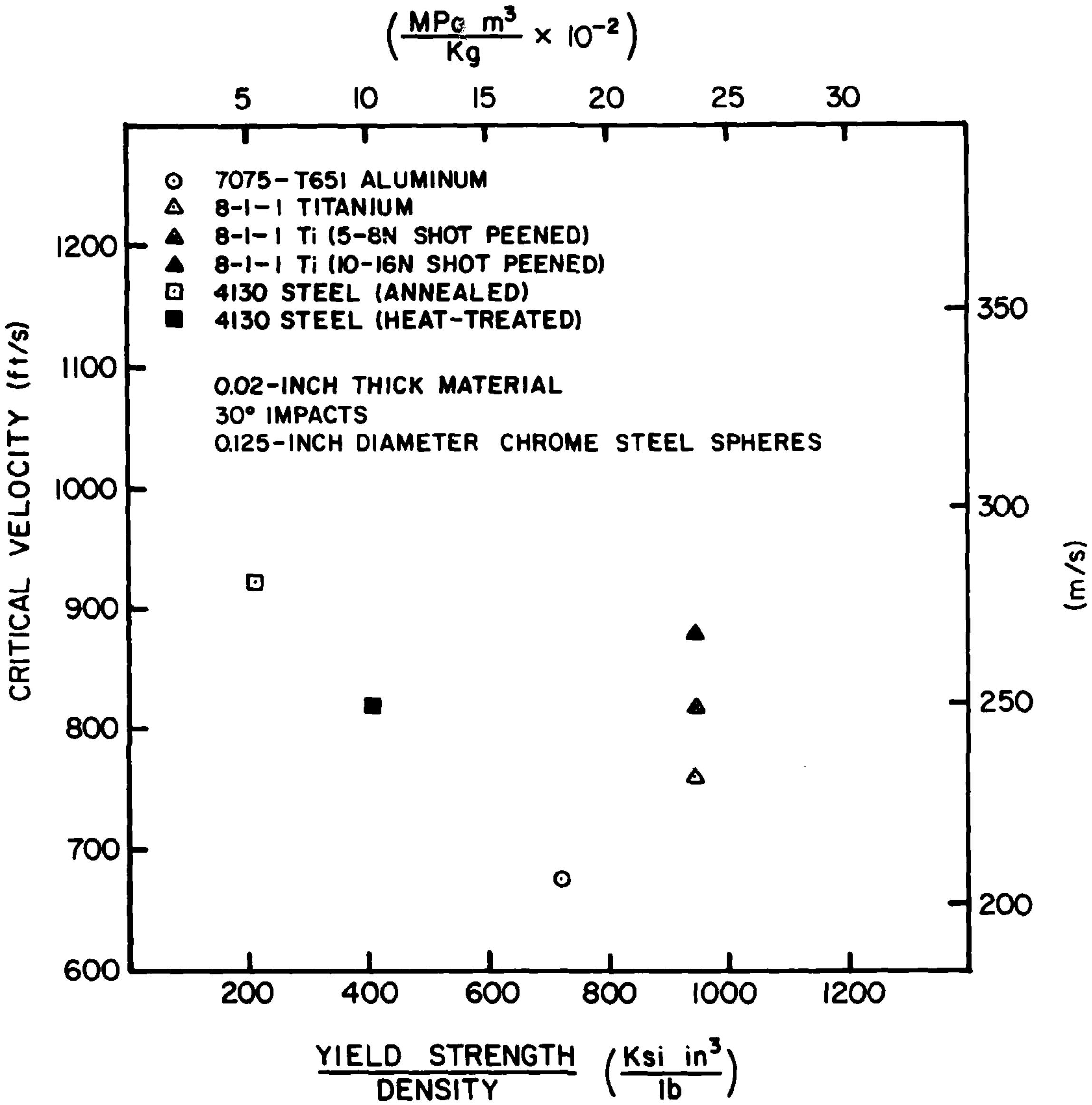

Figure 18. Critical Velocity versus Material Yield Strength/ Density Plot for All Materials.

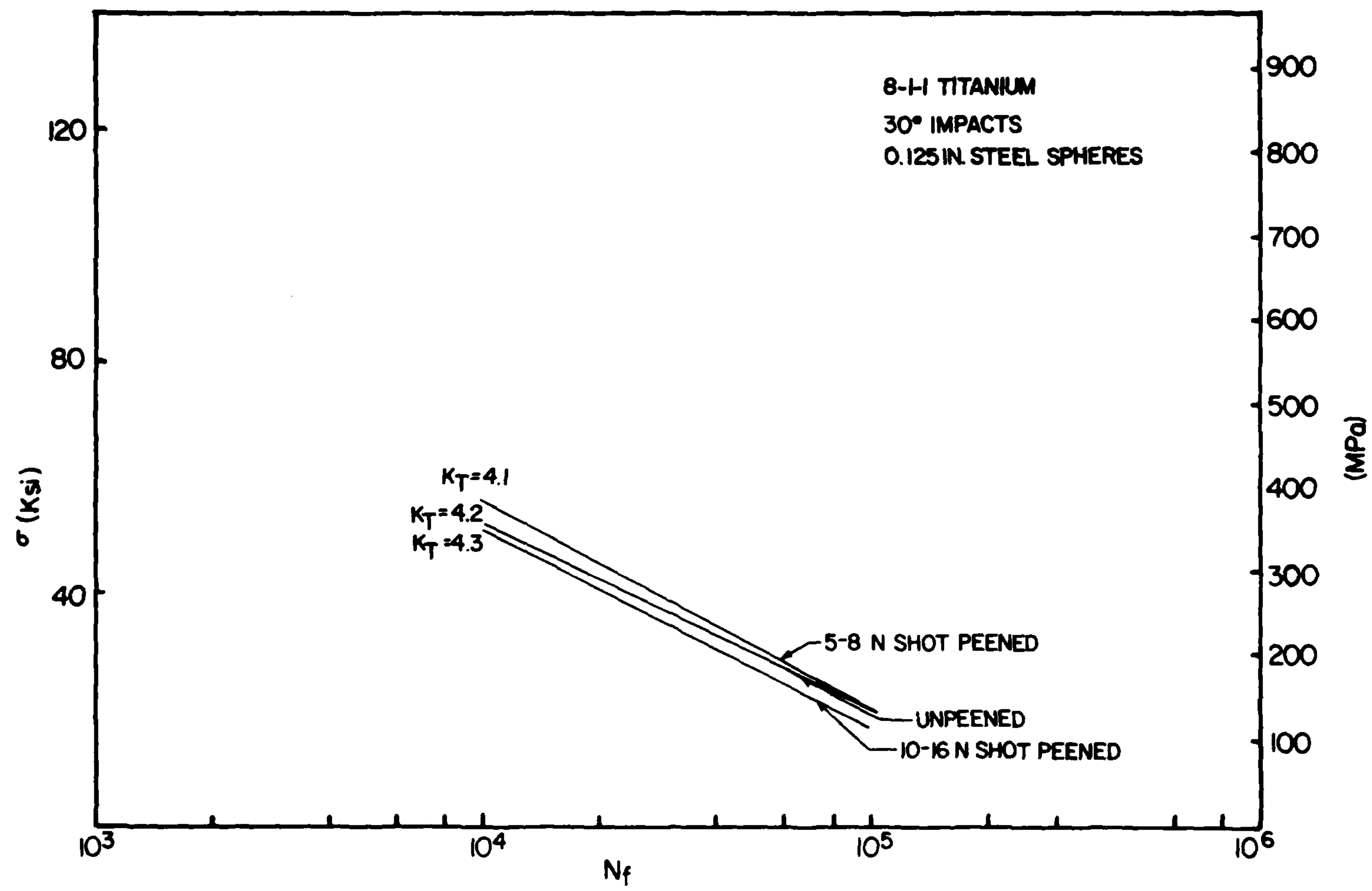

Figure 19. Fatigue Data Comparison Between Shot Peened and Unpeened Titanium Material. NOTE: Critical velocities are different.

(1) Effect of Incidence Angle on Critical Velocity

The effect of the incidence angle on the critical velocity is shown in Figure 20. Figure 20 gives a plot of the critical velocity versus the impact angle for the steel sphere impacts on the 8-1-1 titanium material. The data of Figure 20 shows that the angle of incidence has very little effect on the critical velocity.

The effect of the incidence angle on the damage received is shown in Figure 21. Figure 21 gives a plot of the average net-section stress (σ) versus the number of cycles of failure (N_f) for the various angles of incidence. Based on the results of this plot and Table 2, the curves tend to flatten out for the 7.5, 15 and 45 degree impacts compared to the 30 degree impacts. The slope for the 15 and 45 degree impacts is very similar. The equivalent stress concentration factors (K_T) were determined to be 3.6, 3.4, 4.2, and 4.1 for the 7.5, 15, 30, and 45 degree impacts, respectively. Thus, K_T increased appreciably between 15 and 30 degrees. The 30 degree impacts gave the highest K_T value for the various angles of incidence. One would expect the greatest damage for the 45 degree impacts and this difference may be attributed to the scatter in impacting the exact center of the leading edge repeatedly.

d. <u>Specimen Geometry</u>

The specimen geometrical parameter investigated in the testing was the leading edge thickness.

(1) Effect of Leading Edge Thickness on Critical Velocity

The effect of the leading edge thickness on the critical velocity is shown in Figure 22. Data for glass and sand particle impacts of Reference 1 are included in the figure. Figure 22 plots the critical velocity against the leading edge thickness of the titanium material for 30 degree impacts. All of the data were normalized using linear scaling

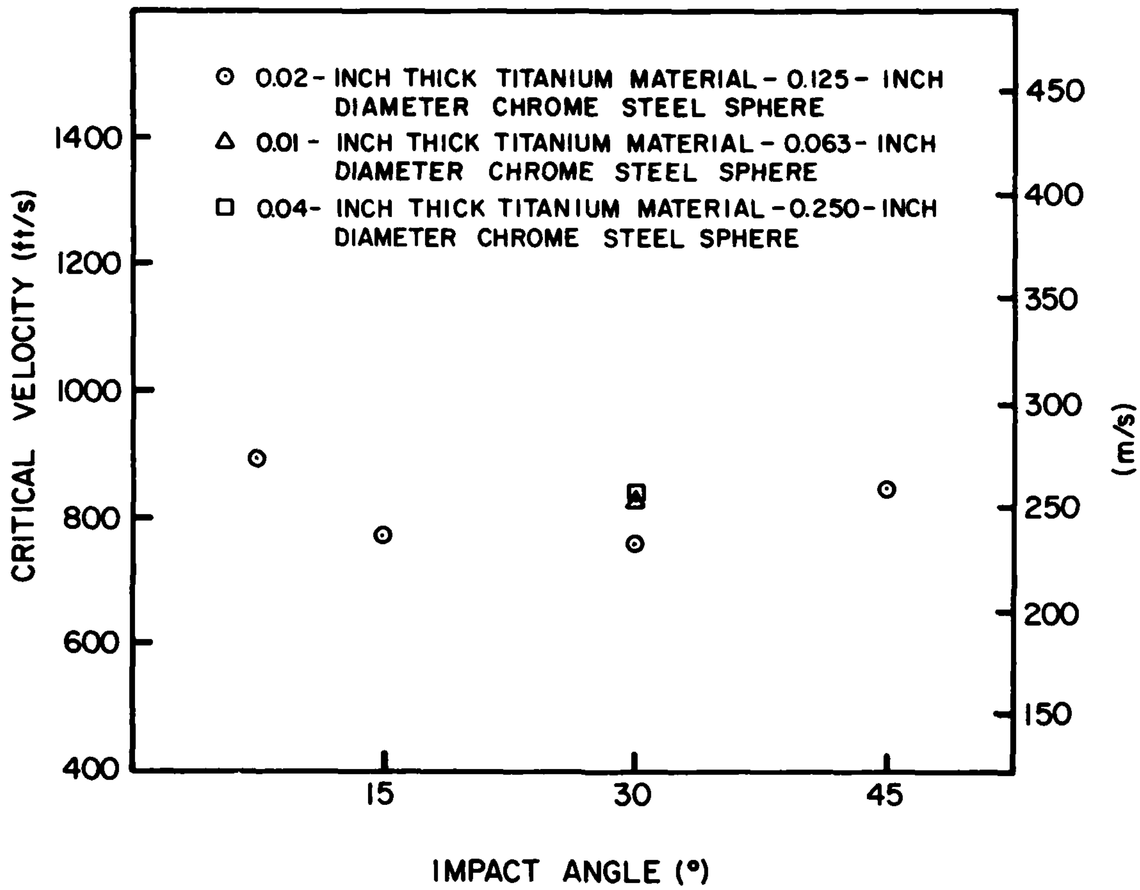

Figure 20. Critical Velocity versus Impact Angle Plot for Titanium Material.

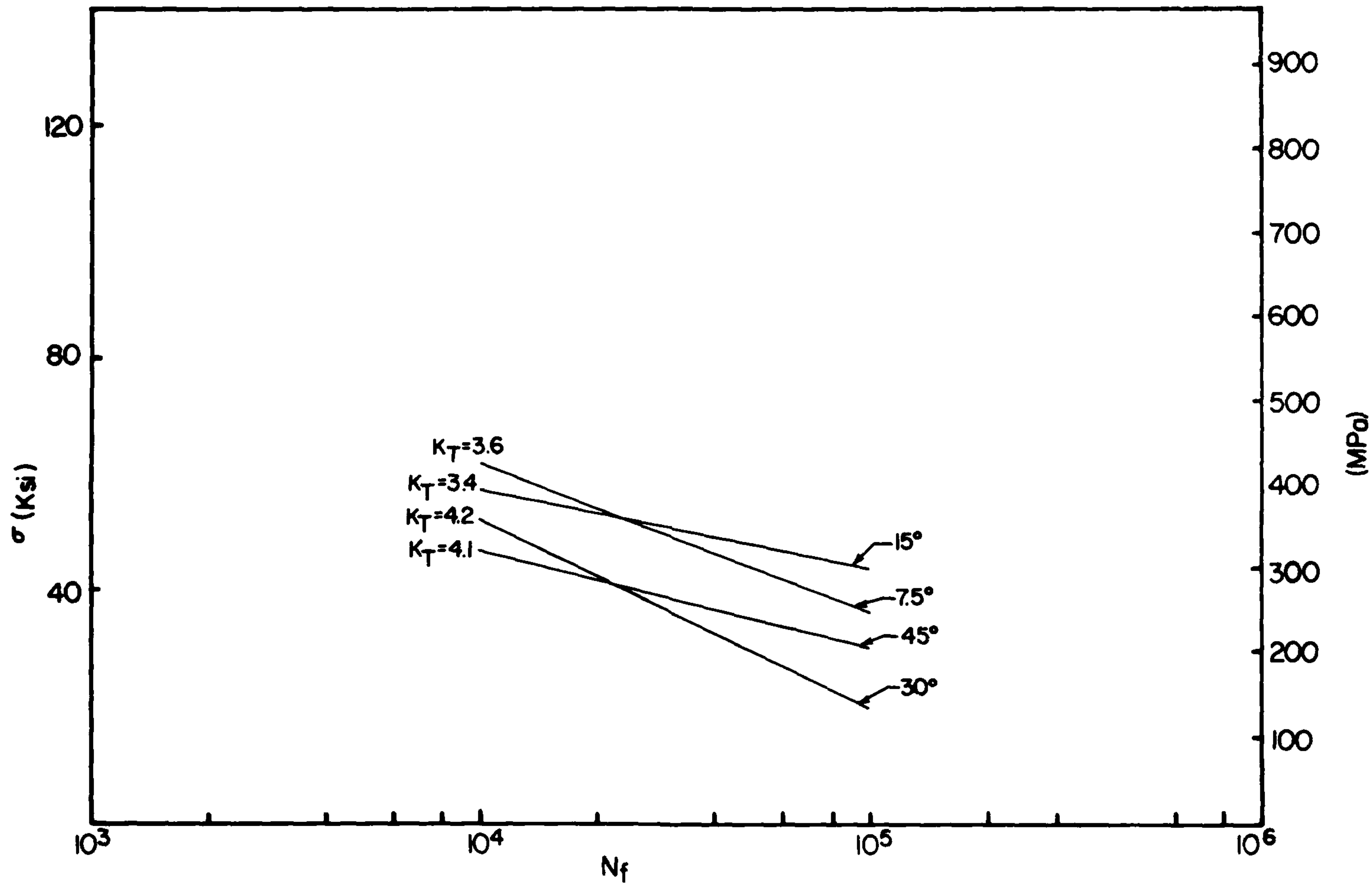

Figure 21. Fatigue Data Results for Various Angles of Incidence Impacts on Titanium Material.

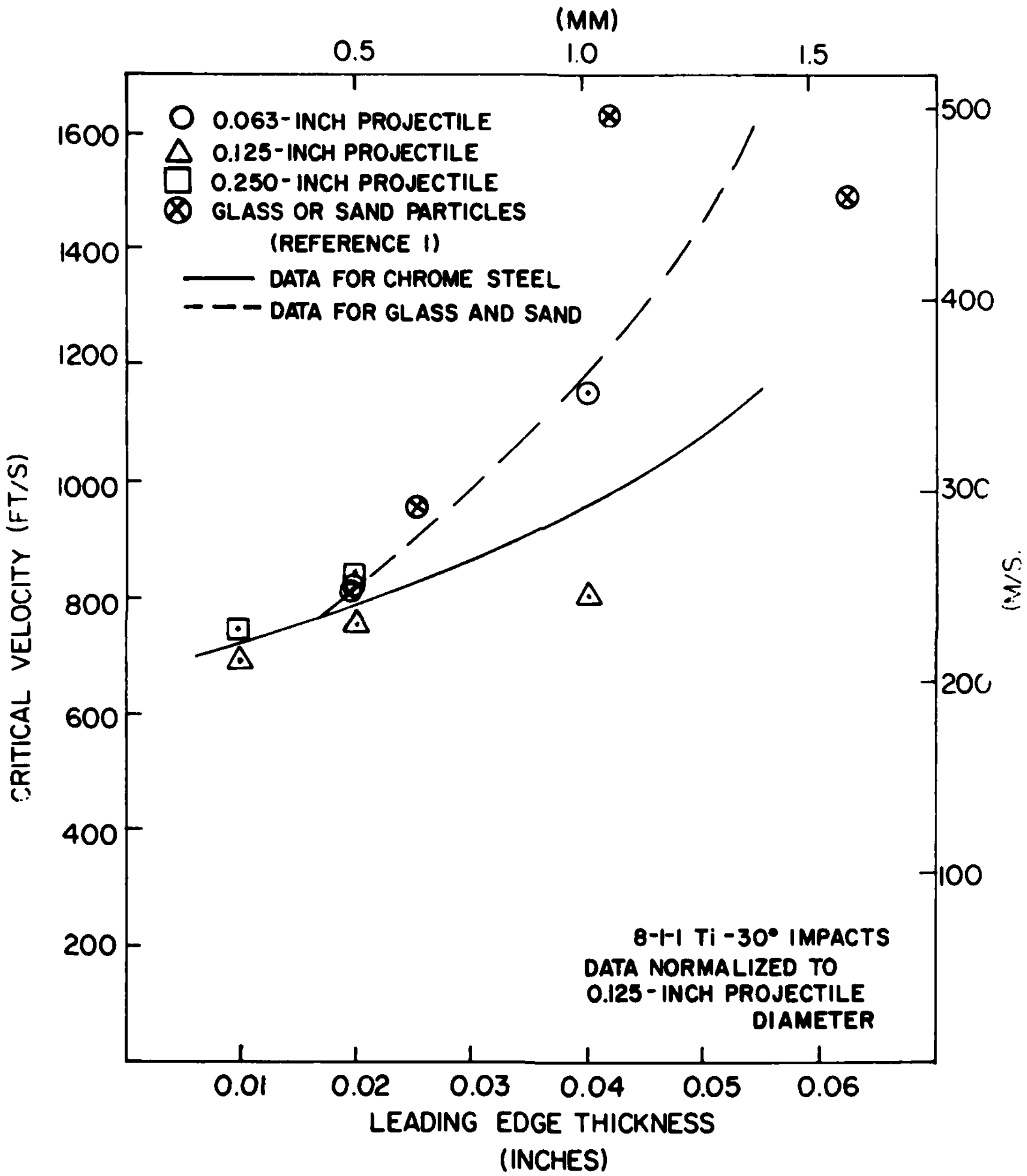

Figure 22. Critical Velocity versus Leading Edge Thickness Plot for Titanium Material.

to a 0.125 inch (3.18 mm) diameter projectile. The solid line presents the data for the chrome steel sphere and it shows a trend of increasing critical velocity as the leading edge thickness is increased as one would expect. The dashed line curve for the glass and sand particle impacts of Reference 1 shows the same trend except that it has a much greater slope than for the steel sphere impacts. This greater slope may be attributed to particle breakup which was experienced in the Reference 1 work for the glass particles.

The damage received for the various leading edge thicknesses is quantified in Figure 23. Figure 23 gives a plot of the average net-section stress (σ) against the number of cycles to failure. The equivalent stress concentration factors (K_T) for the 0.02 and 0.04 inch (0.254 and 0.508 mm) thick titanium specimens were determined to be 4.2 and 3.6, respectively for the 0.125 inch (3.18 mm) diameter steel sphere impacts at 30 degrees. For the larger 0.250 inch (6.35 mm) diameter steel sphere impacts at 30 degrees, the K_T values from Figure 10 and Table 2 were determined to be 4.1 and 4.9 for the 0.02 and 0.04 inch (0.254 and 0.508 mm) thick leading edge specimens. Thus, the trend for the 0.125 inch (3.18 mm) diameter projectile impacts was that the damage decreased as the leading edge thickness was increased. For the larger 0.250 inch (6.25 mm) projectile impacts, the trend was opposite that for the 0.125 inch (3.18 mm) projectile impacts. The trend for the larger projectile impacts was that the damage increased as the leading edge increased. This may be attributed to the much higher critical velocity required for the larger projectile impacts on the thicker leading edge. For the 0.04 inch (1.016 mm) thick specimens, the critical velocity was 802 ft/s (244 m/s) for the 0.125 inch (3.18 mm) diameter projectiles and 836 ft/s (255 m/s) for the 0.250 inch (6.35 mm) diameter spheres. For the 0.02 inch (3.18 mm) thick specimens, the critical velocity was 760 ft/s (232 m/s) for the 0.125 inch (3.18 mm) projectiles

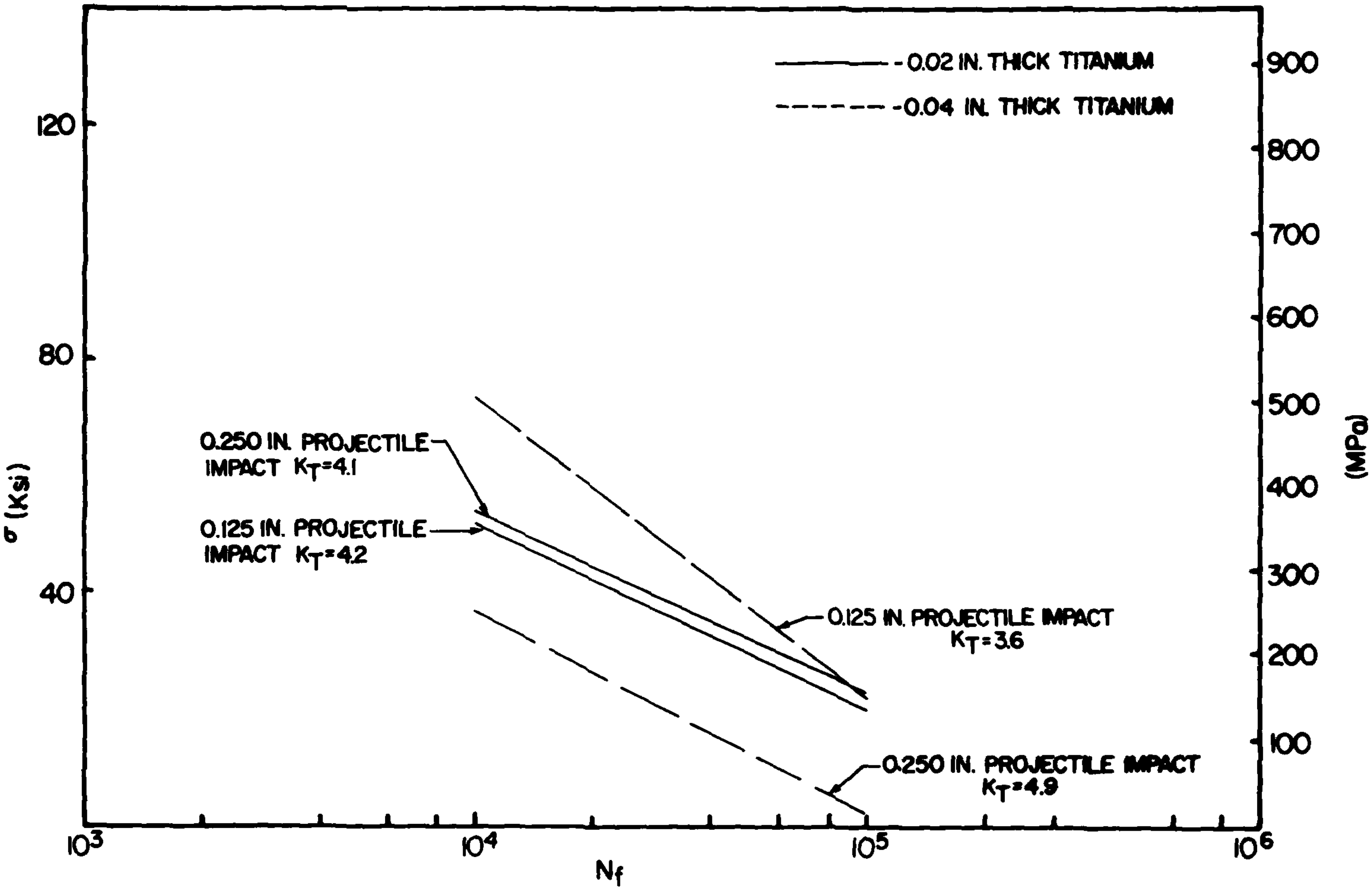

Figure 23. Fatigue Data Results for Various Leading Edge Thickness Impacted on Titanium Material.

and 745 ft/s (227 m/s) for the 0.250 inch (6.35 mm) projectiles. Note that the larger projectile impacts on the thicker targets required a higher critical velocity than for the smaller projectile impacts on the thicker targets. This is opposite of what one would expect; however, the mode of damage for the smaller projectile impacts was a nick with mass removal at the impact site while the damage mode for the larger projectile impacts was bulging with tearing at the impact site. The data for the 0.125 inch (3.18 mm) diameter sphere impacts on the 0.04 inch (1.016 mm) thick leading edge is tending to indicate that this projectile size may be too small for this leading edge thickness.

SECTION IV
SUMMARY AND CONCLUSIONS

Leading edge impact damage was studied by performing a series of hard particle impact tests on three materials and visually observing the damage. The materials investigated were 8-1-1 titanium, 4130 steel in the annealed and heat-treated conditions, and 7075-T651 aluminum. The concept of a critical velocity to quantitatively evaluate damage was investigated. Fatigue and residual tensile tests also were used as a measure of damage and the concept of an equivalent elastic stress concentration factor to characterize severity of damage was investigated. Fatigue and residual tensile tests also were used as a measure of damage and the concept of an equivalent elastic stress concentration factor to characterize severity of damage was investigated. Finally, geometric scaling was examined by using different leading edge thicknesses and various projectile sizes.

The conclusions for the various parameters investigated in the study are given in the following paragraphs.

1. CRITICAL VELOCITY

The study involved determining the critical velocity region for various material and test conditions where the damage was either in the form of bulging with tearing of the leading edge or nicks with mass removal at the impact site.

The aluminum sphere impacts on titanium material required the highest impact velocities to generate damage where tears or rips were received with bulging at the impact site. The aluminum spheres were not suitable for testing because they were observed to be substantially deforming plastically during the impact event; therefore chrome steel spheres were substituted for the aluminum spheres. This switch was made to avoid the uncertainty surrounding the effect of projectile deformation upon the damage inflicted on the test specimens.

For the steel sphere impacts using a projectile diameter of 0.125 inches (3.18 mm) and similar test conditions, the 4130 steel in the annealed condition had the highest critical velocity of 922 ft/s (281 m/s). The shot peened (10-16 N intensity titanium had the next highest critical velocity of 883 ft/s (269 m/s). The shot peened titanium (5-8 N intensity) and 4130 steel in the heat-treated condition had a similar critical velocity of 819 ft/s (250 m/s). The basic titanium material had a critical velocity of 760 ft/s (227 m/s) while the alumunum material had the lowest critical velocity of 675 ft/s (206 m/s).

2. FATIGUE

Small sphere particle leading edge impacts do cause damage and have a detrimental effect on the fatigue strength of the target material. The technique used to characterize the impact damage was to use fatigue tests to determine an equivalent elastic stress concentration factor for the severity of damage using machined notch specimens which were fatigue tested to provide the baseline data. This technique was developed in a previous study (Reference 1). The extent of damage from a range of particle sizes on the various materials was evaluated quantitatively by performing a series of fatigue tests at various load levels on specimens impacted under nominally identical conditions. The data demonstrated reasonable reproducibility and the extent of a particular type of damage was categorized in terms of an equivalent elastic stress concentration factor (K_T) using notch fatigue data for the various materials. For similar test conditions, the 4130 steel in the annealed condition had the lowest K_T of 1.4 followed by the heat-treated material with a K_T of 2.1. The basic and shot peened titanium material had a similar K_T value of about 4.2. Damage for the aluminum material was substantial; therefore, the tensile test was substituted for the fatigue test and its residual tensile strength was 77.4 ksi (533.3 MPa).

Based on this information, the 4130 steel was less sensitive to fatigue degredation than the other materials.

3. SCALING

The concept of geometric scaling was investigated by performing a series of impact tests using different leading edge thicknesses of titanium and different projectile sizes. Observation of the type of damage, the damage measurements, and the fatigue tests appeared to validate the scaling concept. It was demonstrated that the tear lengths were high as much as 15 percent for the larger projectile impacts for linear scaling to be applicable. For damage in the form of a nick, the width and depth damage for the larger projectile impacts was low 6 percent and 25 percent respectively for the linear scaling. Also, the K_T values for the larger projectile impacts determined from the fatigue tests were high about 17 percent for linear scaling to be applicable.

A plot of critical velocity versus particle size (in relation to leading edge thickness) also appeared to validate the scaling concepts. Use of scaling allows one to consider d/t (projectile diameter/leading edge thickness) as a useful impact parameter. The data showed that the critical velocity increases dramatically when $d/t < 4$. Considering the amount of scatter in the data due to the difficulty in hitting the leading edge at the same central location in every impact tests, the scaling law seemed to work quite well over the ranges investigated.

4. PROJECTILE DENSITY

The effect of projectile density was considerable for critical velocity determination. The more dense projectiles cause greater damage. The aluminum spheres required a much higher velocity to obtain critical damage on the specimens than for the chrome steel spheres. As indicated earlier, the steel spheres were substituted for the aluminum spheres when the aluminum spheres were observed to be plastically deforming during the impact event.

5. BLADE MATERIAL PARAMETERS

No correlation could be established between the critical velocity and the material density, modulus of elasticity, or yield strength.

An attempt was made to establish some correlation by plotting the critical velocity versus the yield strength divided by the material density. Again, the plot showed that no correlation could be established.

6. ANGLE OF INCIDENCE

The effect of angle of incidence on the critical velocity was examined very briefly. Within the range of projectile and target dimensions investigated, the change in the critical velocity as a function of the impact angle was minor.

Specimen damage is shown in Figure 21, both as failure stress for various numbers of cycles and as K_T values. Damage increased as the impact angle increased from 15 to 45 degrees. However, no consistent ranking between 7.5 and 15 degrees or 30 and 45 degrees was possible.

7. LEADING EDGE THICKNESS

As the leading edge thickness was increased, the critical velocity also increased. This is what would be expected.

REFERENCES

1. Nicholas, Dr. T., Barber, Dr. J., and Bertke, R. S., "Impact Damage on Titanium Leading Edges from Small Hard Objects", Technical Report AFML-TR-78-173, November 1978.

2. Peterson, R. E., Stress Concentration Design Factors, John Wiley and Sons, Inc., Chapman and Hall, LTD., 1953.

APPENDIX A

PHOTOGRAPHS AND RESULTS OF DAMAGE

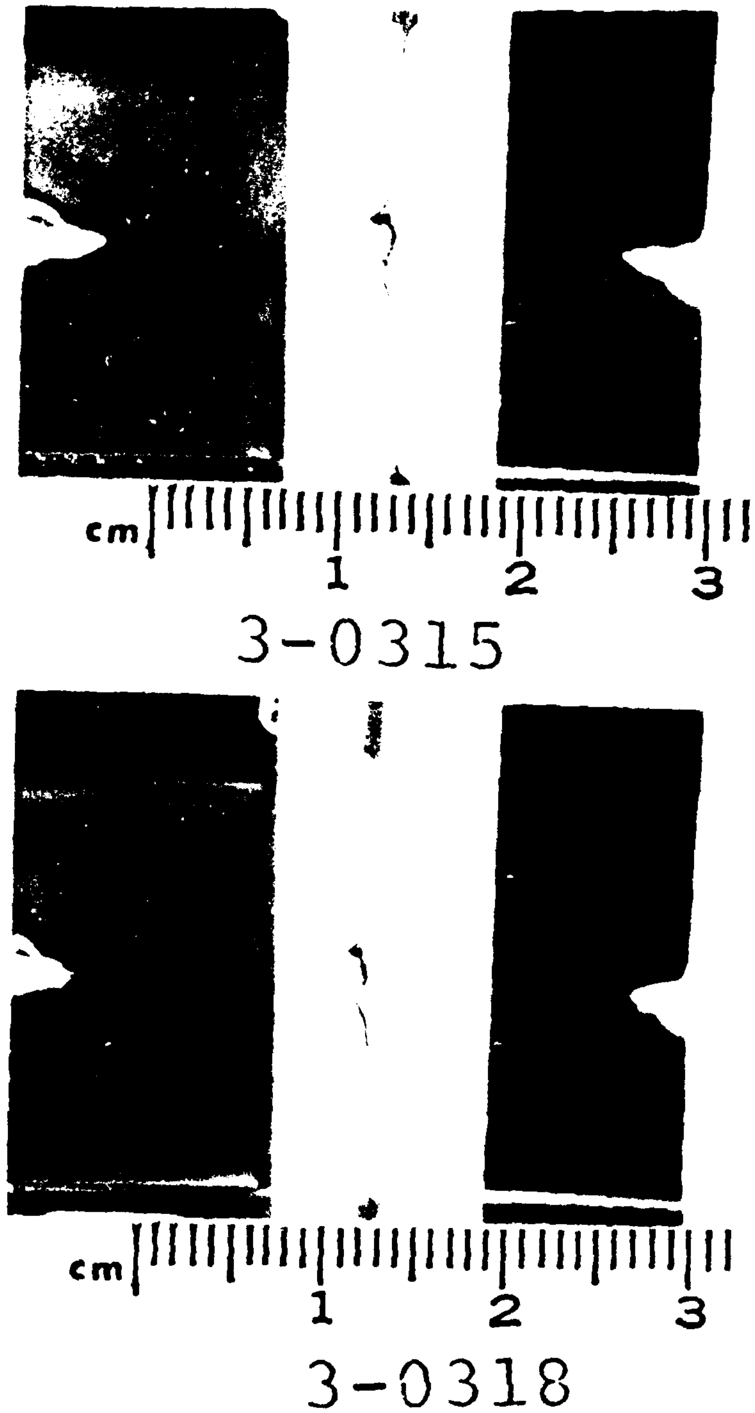

Figure A.1. Typical Damage on 0.254 mm Thick Titanium Due to 1.60 mm Diameter Aluminum Sphere Impact at 30°.

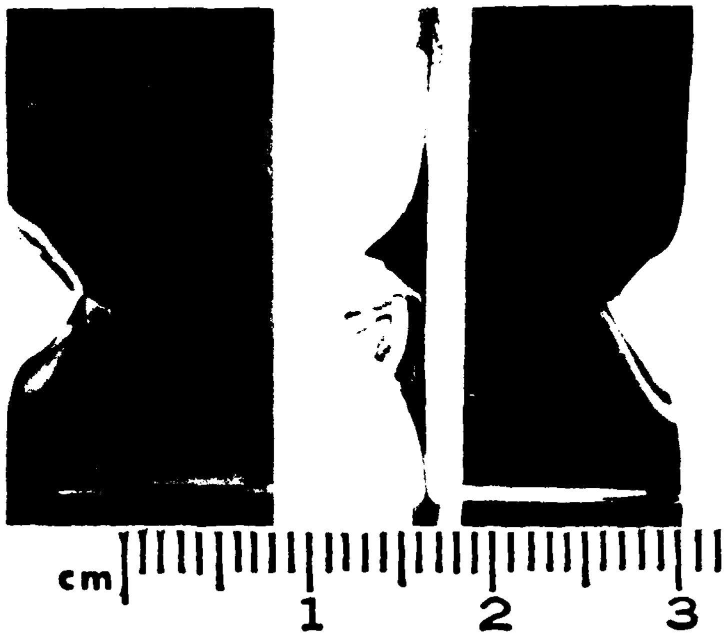

3-0307

3-0314

Figure A.2. Typical Damage on 0.254 mm Thick Titanium Due to 3.18 mm Diameter Aluminum Sphere Impact at 30°.

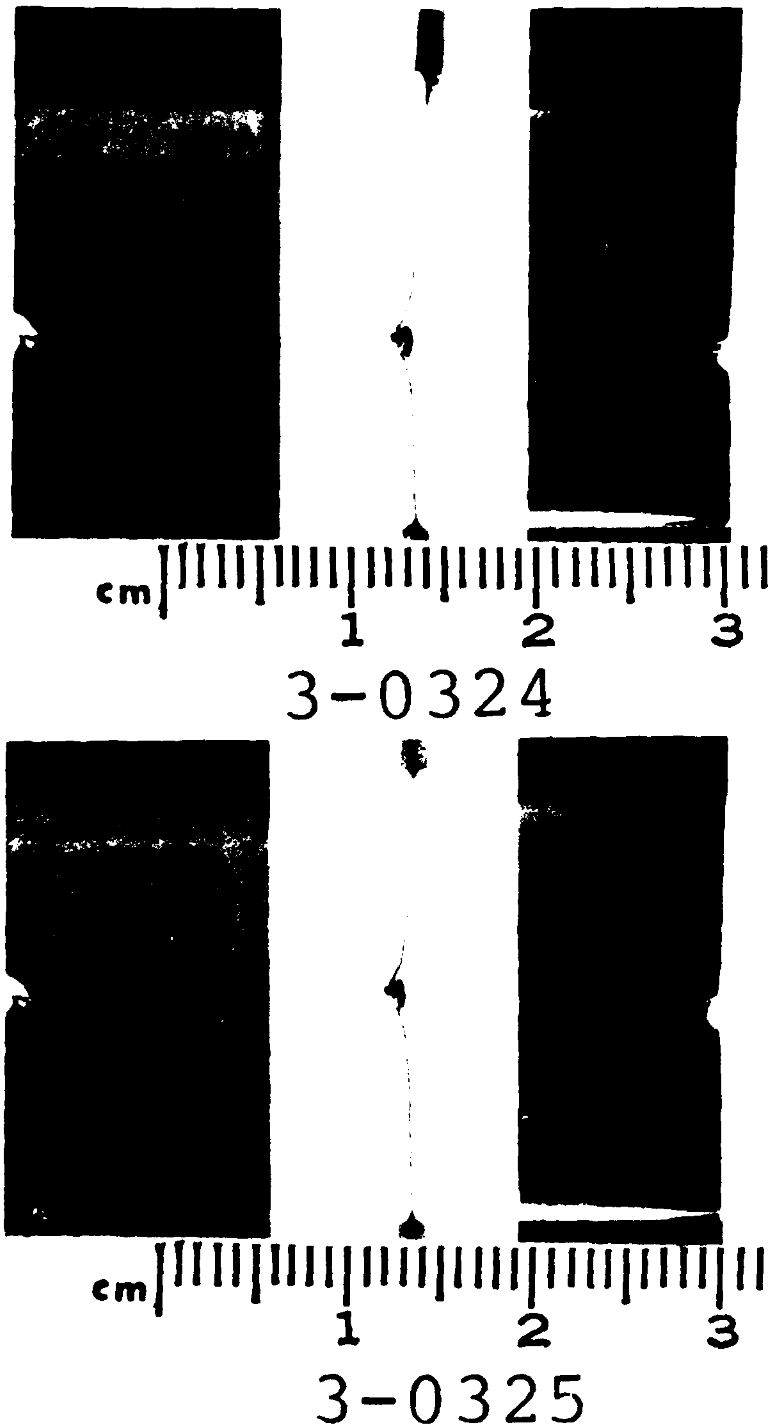

Figure A.3. Typical Damage on 0.254 mm Thick Titanium Due to 1.60 mm Diameter Chrome Steel Sphere Impact at 30°.

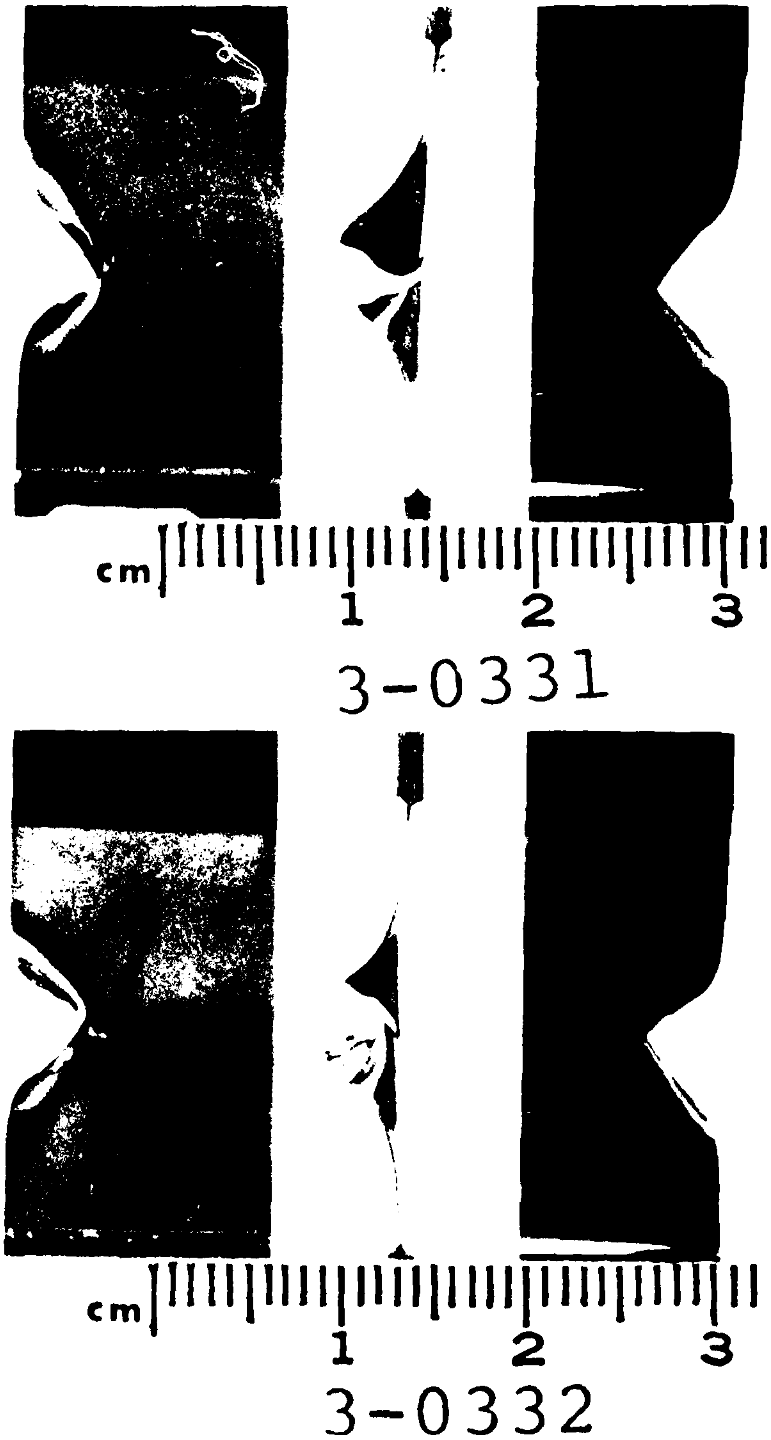

Figure A.4. Typical Damage on 0.254 mm Thick Titanium Due to 3.18 mm Diameter Chrome Steel Sphere Impact at 30°.

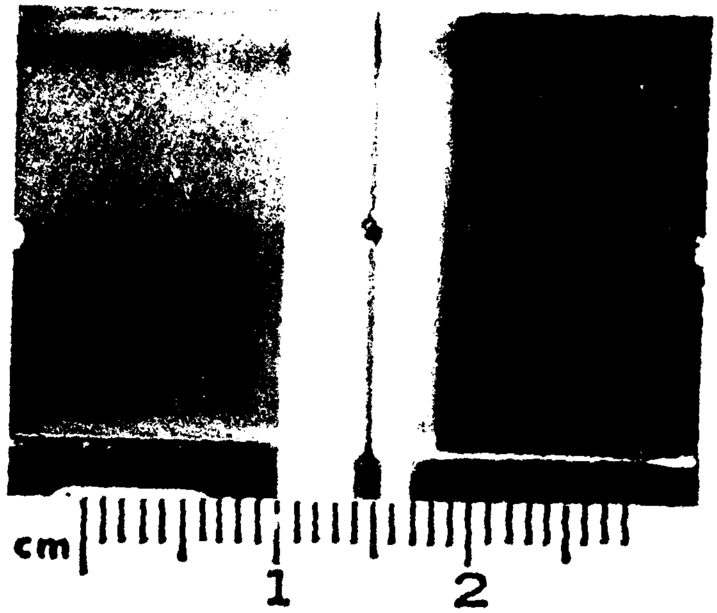

3-0345

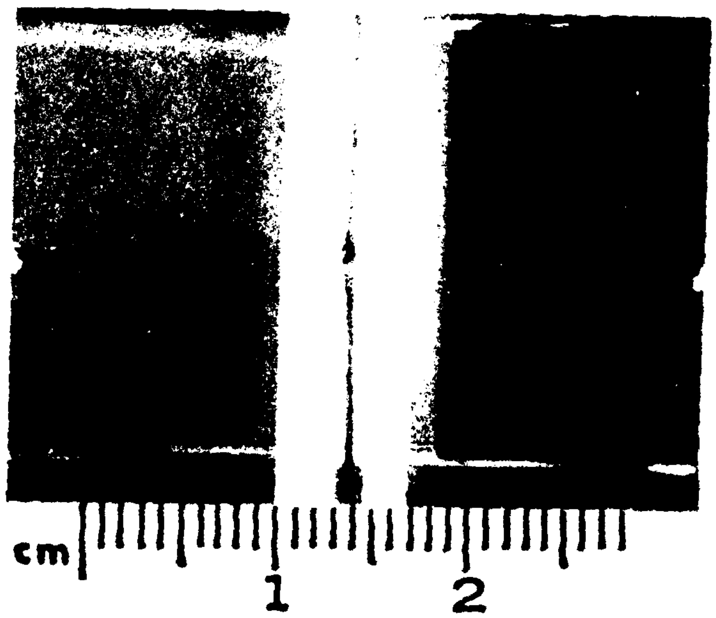

3-0346

Figure A.5. Typical Damage on 0.508 mm Thick Titanium Due to 1.60 mm Diameter Chrome Steel Sphere Impact at 30°.

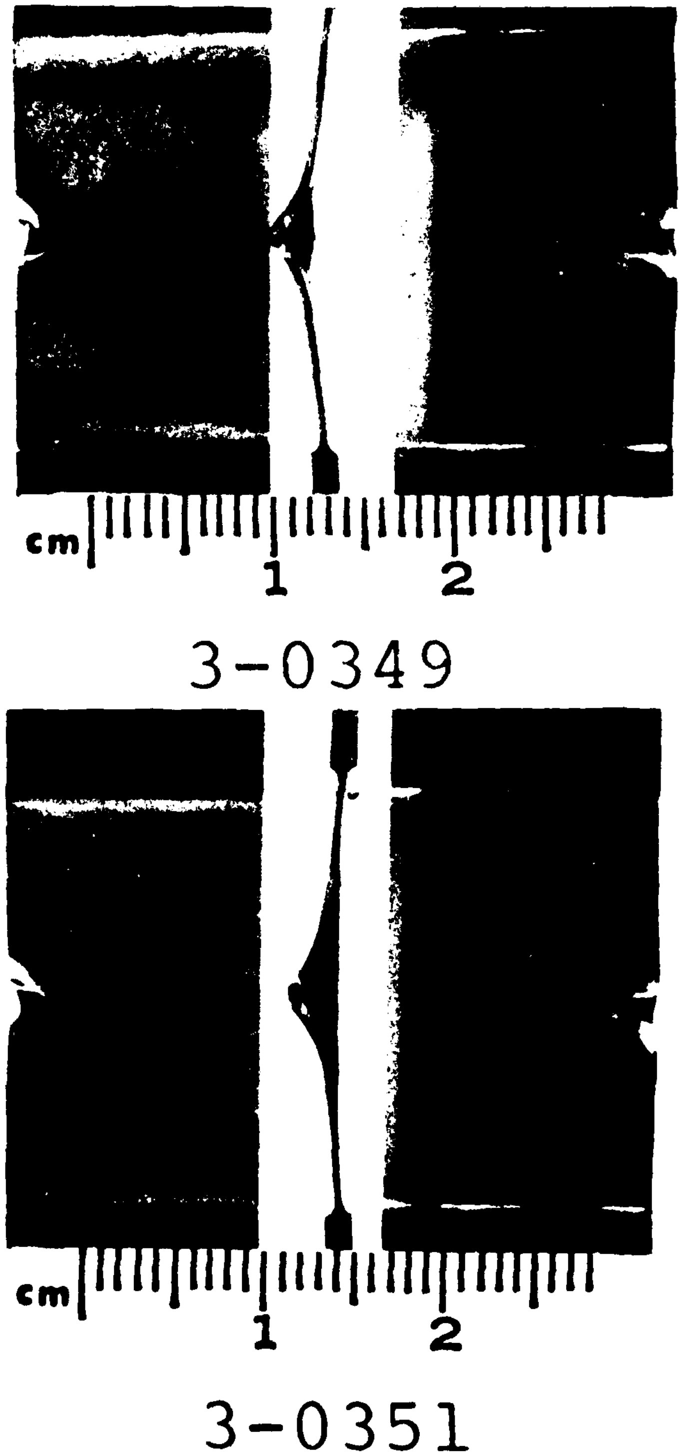

Figure A.6. Typical Damage on 0.508 mm Thick Titanium Due to 3.18 mm Diameter Chrome Steel Sphere Impact at 30°.

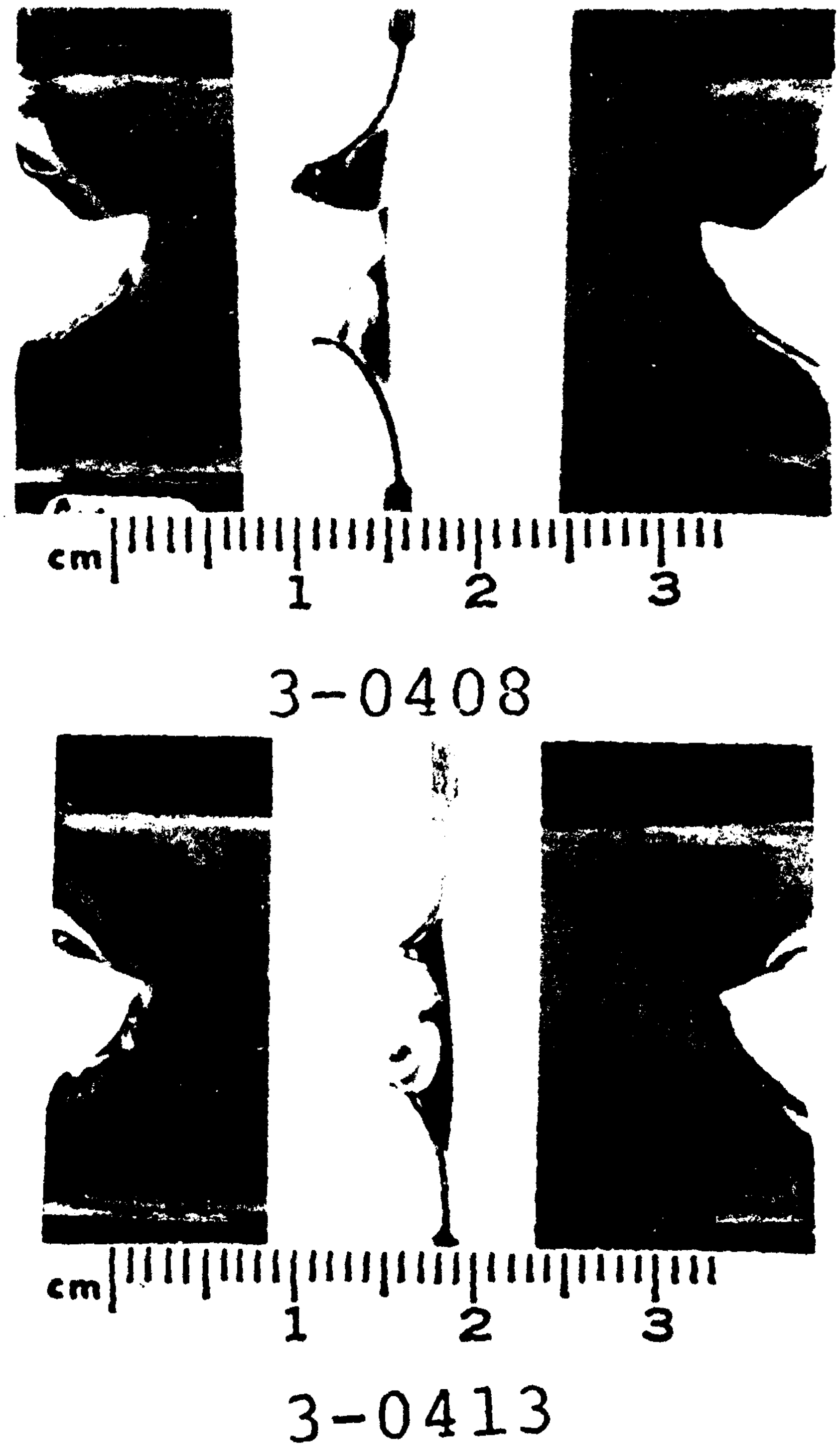

Figure A.7. Typical Damage on 0.508 mm Thick Titanium Due to 6.35 mm Diameter Chrome Steel Sphere Impact at 30°.

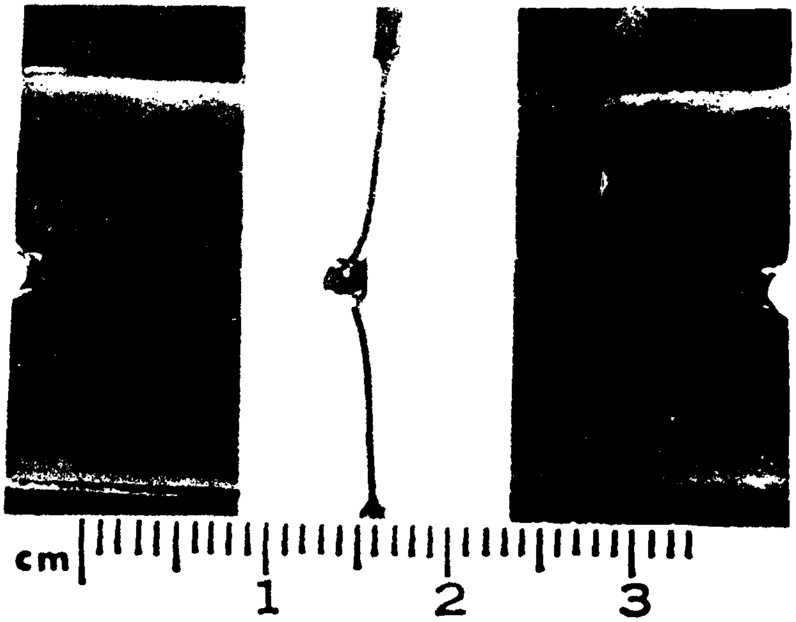

3-0423

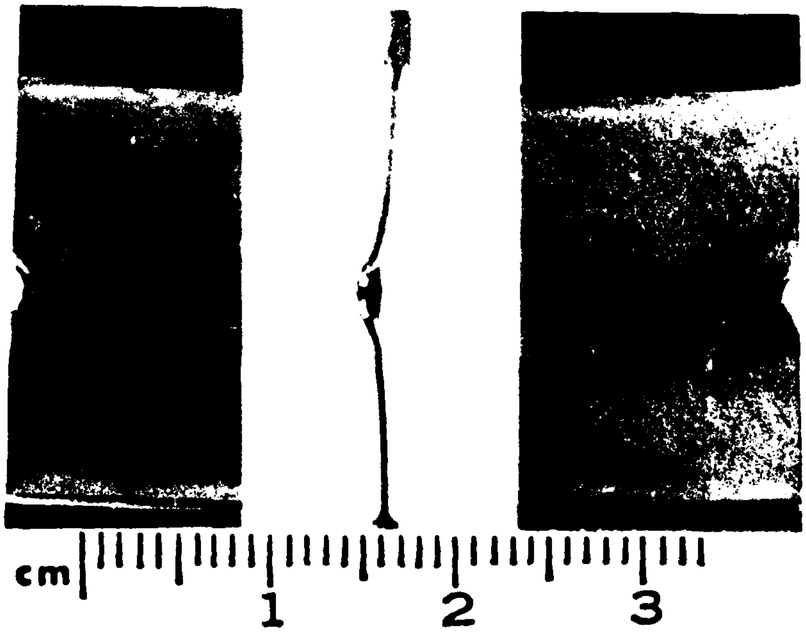

3-0424

Figure A.8. Typical Damage on 0.508 mm Thick Titanium Due to 3.18 mm Diameter Chrome Steel Sphere Impact at 7.5°.

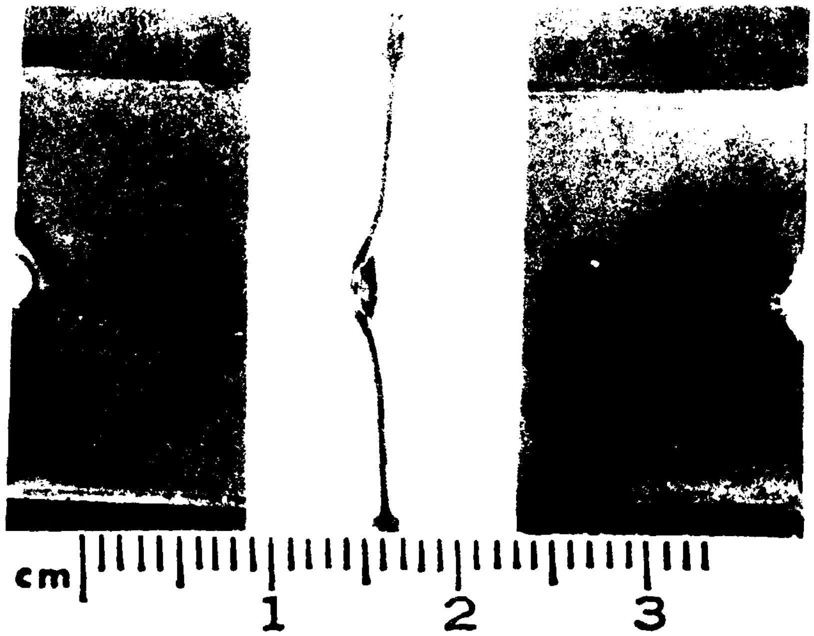

3-0435

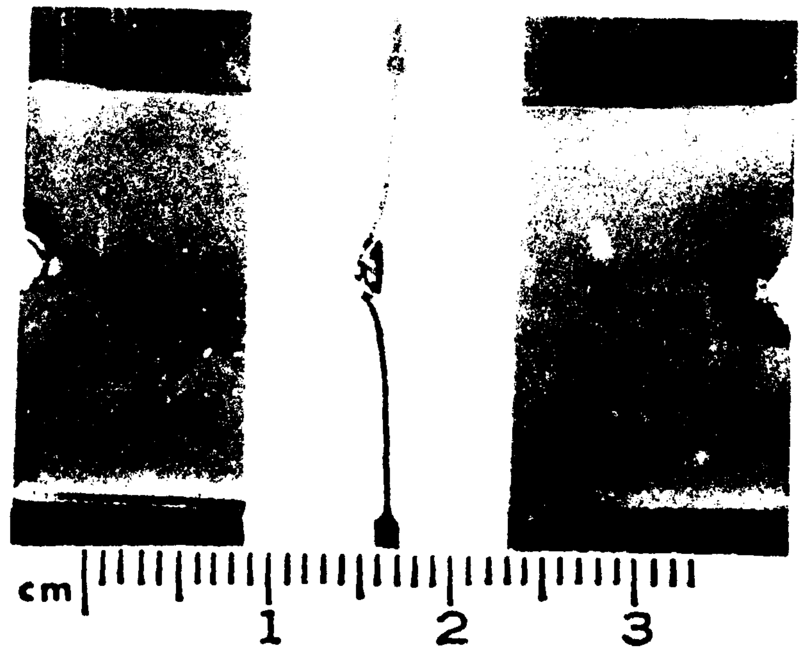

3-0436

Figure A.9. Typical Damage on 0.508 mm Thick Titanium Due to 3.18 mm Diameter Chrome Steel Sphere Impact at 15°.

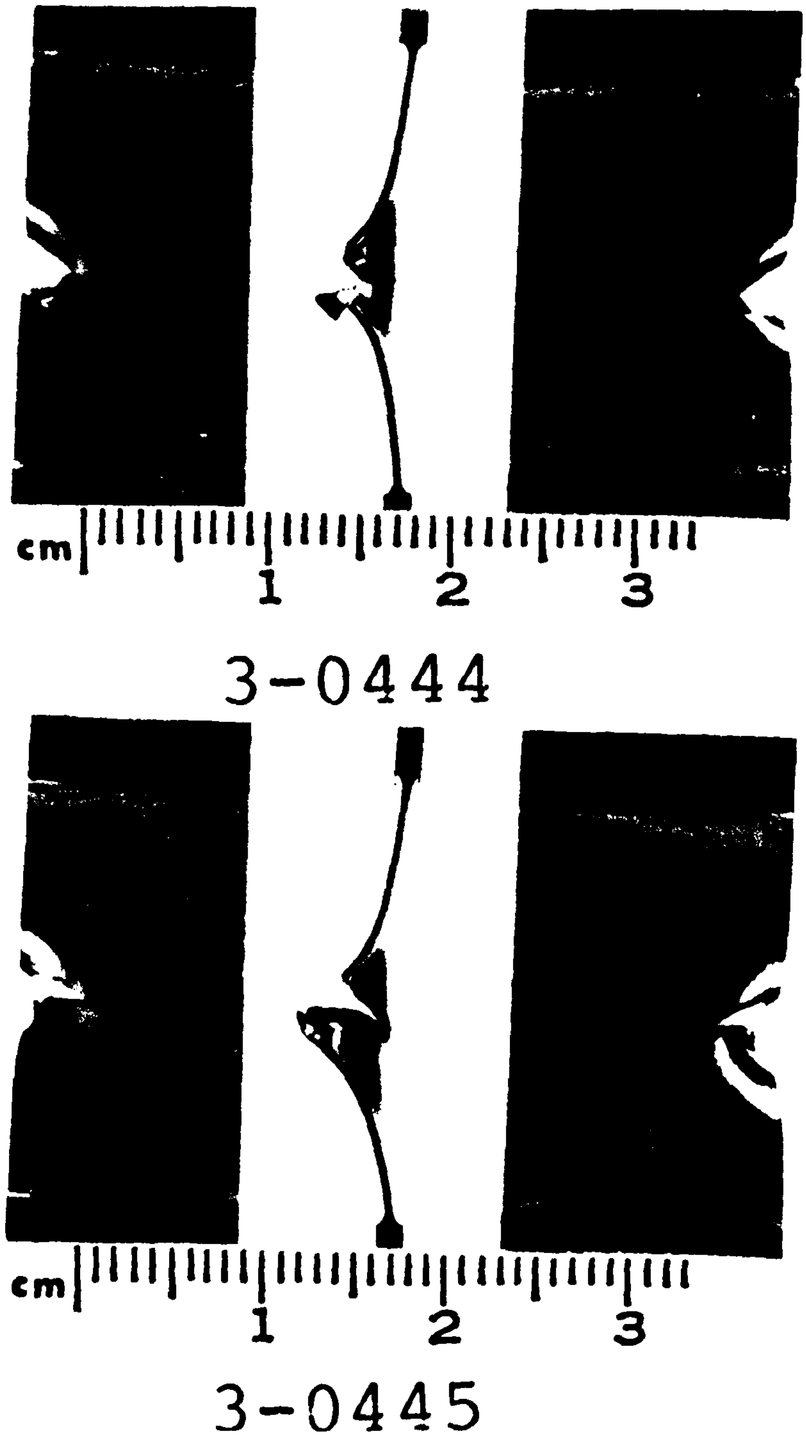

Figure A.10. Typical Damage on 0.508 mm Thick Titanium Due to 3.18 mm Diameter Chrome Steel Sphere Impact at 45°.

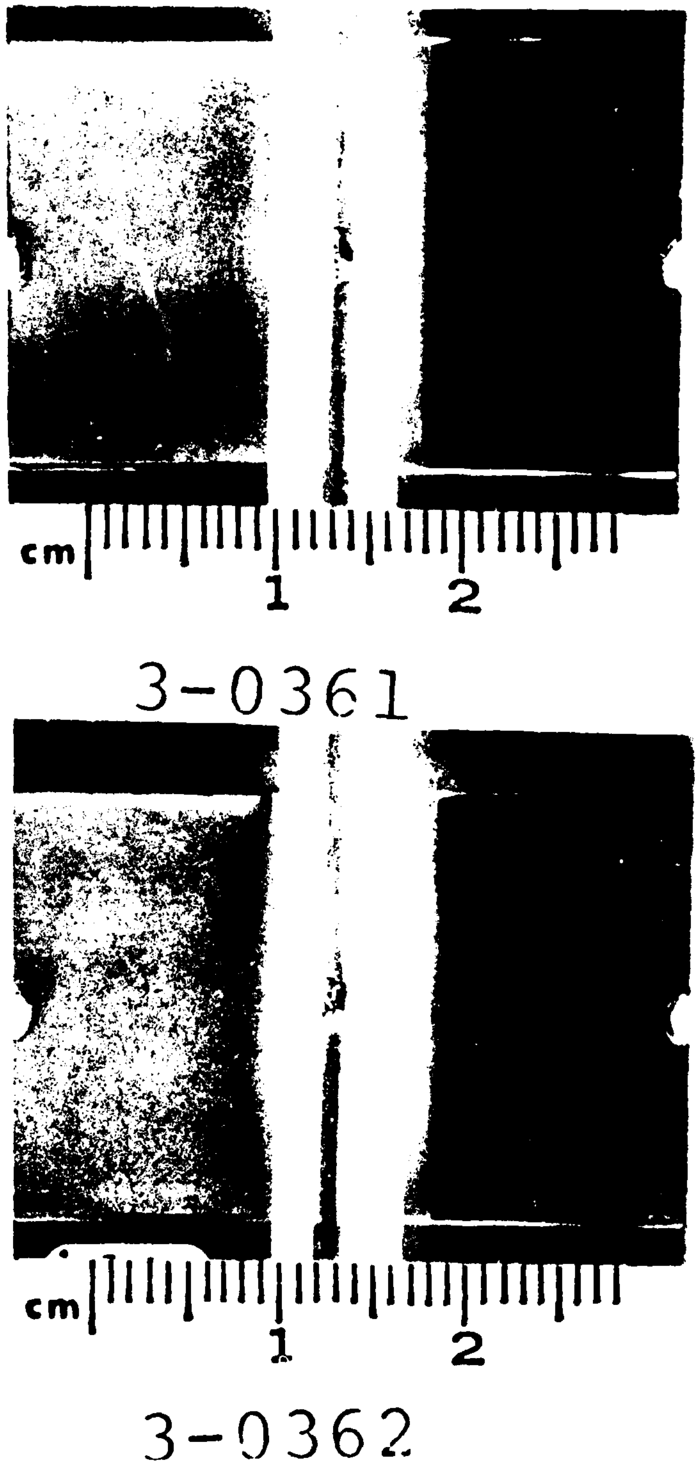

Figure A.11. Typical Damage on 1.016 mm Thick Titanium Due to 3.18 mm Diameter Chrome Steel Sphere Impact at 30°.

3-0375

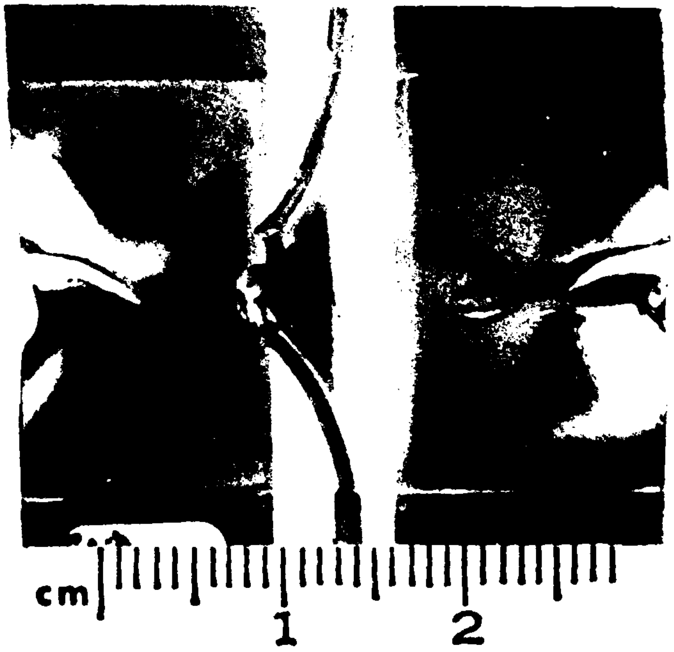

3-0376

Figure A.12. Typical Damage on 1.016 mm Thick Titanium Due to 6.35 mm Diameter Chrome Steel Sphere Impact at 30°.

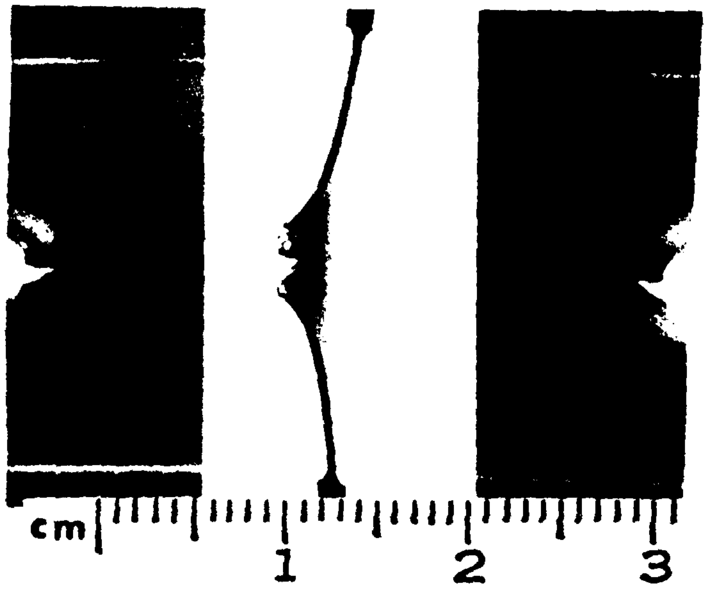

3-0525

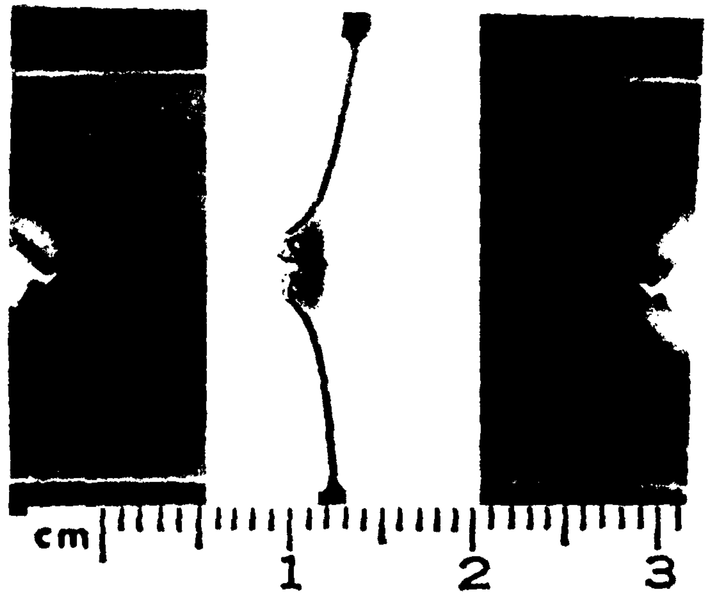

5-0526

Figure A.13. Typical Damage on 0.508 mm Thick (5-8N Shot Peened) Titanium Due to 3.18 mm Diameter Chrome Steel Sphere Impact at 30°.

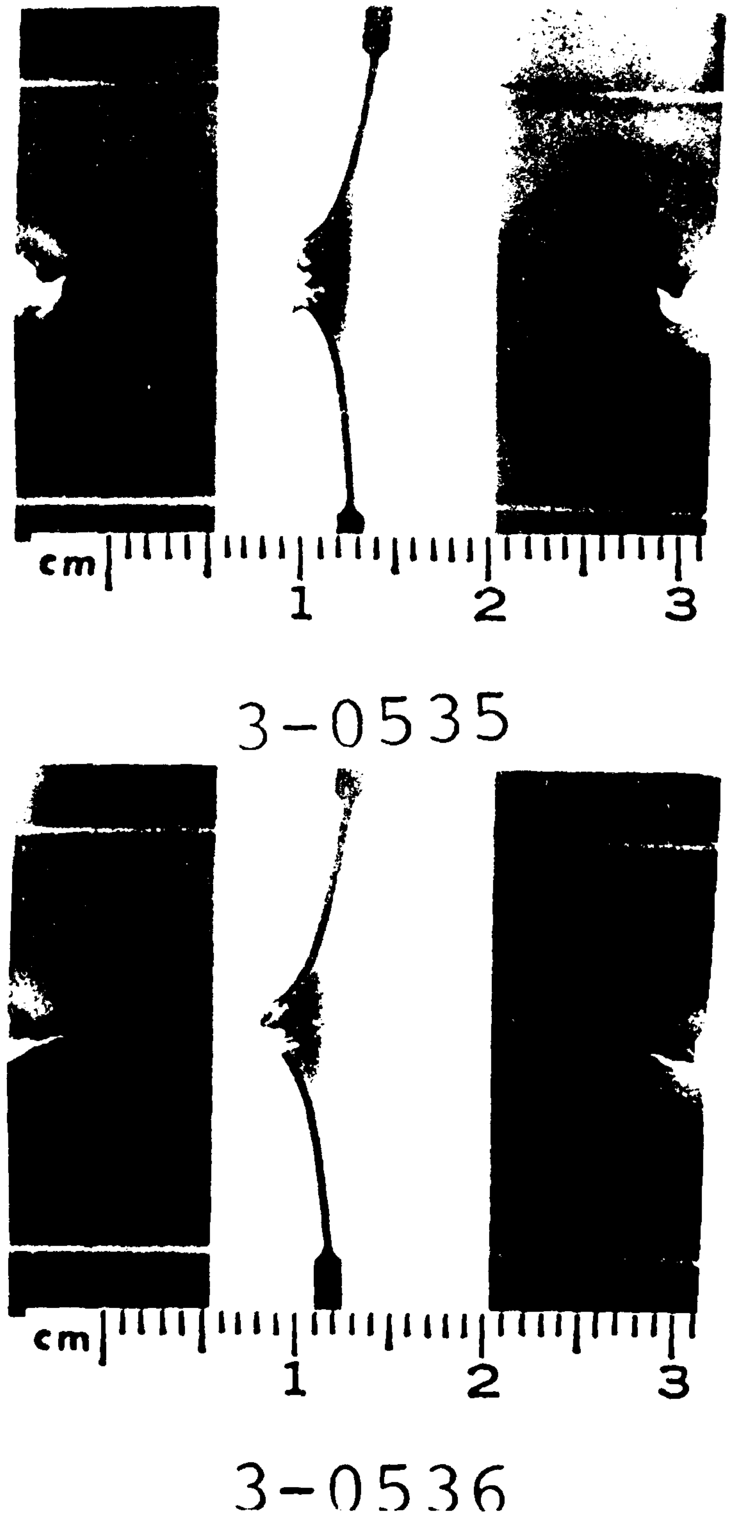

Figure A.14. Typical Damage on 0.508 mm Thick (10-16N Shot Peened) Titanium Due to 3.18 mm Diameter Chrome Steel Sphere Impact at 30°.

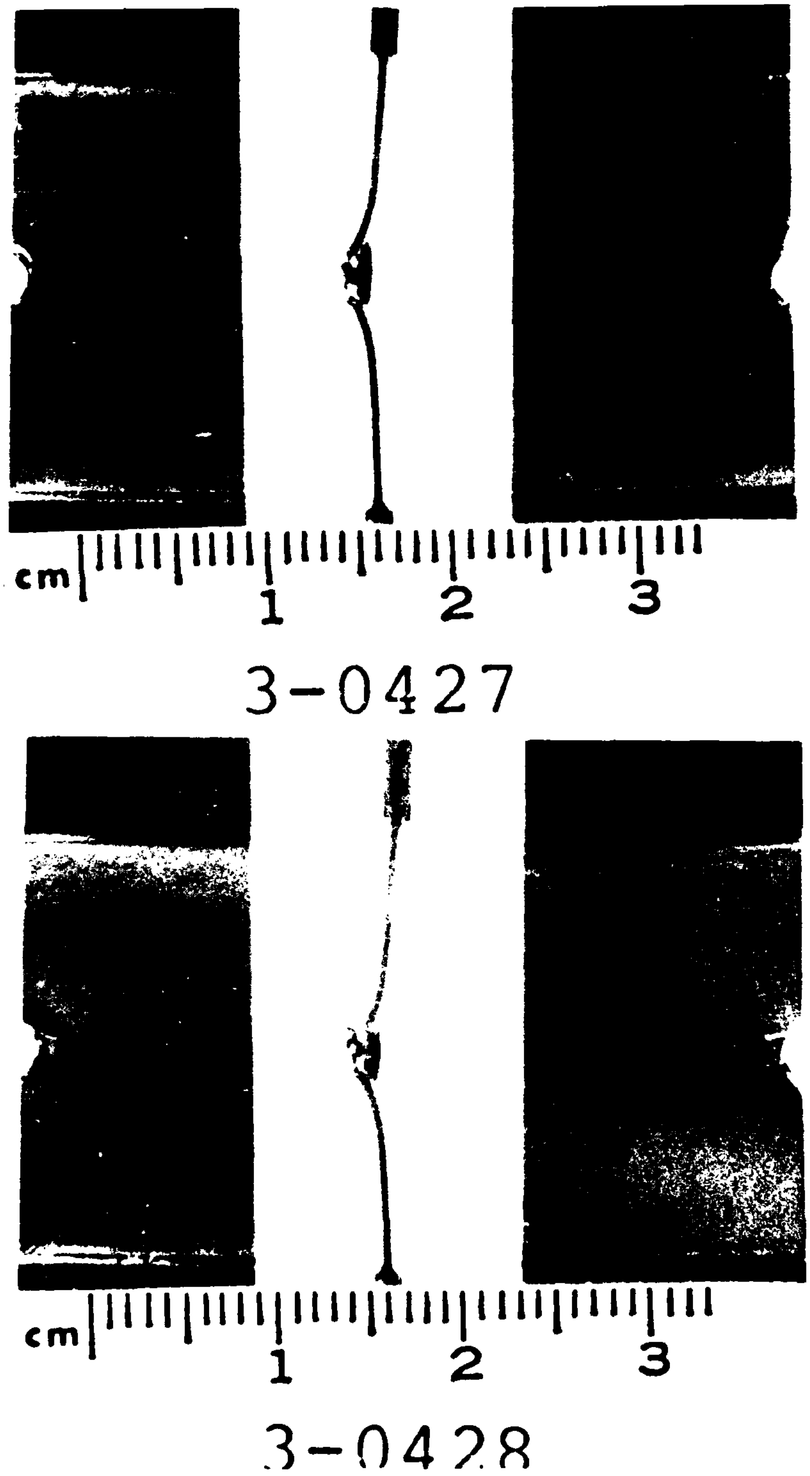

Figure A.15. Typical Damage on 0.508 mm Thick Steel in Annealed Condition Due to 3.18 mm Diameter Chrome Steel Sphere Impact at 30°.

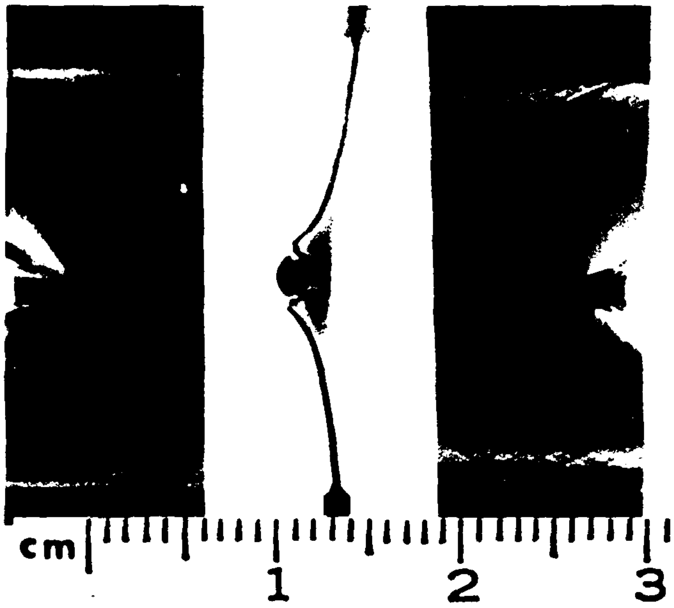

3-0511

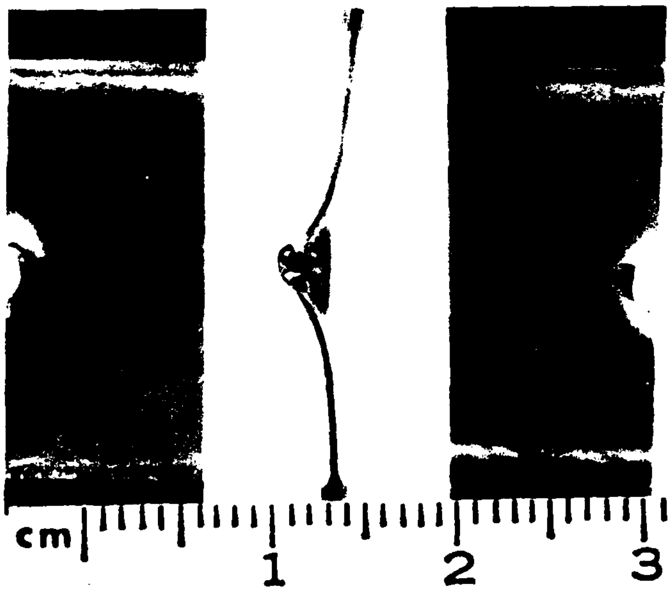

3-0512

Figure A.16. Typical Damage on 0.508 mm Thick Steel in Heat-Treated Condition Due to 3.18 mm Diameter Chrome Steel Sphere Impact at 30°.

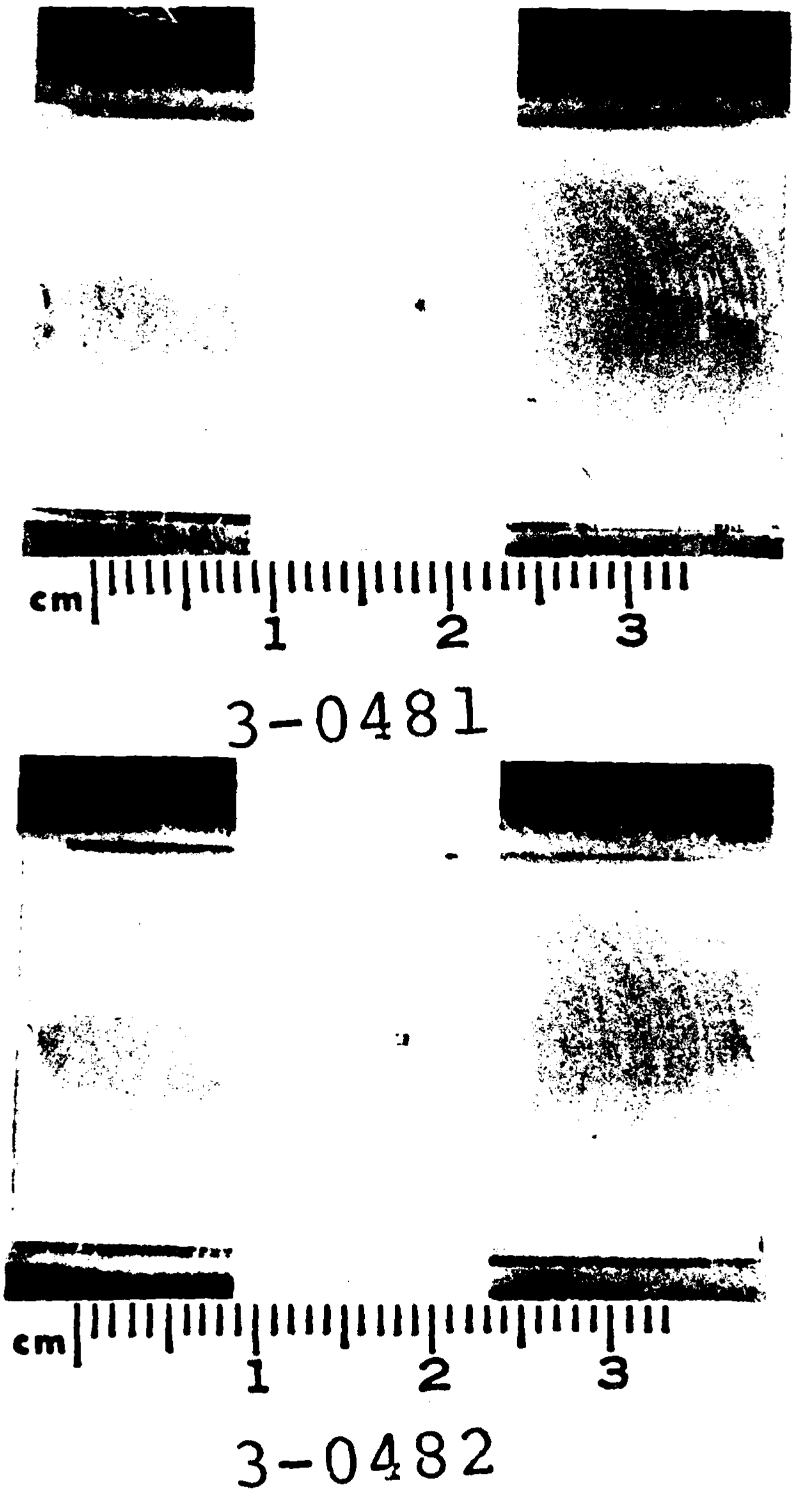

Figure A.17. Typical Damage on 0.508 mm Thick Aluminum Due to 1.60 mm Diameter Chrome Steel Sphere Impact at 30°.

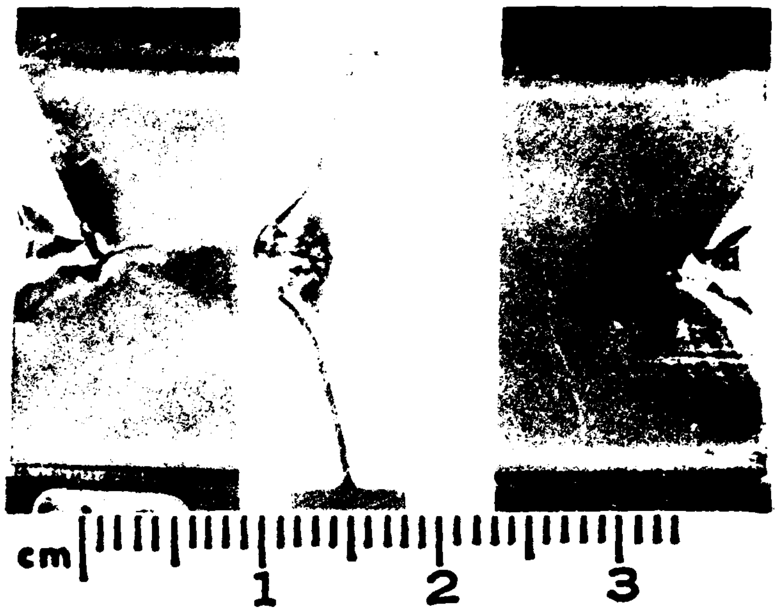

3-0461

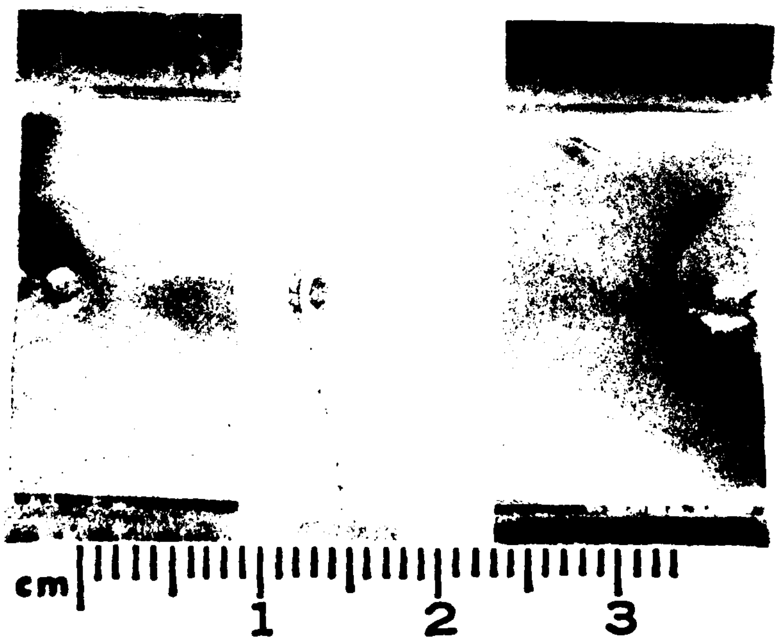

3-0462

Figure A.18. Typical Damage on 0.508 mm Thick Aluminum Due to 3.18 mm Diameter Chrome Steel Sphere Impact at 30°.

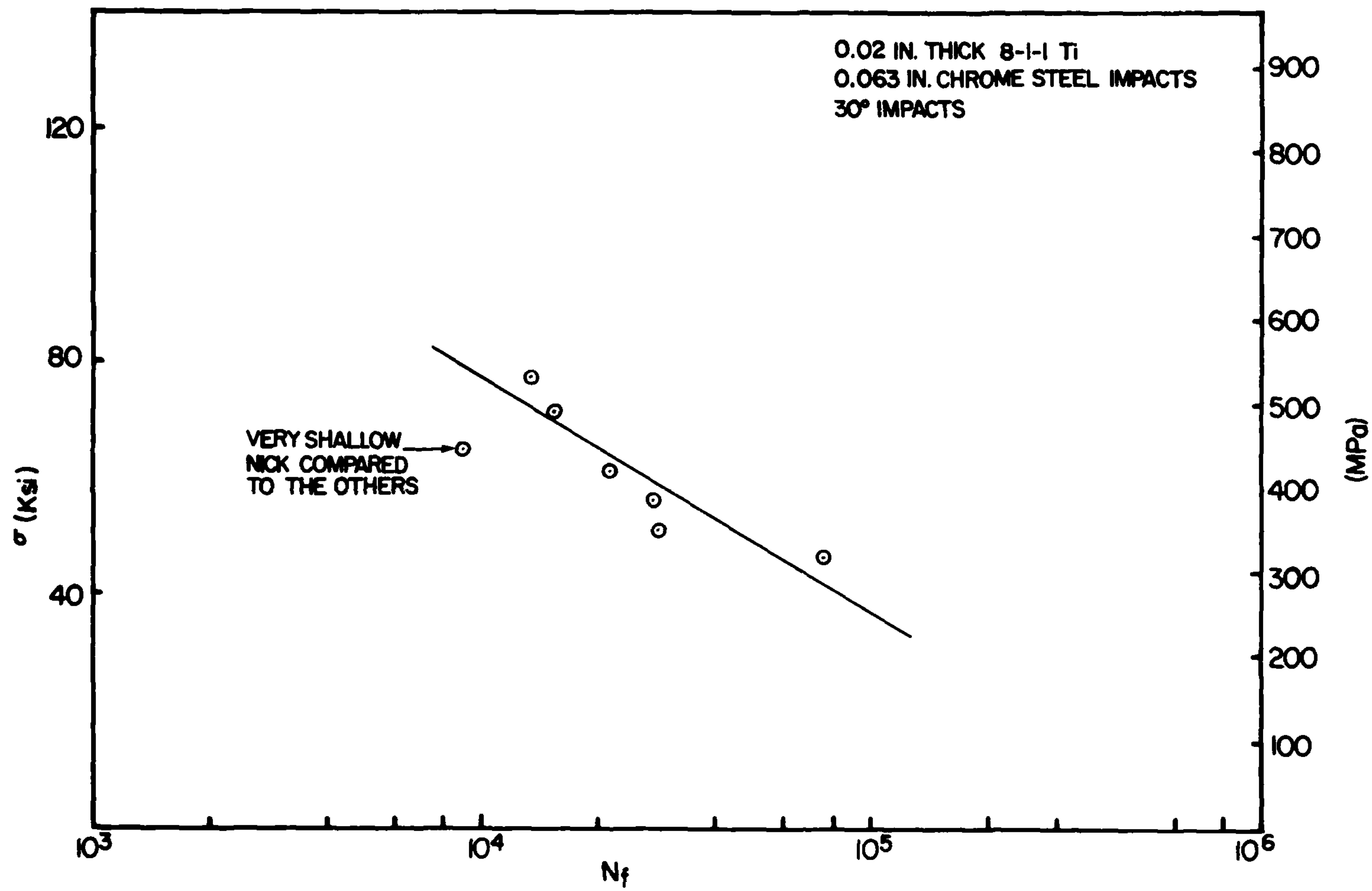

Figure A.19. Fatigue Data Results for 1.60 mm Chrome Steel Sphere Impacts on 0.508 mm Thick Titanium (30°).

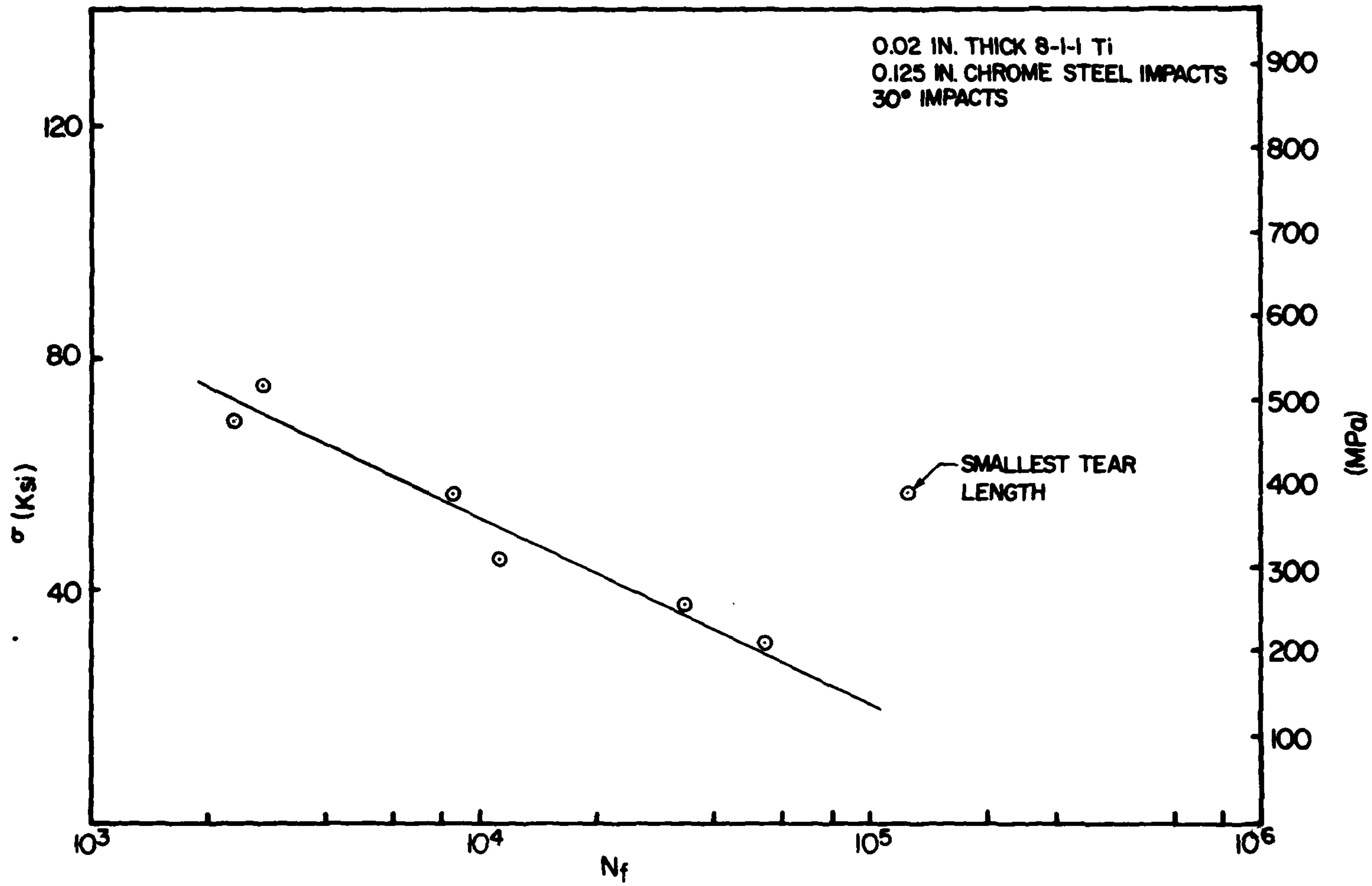

Figure A.20. Fatigue Data Results for 3.18 mm Chrome Steel Sphere Impacts on 0.508 mm Thick Titanium (30°).

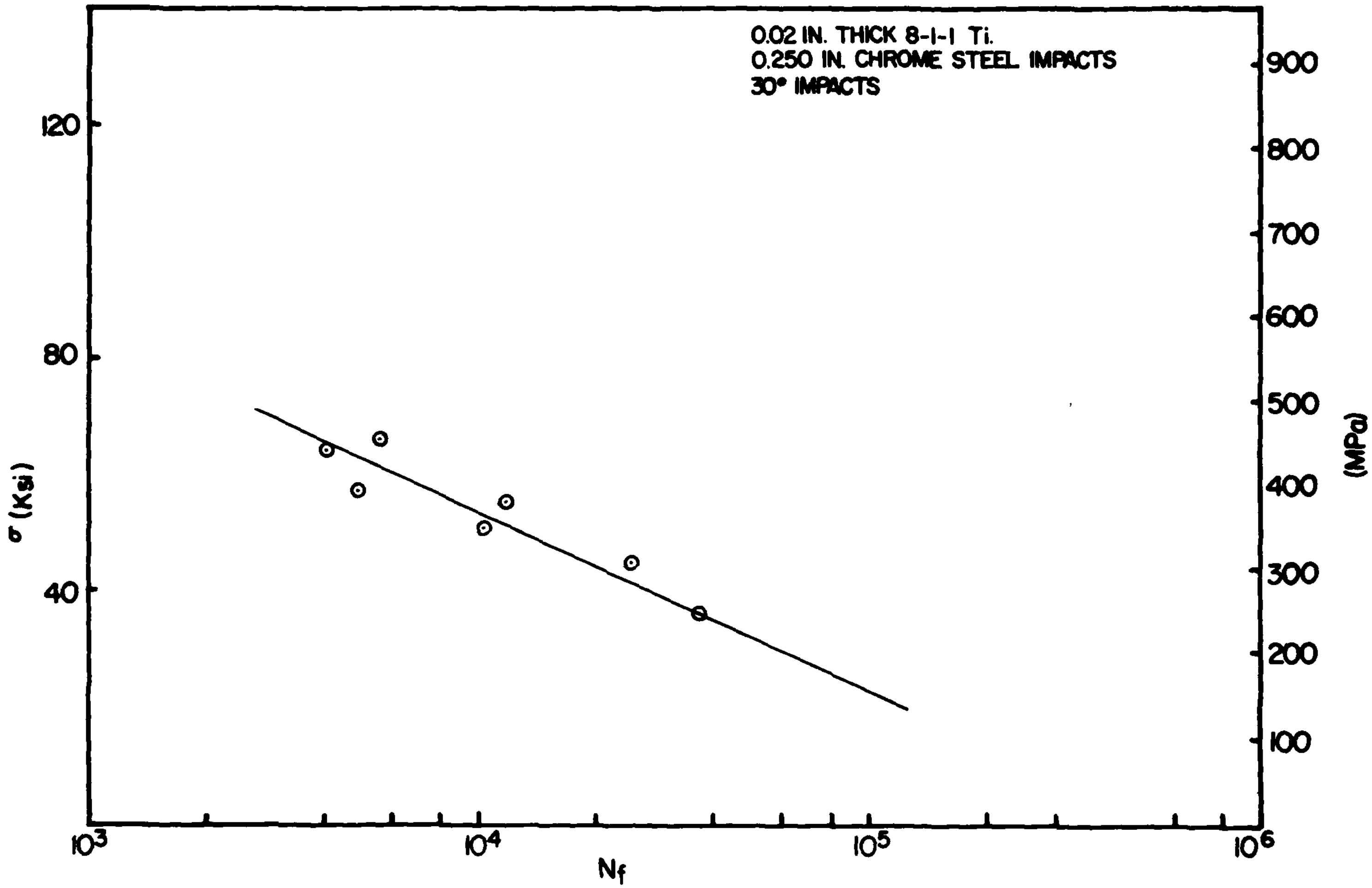

Figure A.21. Fatigue Data Results for 6.35 *mm Chrome* Steel Sphere Impacts on 0.508 mm Thick Titanium (30°).

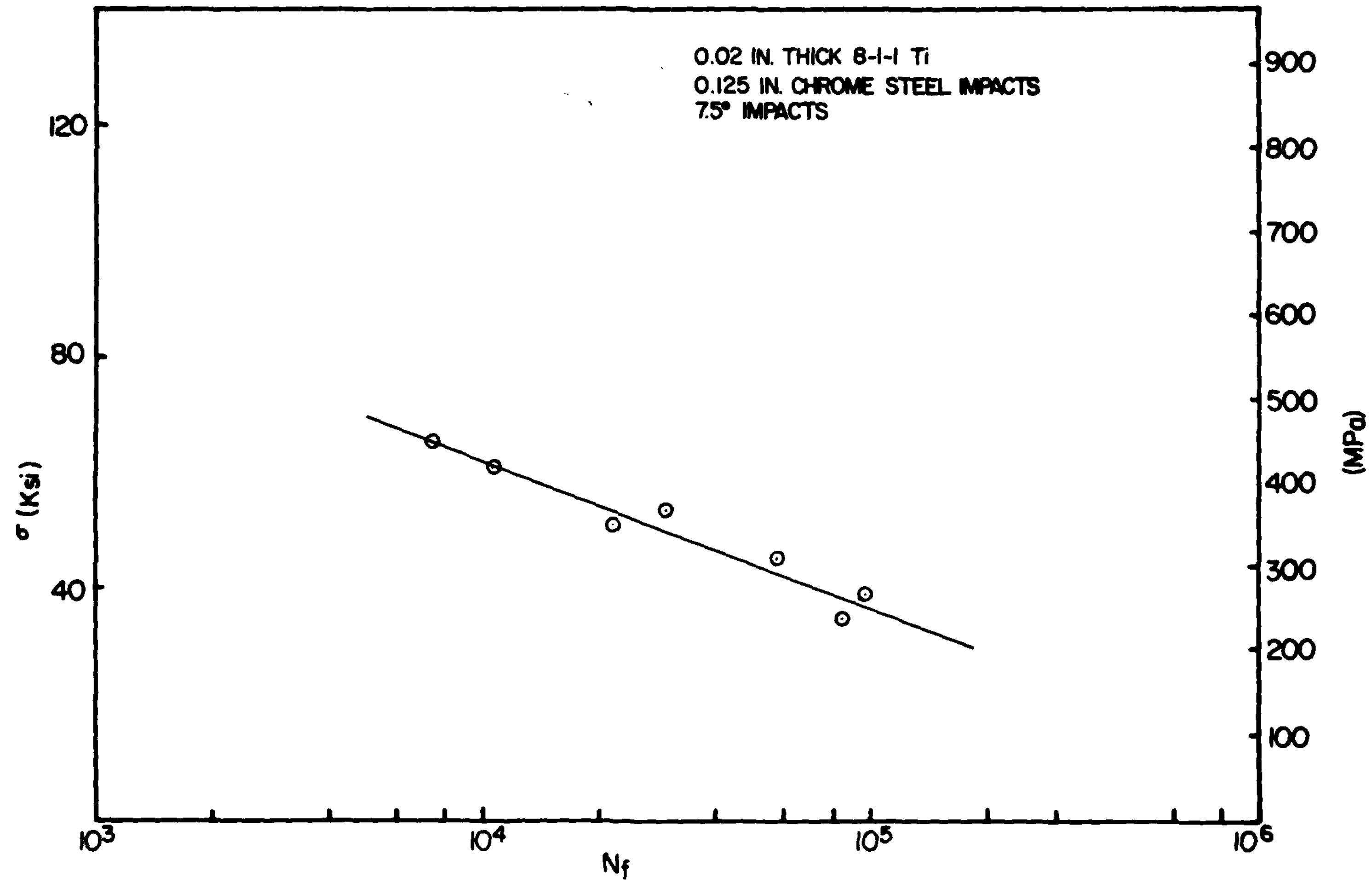

Figure A.22. Fatigue Data Results for 3.18 mm Chrome Steel Sphere Impacts on 0.508 mm Thick Titanium (7.5°).

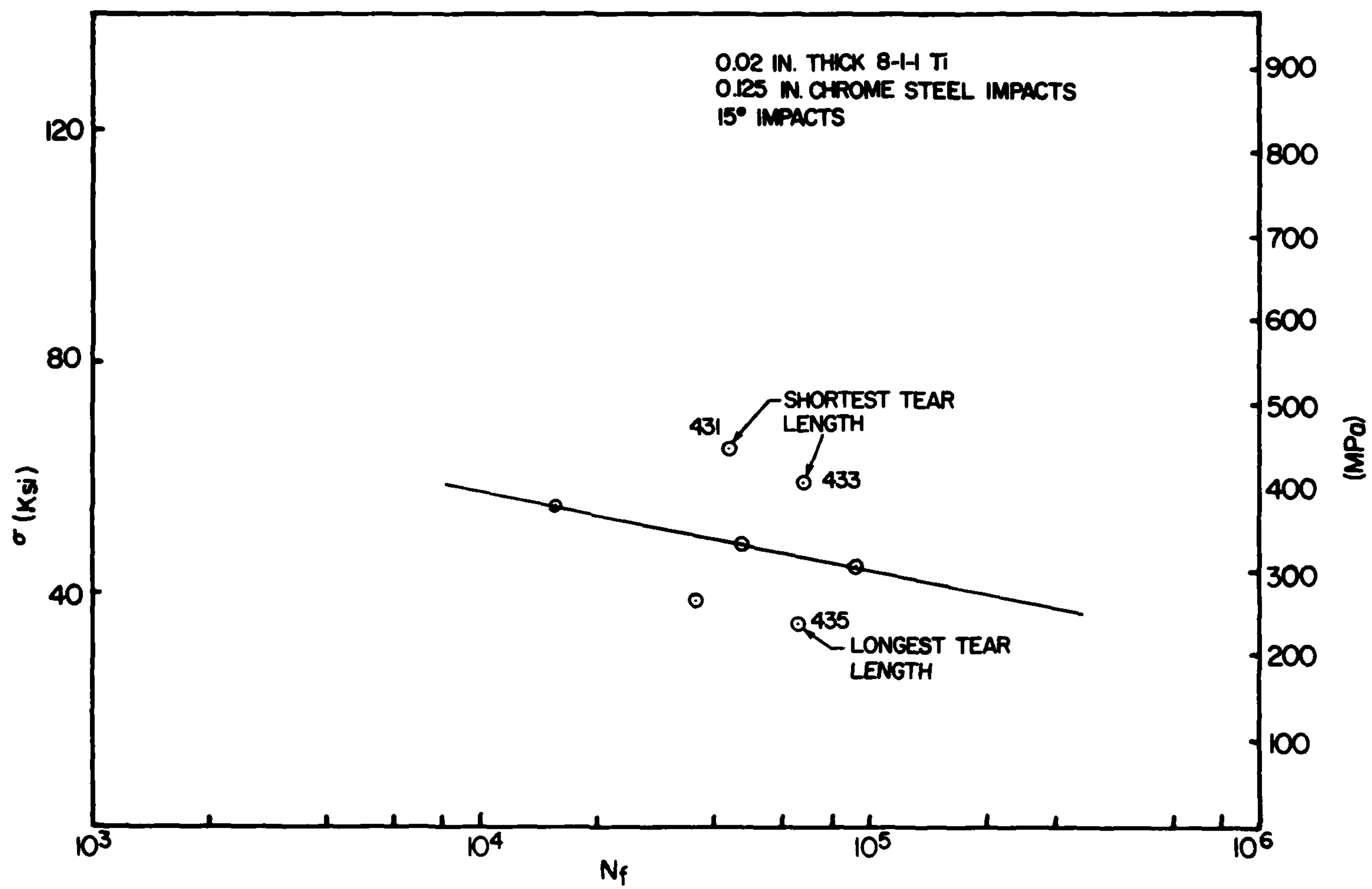

Figure A.23. Fatigue Data Results for 3.18 mm Chrome Steel Sphere Impacts on 0.508 mm Thick Titanium (15°).

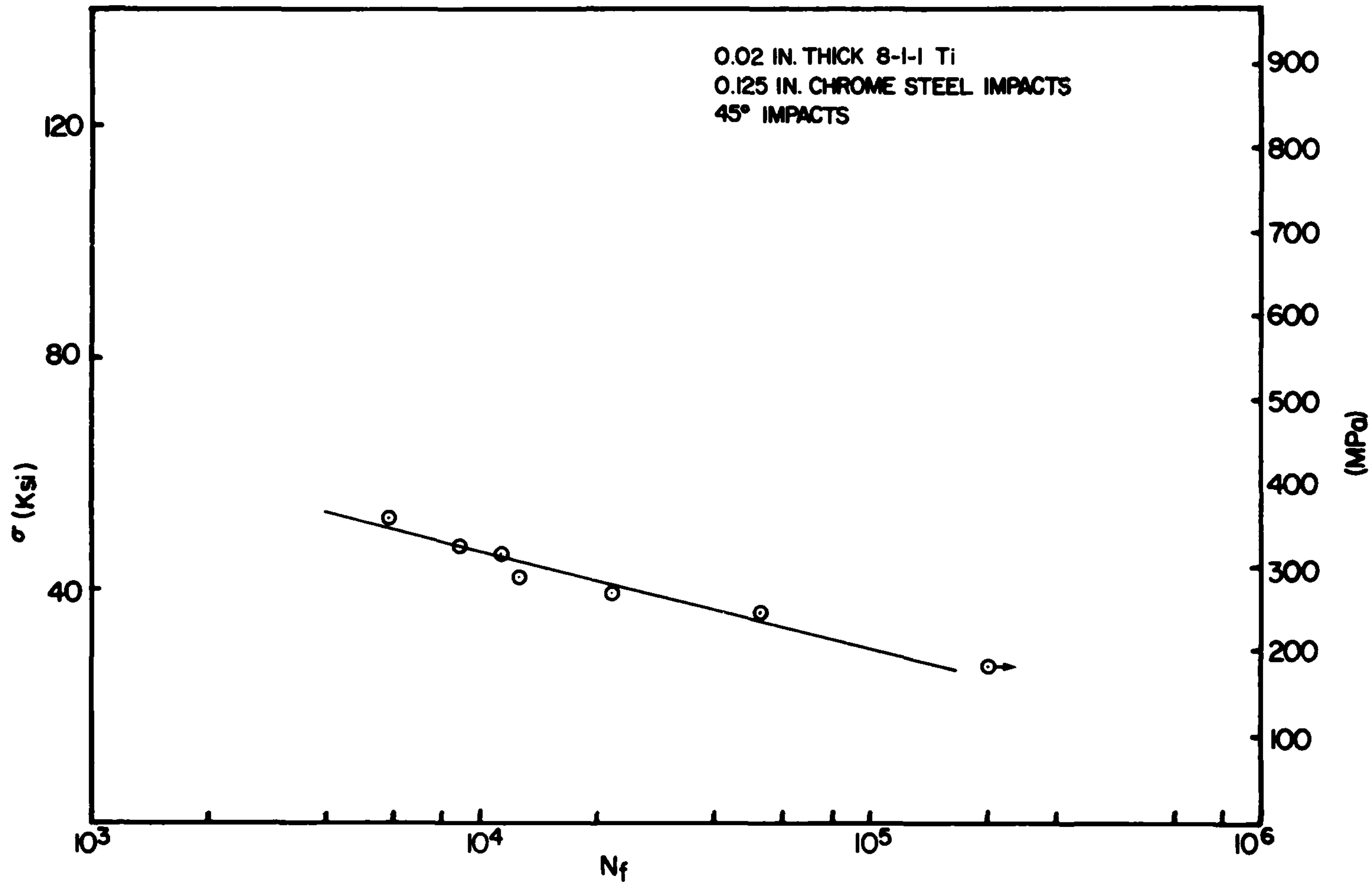

Figure A.24. Fatigue Data Results for 3.18 mm Chrome Steel Sphere Impacts on 0.508 mm Thick Titanium (45°).

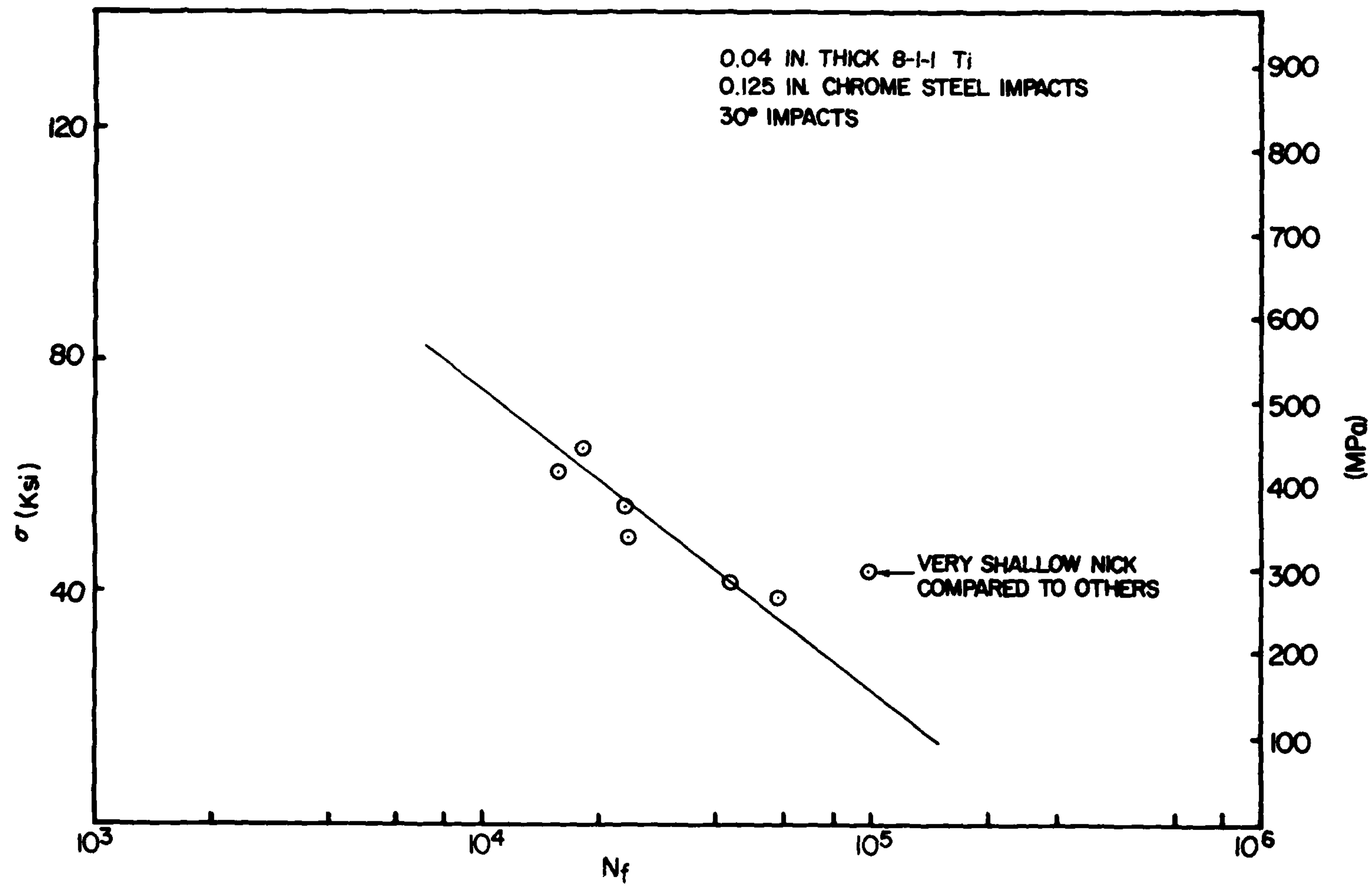

Figure A.25. Fatigue Data Results for 3.18 mm Chrome Steel Sphere Impacts on 1.016 mm Thick Titanium (30°).

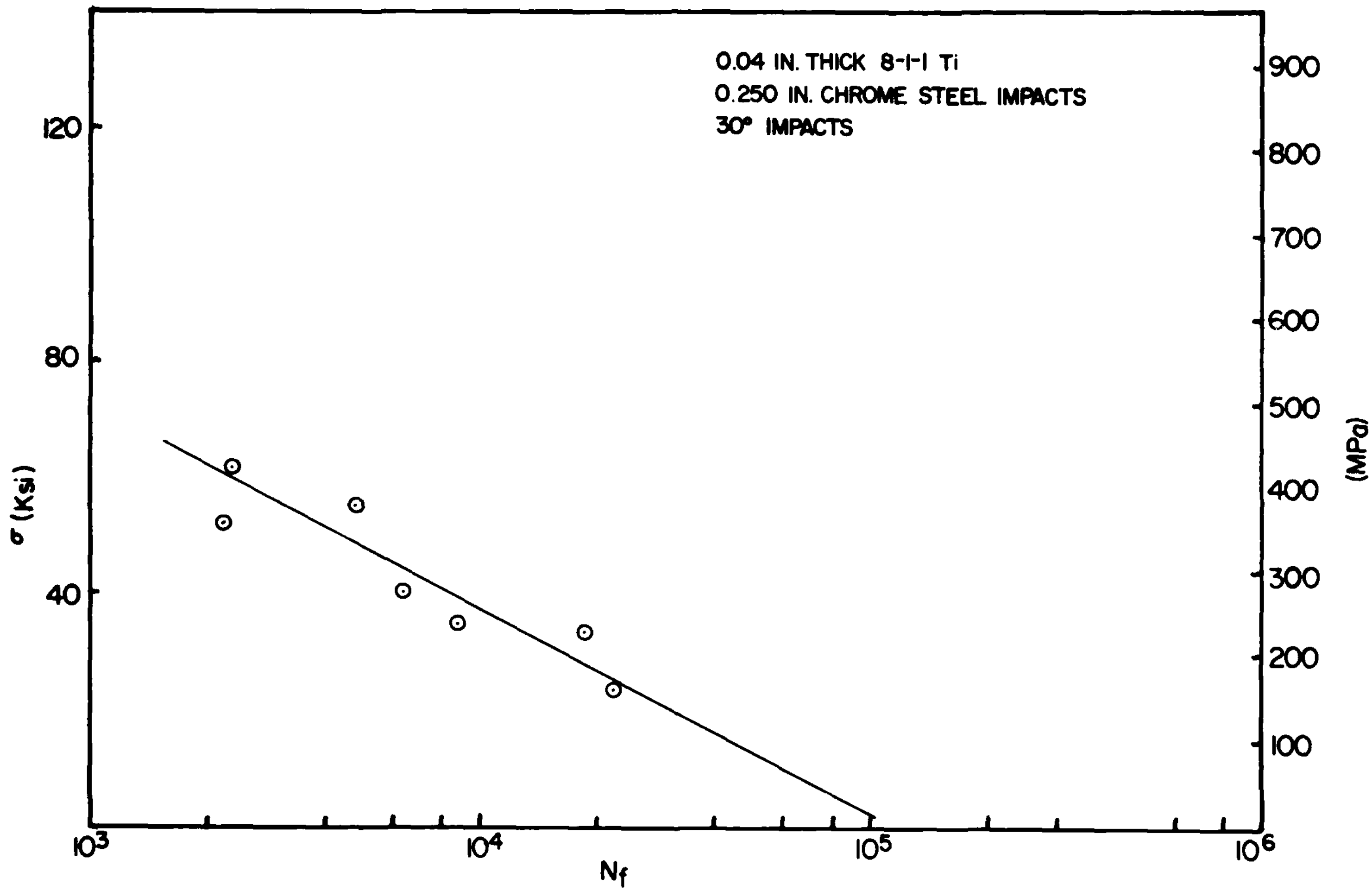

Figure A.26. Fatigue Data Results for 6.35 mm Chrome Steel Sphere Impacts on 1.016 mm Thick Titanium (30°).

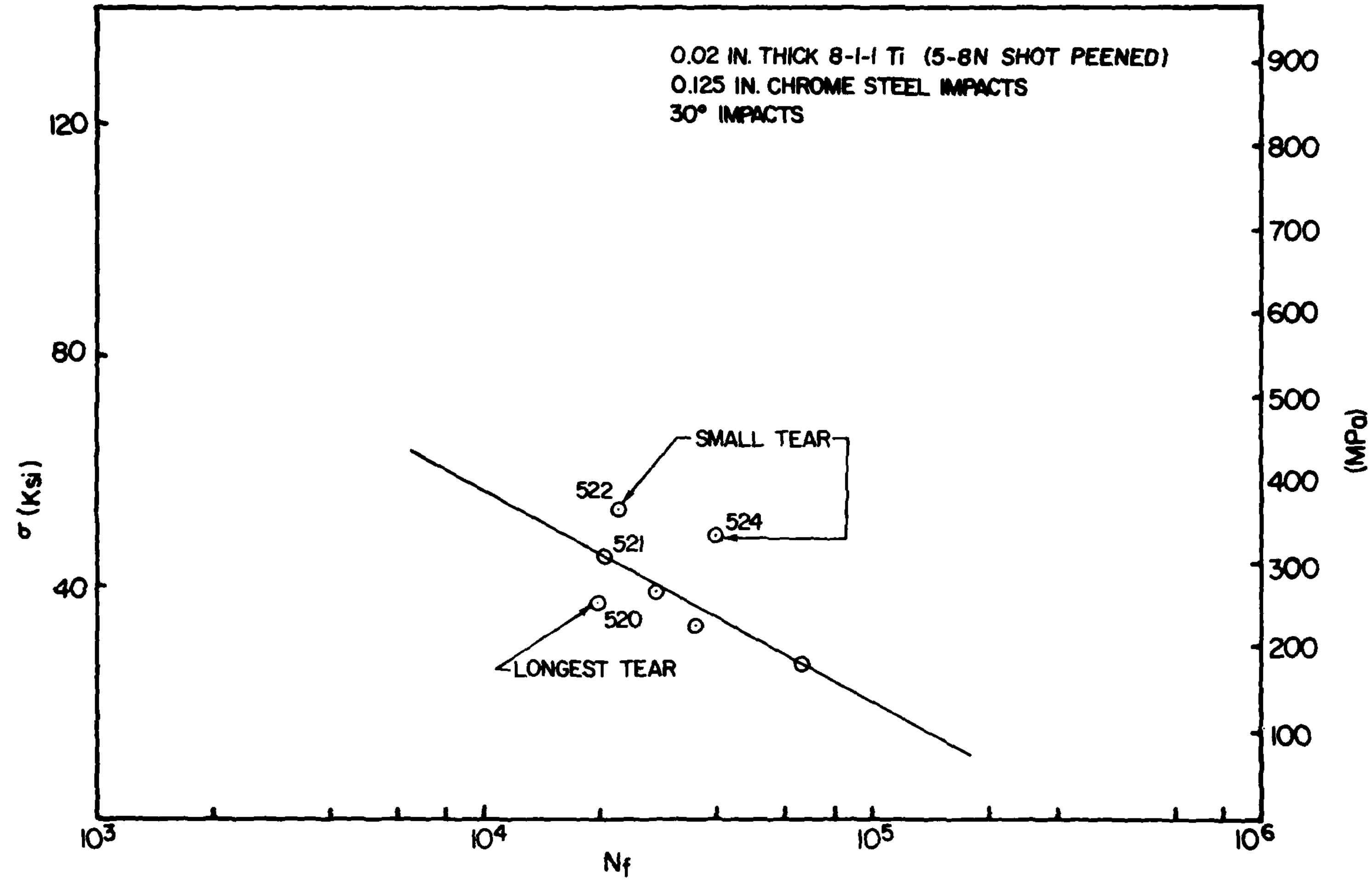

Figure A.27. Fatigue Data Results for 3.18 *mm Chrome Steel* Sphere Impacts on 0.508 mm Thick Titanium (5-8N Shot Peened) (30°).

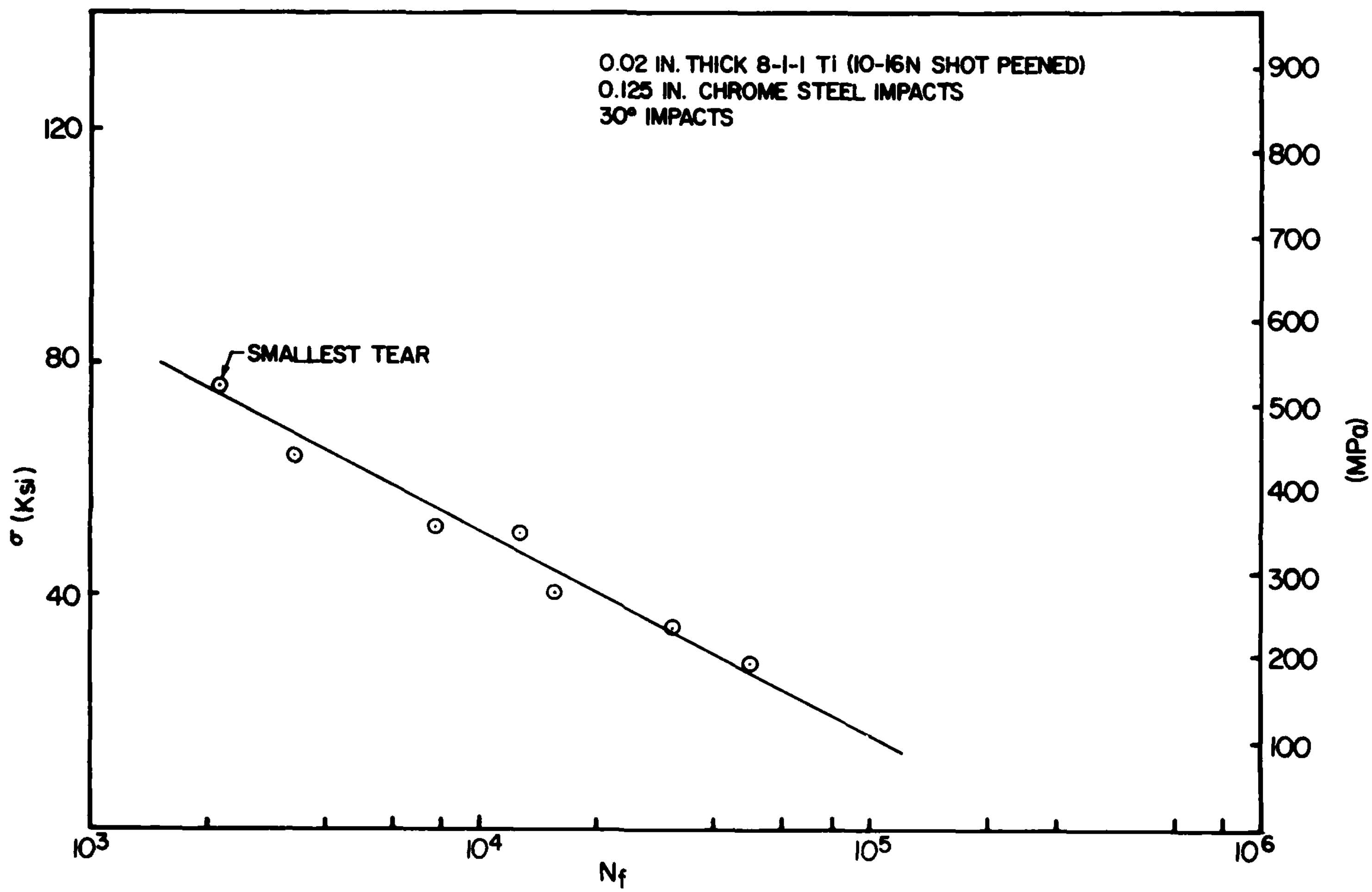

Figure A.28. Fatigue Data Results for 3.18 mm Chrome Steel Sphere Impacts on 0.508 mm Thick Titanium (10-16N Shot Peened).

AD-A109 676 DAYTON UNIV OH RESEARCH INST F/G 11/6
IMPACT DAMAGE ON VARIOUS METAL LEADING EDGES FROM SMALL HARD OB--ETC(U)
AUG 81 R S BERTKE F33615-76-C-5124
UNCLASSIFIED UDR-TR-81-06 AFWAL-TR-81-4066 NL

2 OF 2
AD A
109676

END
DATE
FILMED
02-82
DTIC

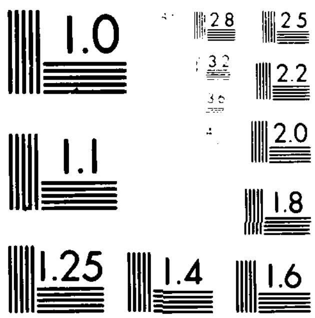

MICROCOPY RESOLUTION TEST CHART

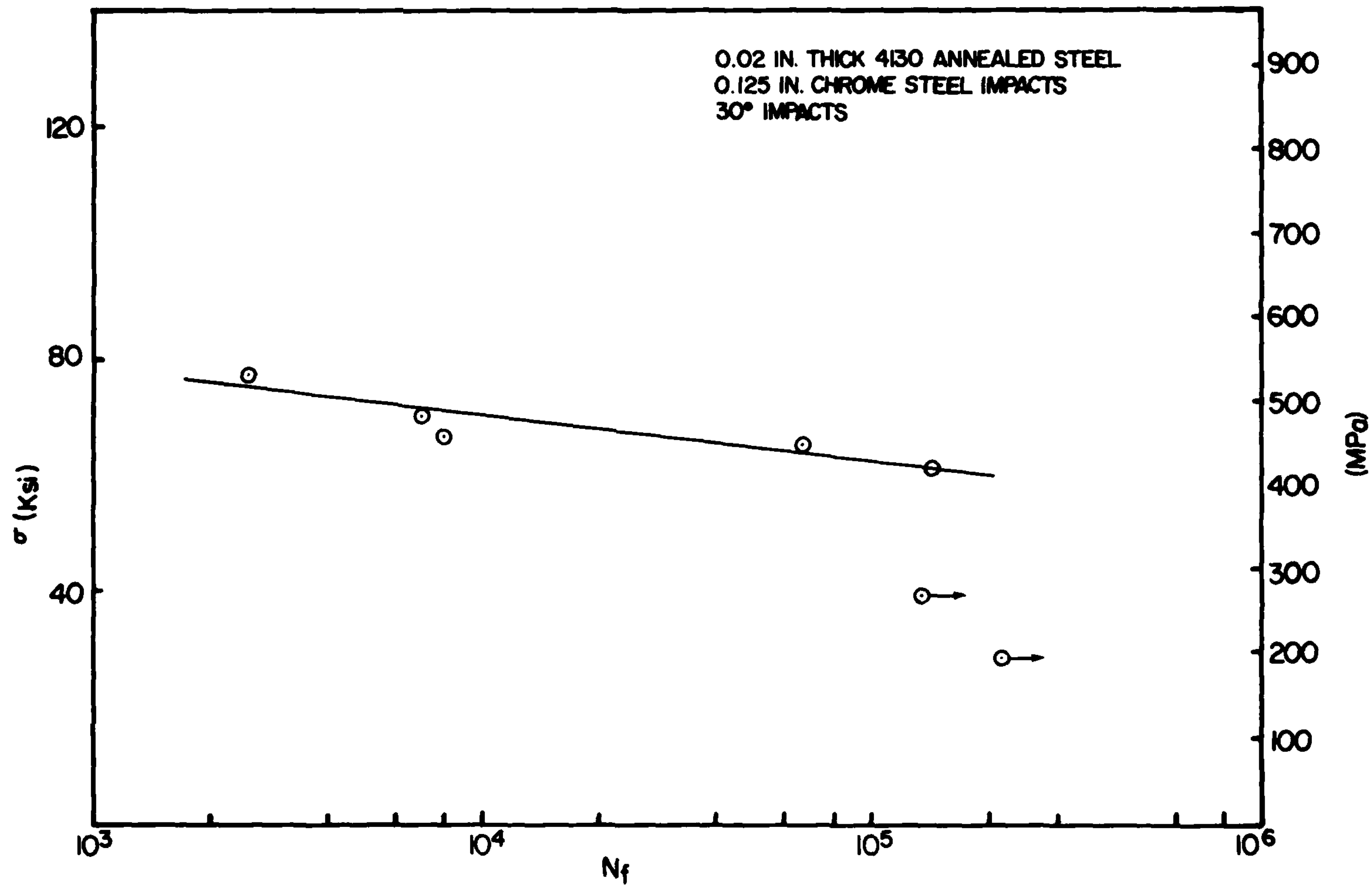

Figure A.29. Fatigue Data Results for 3.18 mm Chrome Steel Sphere Impacts on 0.508 mm Thick 4130 Steel (Annealed) (30°).

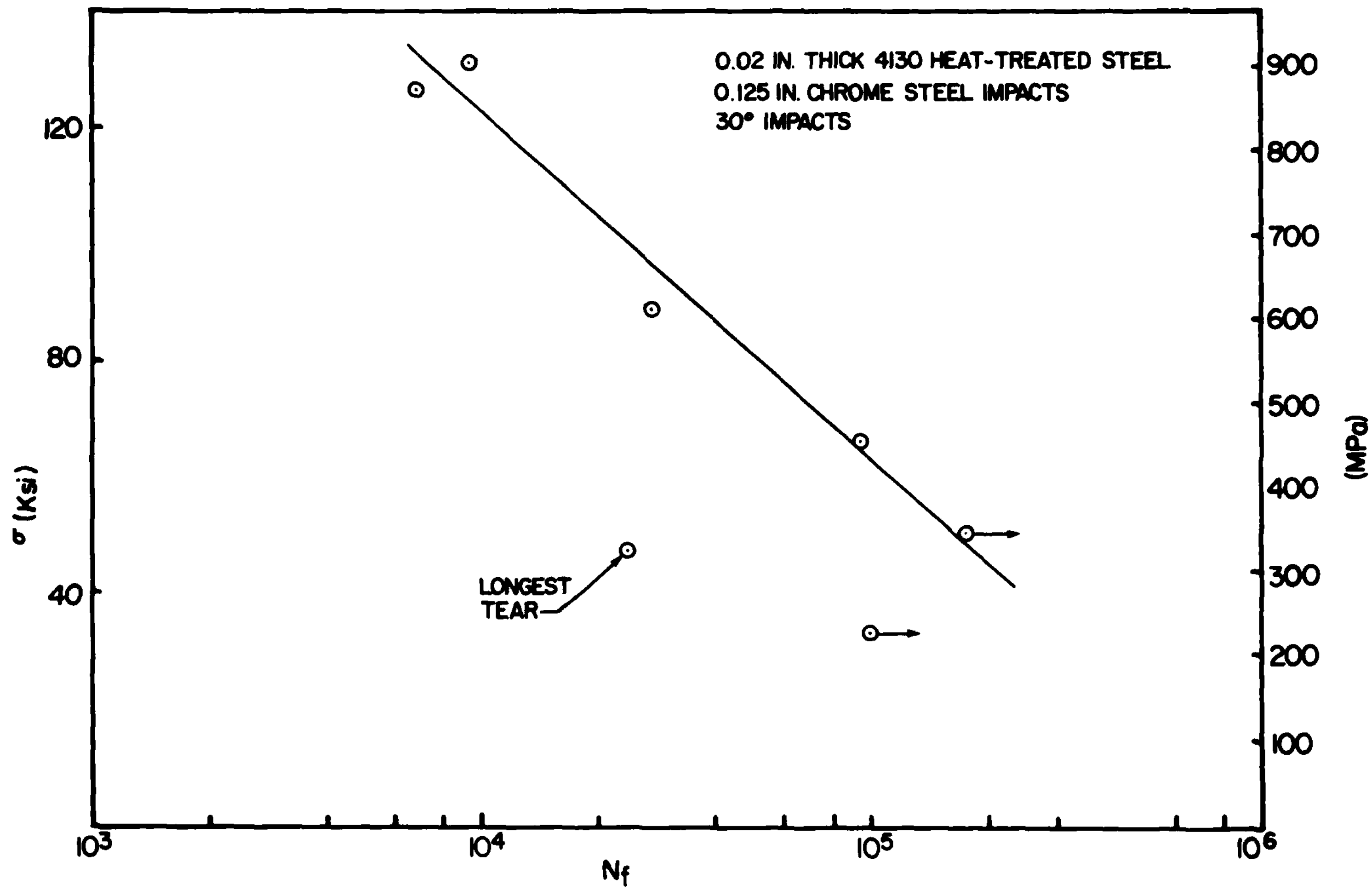

Figure A.30. Fatigue Data Results for 3.18 mm Chrome Steel Sphere Impacts on 0.508 mm Thick 4130 Steel (Heat-Treated) (30°).

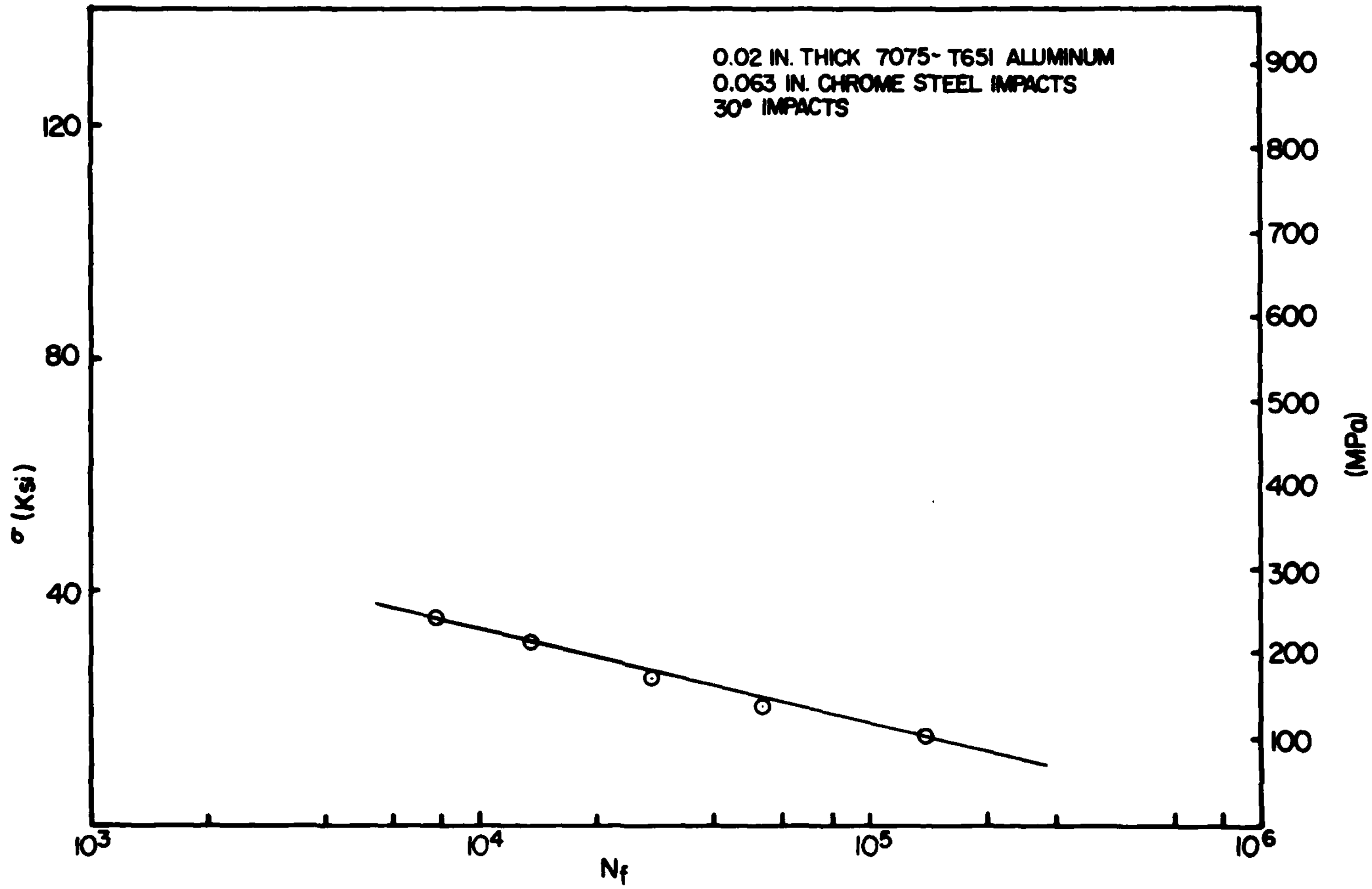

Figure A.31. Fatigue Data Results for 1.60 mm Chrome Steel Sphere Impacts on 0.508 mm Thick 7075-T651 Aluminum (30°).

APPENDIX B

IMPACT TESTS

TABLE 1. IMPACT RESULTS FOR ALUMINUM (1.60 mm) and SPHERE IMPACTS ON 0.254 mm THICK TITANIUM (30°)

Shot No.	Material	Size (cm)	Type of Impact	Thickness at Impact (mm)	Impact Angle (°)	Support Method	Projectile Type	Projectile Size (mm)	Velocity (m/s)	Remarks	Tear Length	Single Impact Nicks Width (mm)	Single Impact Nicks Depth (mm)	Edge On
3-0315	8-1-1 Ti	15.24x2.54x0.16	Edge On	0.25	30	Simple	Aluminum	1.58	884	Roll back with tear also mass loss		2.51	4.95	
3-0316	8-1-1 Ti	15.24x2.54x0.16	Edge On	0.25	30	Simple	Aluminum	1.58	871	Roll back with tear also mass loss		1.85	3.22	
3-0317	8-1-1 Ti	15.24x2.54x0.16	Edge On	0.25	30	Simple	Aluminum	1.58	884	Roll back with tear also mass loss		1.93	3.60	
3-0318	8-1-1 Ti	15.24x2.54x0.16	Edge On	0.25	30	Simple	Aluminum	1.58	838	Roll back with tear also mass loss		2.31	3.47	

TABLE 2. IMPACT RESULTS FOR ALUMINUM (3.18 mm) SPHERE IMPACTS ON 0.254 mm THICK TITANIUM (30°)

Shot No.	Material	Size (cm)	Type of Impact	Thickness at Impact (mm)	Impact Angle (°)	Support Method	Projectile Type	Projectile Size (mm)	Velocity (m/s)	Remarks	Tear Length (mm)	Single Impact Nicks Width (mm)	Single Impact Nicks Depth (mm)	Edge On
J-0301	8-1-1 Ti	15.24x2.54x0.16	Edge On	0.25	30	Simple	Aluminum	3.18	325	Roll back no tear multiple impacts				
J-0302	8-1-1 Ti	15.24x2.54x0.16	Edge On	0.25	30	Simple	Aluminum	3.18	388	Roll back no tear multiple impacts				
J-0303	8-1-1 Ti	15.24x2.54x0.16	Edge On	0.25	30	Simple	Aluminum	3.18	330	Roll back with tear on edge of test area				
J-0304	8-1-1 Ti	15.24x2.54x0.16	Edge On	0.25	30	Simple	Aluminum	3.18	362	Roll back with tear	4.08			
J-0305	8-1-1 Ti	15.24x2.54x0.16	Edge On	0.25	30	Simple	Aluminum	3.18	346	Roll back with tear	8.02			
0-0306	8-1-1 Ti	15.24x2.54x0.16	Edge On	0.25	30	Simple	Aluminum	3.18	372	Roll back with tear	9.09			
0-0307	8-1-1 Ti	15.24x2.54x0.16	Edge On	0.25	30	Simple	Aluminum	3.18	341	Roll back with tear	5.97			
0-0308	8-1-1 Ti	15.24x2.54x0.16	Edge On	0.25	30	Simple	Aluminum	3.18	329	Roll back with tear	8.69			
0-0309	8-1-1 Ti	15.24x2.54x0.16	Edge On	0.25	30	Simple	Aluminum	3.18	317	Roll back with tear	7.70			
0-0310	8-1-1 Ti	15.24x2.54x0.16	Edge On	0.25	30	Simple	Aluminum	3.18	309	Roll back with tear on edge of test area				
0-0311	8-1-1 Ti	15.24x2.54x0.16	Edge On	0.25	30	Simple	Aluminum	3.18	316	Roll back with tear	4.11			
0-0312	8-1-1 Ti	15.24x2.54x0.16	Edge On	0.25	30	Simple	Aluminum	3.18	316	Roll back with tear	4.52			
0-0313	8-1-1 Ti	15.24x2.54x0.16	Edge On	0.25	30	Simple	Aluminum	3.18	313	Roll back with tear	6.09			
0-0314	8-1-1 Ti	15.24x2.54x0.16	Edge On	0.25	30	Simple	Aluminum	3.18	319	Roll back with tear	8.71			

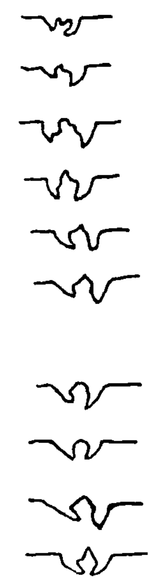

TABLE 3. IMPACT RESULTS OF CHROME STEEL (1.60 mm) SPHERE IMPACTS ON 0.254 mm THICK TITANIUM (30°)

Shot No.	Material	Size (cm)	Type of Impact	Thickness at Impact (mm)	Impact Angle (°)	Support Method	Projectile Type	Projectile Size (mm)	Velocity (m/s)	Remarks	Tear Length (mm)	Single Impact Nicks Width (mm)	Single Impact Nicks Depth (mm)	Edge On
3-0319	8-1-1 Ti	15.24x2.54x0.16	Edge On	0.25	30	Simple	Chrome Steel	1.58	248	Roll back with tear	1.72			
3-0320	8-1-1 Ti	15.24x2.54x0.16	Edge On	0.25	30	Simple	Chrome Steel	1.58	251	Roll back with crease				
3-0321	8-1-1 Ti	15.24x2.54x0.16	Edge On	0.25	30	Simple	Chrome Steel	1.58	250	Roll back with tear	1.65			
3-0322	8-1-1 Ti	15.24x2.54x0.16	Edge On	0.25	30	Simple	Chrome Steel	1.58	249	Roll back with tear	2.38			
3-0323	8-1-1 Ti	15.24x2.54x0.16	Edge On	0.25	30	Simple	Chrome Steel	1.58	249	Roll back with crease				
3-0324	8-1-1 Ti	15.24x2.54x0.16	Edge On	0.25	30	Simple	Chrome Steel	1.58	251	Roll back with tear	2.48			
3-0325	8-1-1 Ti	15.24x2.54x0.16	Edge On	0.25	30	Simple	Chrome Steel	1.58	251	Roll back with tear	2.79			
3-0326	8-1-1 Ti	15.24x2.54x0.16	Edge On	0.25	30	Simple	Chrome Steel	1.58	252	Roll back with crease				
3-0327	8-1-1 Ti	15.24x2.54x0.16	Edge On	0.25	30	Simple	Chrome Steel	1.58	256	Roll back with tear	1.98			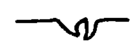

TABLE 4. IMPACT RESULTS FOR CHROME STEEL (3.18 mm) SPHERE IMPACTS ON 0.254 mm THICK TITANIUM (30°)

Shot No.	Material	Size (cm)	Type of Impact	Thickness at Impact (mm)	Impact Angle (°)	Support Method	Projectile Type	Projectile Size (mm)	Velocity (m/s)	Remarks	Tear Length (mm)	Single Impact Nicks Width (mm)	Single Impact Nicks Depth (mm)	Edge On
3-0328	8-1-1 Ti	15.24x2.54x0.16	Edge On	0.25	30	Simple	Chrome Steel	3.18	251	Roll back with tear	5.13			
3-0329	8-1-1 Ti	15.24x2.54x0.16	Edge On	0.25	30	Simple	Chrome Steel	3.18	248	Roll back with tear	5.89			
3-0330	8-1-1 Ti	15.24x2.54x0.16	Edge On	0.25	30	Simple	Chrome Steel	3.18	248	Roll back with tear	5.08			
3-0331	8-1-1 Ti	15.24x2.54x0.16	Edge On	0.25	30	Simple	Chrome Steel	3.18	239	Roll back with tear	5.89			
3-0332	8-1-1 Ti	15.24x2.54x0.16	Edge On	0.25	30	Simple	Chrome Steel	3.18	231	Roll back with tear	5.99			
3-0333	8-1-1 Ti	15.24x2.54x0.16	Edge On	0.25	30	Simple	Chrome Steel	3.18	219	Roll back with tear	5.61			
3-0334	8-1-1 Ti	15.24x2.54x0.16	Edge On	0.25	30	Simple	Chrome Steel	3.18	205	Roll back with tear	6.88			
3-0335	8-1-1 Ti	15.24x2.54x0.16	Edge On	0.25	30	Simple	Chrome Steel	3.18	197	Roll back with tear	10.36			
3-0336	8-1-1 Ti	15.24x2.54x0.16	Edge On	0.25	30	Simple	Chrome Steel	3.18	184	Roll back with tear along sides of test area				
3-0337	8-1-1 Ti	15.24x2.54x0.16	Edge On	0.25	30	Simple	Chrome Steel	3.18	204	Roll back with tear also projectile hit low	12.49			
3-0338	8-1-1 Ti	15.24x2.54x0.16	Edge On	0.25	30	Simple	Chrome Steel	3.18	202	Roll back with tear	4.69			
3-0339	8-1-1 Ti	15.24x2.54x0.16	Edge On	0.25	30	Simple	Chrome Steel	3.18	201	Roll back with tear	5.0			

TABLE 5. IMPACT RESULTS FOR CHROME STEEL (1.60 mm) SPHERE IMPACTS ON 0.508 mm THICK TITANIUM (30°)

Shot No.	Material	Size (cm)	Type of Impact	Thickness at Impact (mm)	Impact Angle (°)	Support Method	Projectile Type	Projectile Size (mm)	Velocity (m/s)	Remarks	Tear Length	Single Impact Width (mm)	Single Nicks Depth (mm)	Edge On
3-0340	8-1-1 Ti	15.24x2.54x0.16	Edge On	0.50	30	Simple	Chrome Steel	1.58	363	Nick also mass loss		1.24	0.54	
3-0341	8-1-1 Ti	15.24x2.54x0.16	Edge On	0.50	30	Simple	Chrome Steel	1.58	354	Bulge also started to plug		1.11	0.16	
3-0342	8-1-1 Ti	15.24x2.54x0.16	Edge On	0.50	30	Simple	Chrome Steel	1.58	348	Nick also mass loss		1.23	0.56	
3-0343	8-1-1 Ti	15.24x2.54x0.16	Edge On	0.50	30	Simple	Chrome Steel	1.58	334	Nick also mass loss		1.26	0.45	
3-0344	8-1-1 Ti	15.24x2.54x0.16	Edge On	0.50	30	Simple	Chrome Steel	1.58	372	Nick also mass loss		1.26	0.60	
3-0345	8-1-1 Ti	15.24x2.54x0.16	Edge On	0.50	30	Simple	Chrome Steel	1.58	324	Nick also mass loss		1.48	0.60	
3-0346	8-1-1 Ti	15.24x2.54x0.16	Edge On	0.50	30	Simple	Chrome Steel	1.58	361	Nick also mass loss		1.26	0.66	
3-0467	8-1-1 Ti	15.24x2.54x0.16	Edge On	0.50	30	Simple	Chrome Steel	1.58	361	Nick also mass loss		1.11	0.36	

TABLE 6. IMPACT RESULTS FOR CHROME STEEL (3.18 mm) SPHERE IMPACTS ON 0.508 mm THICK TITANIUM (30°)

Shot No.	Material	Size (cm)	Type of Impact	Thickness at Impact (mm)	Impact Angle (°)	Support Method	Projectile Type	Projectile Size (mm)	Velocity (m/s)	Remarks	Tear Length (mm)	Single Impact Nicks Width (mm)	Single Impact Nicks Depth (mm)	Edge On
3-0347	8-1-1 Ti	15.24x2.54x0.16	Edge On	0.50	30	Simple	Chrome Steel	3.18	230	Roll back with tear	2.84			
3-0348	8-1-1 Ti	15.24x2.54x0.16	Edge On	0.50	30	Simple	Chrome Steel	3.18	231	Roll back with tear	4.95			
3-0349	8-1-1 Ti	15.24x2.54x0.16	Edge On	0.50	30	Simple	Chrome Steel	3.18	230	Roll back with tear	5.23			
3-0350	8-1-1 Ti	15.24x2.54x0.16	Edge On	0.50	30	Simple	Chrome Steel	3.18	227	Roll back with crease				
3-0351	8-1-1 Ti	15.24x2.54x0.16	Edge On	0.50	30	Simple	Chrome Steel	3.18	233	Roll back with tear	5.99			
3-0352	8-1-1 Ti	15.24x2.54x0.16	Edge On	0.50	30	Simple	Chrome Steel	3.18	233	Roll back with tear	5.20			
3-0353	8-1-1 Ti	15.24x2.54x0.16	Edge On	0.50	30	Simple	Chrome Steel	3.18	235	Roll back no tear				
3-0354	8-1-1 Ti	15.24x2.54x0.16	Edge On	0.50	30	Simple	Chrome Steel	3.18	232	Roll back with tear also mass loss	5.20			
3-0355	8-1-1 Ti	15.24x2.54x0.16	Edge On	0.50	30	Simple	Chrome Steel	3.18	232	Roll back no tear				
3-0356	8-1-1 Ti	15.24x2.54x0.16	Edge On	0.50	30	Simple	Chrome Steel	3.18	231	Roll back with tear	5.10			

TABLE 7. IMPACT RESULTS FOR CHROME STEEL (6.35 mm) SPHERE IMPACTS ON 0.508 mm THICK TITANIUM (30°)

Shot No.	Material	Size (cm)	Type of Impact	Thickness at Impact (mm)	Impact Angle (°)	Support Method	Projectile Type	Projectile Size (mm)	Velocity (m/s)	Remarks	Tear Length (mm)	Single Impact Nicks Width (mm)	Single Impact Nicks Depth (mm)	Edge On
3-0404	8-1-1 Ti	15.24x2.54x0.16	Edge On	0.50	30	Simple	Chrome Steel	6.35	223	Roll back with tear also mass loss	7.08			
3-0405	8-1-1 Ti	15.24x2.54x0.16	Edge On	0.50	30	Simple	Chrome Steel	6.35	223	Roll back with tear also mass loss	4.26			
3-0406	8-1-1 Ti	15.24x2.54x0.16	Edge On	0.50	30	Simple	Chrome Steel	6.35	265	Roll back with tear also mass loss from plugging	11.45			
3-0407	8-1-1 Ti	15.24x2.54x0.16	Edge On	0.50	30	Simple	Chrome Steel	6.35	464	Roll back with tear also mass loss	11.30			
3-0408	8-1-1 Ti	15.24x2.54x0.16	Edge On	0.50	30	Simple	Chrome Steel	6.35	224	Roll back with tear also mass loss	7.87			
3-0409	8-1-1 Ti	15.24x2.54x0.16	Edge On	0.50	30	Simple	Chrome Steel	6.35	227	Nick also mass loss				
3-0410	8-1-1 Ti	15.24x2.54x0.16	Edge On	0.50	30	Simple	Chrome Steel	6.35	285	Nick also mass loss multiple impact				
3-0411	8-1-1 Ti	15.24x2.54x0.16	Edge On	0.50	30	Simple	Chrome Steel	6.35	224	Roll back with tears on sides of test area				
3-0412	8-1-1 Ti	15.24x2.54x0.16	Edge On	0.50	30	Simple	Chrome Steel	6.35	223	Roll back with tear	8.33			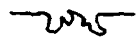
3-0413	8-1-1 Ti	15.24x2.54x0.16	Edge On	0.50	30	Simple	Chrome Steel	6.35	221	Roll back with tear also mass loss	5.63			

TABLE 8. IMPACT RESULTS FOR CHROME STEEL (3.18 mm) SPHERE IMPACTS ON 0.508 mm THICK TITANIUM (7.5°)

Shot No.	Material	Size (cm)	Type of Impact	Thickness at Impact (mm)	Impact Angle (°)	Support Method	Projectile Type	Projectile Size (mm)	Velocity (m/s)	Remarks	Tear Length (mm)	Single Impact Nicks Width (mm)	Single Impact Nicks Depth (mm)	Edge On
3-0416	8-1-1 Ti	15.24x2.54x0.16	Edge On	0.50	7.5	Simple	Chrome Steel	3.18	311	Roll back with tear also mass loss	2.89			
3-0417	8-1-1 Ti	15.24x2.54x0.16	Edge On	0.50	7.5	Simple	Chrome Steel	3.18	308	Nick and mass loss multiple impact				
3-0418	8-1-1 Ti	15.24x2.54x0.16	Edge On	0.50	7.5	Simple	Chrome Steel	3.18	283	Roll back with tear also mass loss (multiple impact)				
3-0419	8-1-1 Ti	15.24x2.54x0.16	Edge On	0.50	7.5	Simple	Chrome Steel	3.18	256	Roll back with tear	2.15			
3-0420	8-1-1 Ti	15.24x2.54x0.16	Edge On	0.50	7.5	Simple	Chrome Steel	3.18	258	Nick and mass loss				
3-0421	8-1-1 Ti	15.24x2.54x0.16	Edge On	0.50	7.5	Simple	Chrome Steel	3.18	274	Roll back with tear also mass loss	1.85			
3-0422	8-1-1 Ti	15.24x2.54x0.16	Edge On	0.50	7.5	Simple	Chrome Steel	3.18	269	Nick and mass loss				
3-0423	8-1-1 Ti	15.24x2.54x0.16	Edge On	0.50	7.5	Simple	Chrome Steel	3.18	280	Roll back with tear	3.20			
3-0424	8-1-1 Ti	15.24x2.54x0.16	Edge On	0.50	7.5	Simple	Chrome Steel	3.18	284	Roll back with tear also mass loss	2.59			
3-0425	8-1-1 Ti	15.24x2.54x0.16	Edge On	0.50	7.5	Simple	Chrome Steel	3.18	280	No damage-projectile strayed off path				
3-0426	8-1-1 Ti	15.24x2.54x0.16	Edge On	0.50	7.5	Simple	Chrome Steel	3.18	277	Roll back with tear	2.64			
3-0427	8-1-1 Ti	15.24x2.54x0.16	Edge On	0.50	7.5	Simple	Chrome Steel	3.18	274	Roll back with tear also mass loss	2.59			
3-0428	8-1-1 Ti	15.24x2.54x0.16	Edge On	0.50	7.5	Simple	Chrome Steel	3.18	310	Roll back with tear also mass loss	2.31			
3-0429	8-1-1 Ti	15.24x2.54x0.16	Edge On	0.50	7.5	Simple	Chrome Steel	3.18	266	Roll back with tear also mass loss				

TABLE 9. IMPACT RESULTS FOR CHROME STEEL (3.18 mm)
SPHERE IMPACTS ON 0.508 mm THICK TITANIUM (15°)

Shot No.	Material	Size (cm)	Type of Impact	Thickness at Impact (mm)	Impact Angle (°)	Support Method	Projectile Type	Projectile Size (mm)	Velocity (m/s)	Remarks	Tear Length (mm)	Single Impact Nicks Width (mm)	Single Impact Nicks Depth (mm)	Edge On
3-0430	8-1-1 Ti	15.24x2.54x0.16	Edge On	0.50	15	Simple	Chrome Steel	3.18	267	Roll back with tear also mass loss	4.14			
3-0431	8-1-1 Ti	15.24x2.54x0.16	Edge On	0.50	15	Simple	Chrome Steel	3.18	230	Roll back with tear also mass loss	1.77			
3-0432	8-1-1 Ti	15.24x2.54x0.16	Edge On	0.50	15	Simple	Chrome Steel	3.18	234	Roll back with tear	2.77			
3-0433	8-1-1 Ti	15.24x2.54x0.16	Edge On	0.50	15	Simple	Chrome Steel	3.18	239	Roll back with tear also mass loss	1.98			
3-0434	8-1-1 Ti	15.24x2.54x0.16	Edge On	0.50	15	Simple	Chrome Steel	3.18	235	Roll back with tear also mass loss	2.38			
3-0435	8-1-1 Ti	15.24x2.54x0.16	Edge On	0.50	15	Simple	Chrome Steel	3.18	239	Roll back with tear also mass loss	3.35			
3-0436	8-1-1 Ti	15.24x2.54x0.16	Edge On	0.50	15	Simple	Chrome Steel	3.18	237	Roll back with tear also mass loss	2.38			
3-0437	8-1-1 Ti	15.24x2.54x0.16	Edge On	0.50	15	Simple	Chrome Steel	3.18	240	Roll back with tear also mass loss	2.59			

TABLE 10. IMPACT RESULTS FOR CHROME STEEL (3.18 mm) SPHERE IMPACTS ON 0.508 mm THICK TITANIUM (45°)

Shot No.	Material	Size (cm)	Type of Impact	Thickness at Impact (mm)	Impact Angle (°)	Support Method	Projectile Type	Projectile Size (mm)	Velocity (m/s)	Remarks	Tear Length (mm)	Single Impact Nicks Width (mm)	Single Impact Nicks Depth (mm)	Edge On
3-0438	8-1-1 Ti	15.24x2.54x0.16	Edge On	0.50	45	Simple	Chrome Steel	3.18	211	Roll back and bulge multiple impact				
3-0439	8-1-1 Ti	15.24x2.54x0.16	Edge On	0.50	45	Simple	Chrome Steel	3.18	234	Roll back and bulge multiple impact				
3-0440	8-1-1 Ti	15.24x2.54x0.16	Edge On	0.50	45	Simple	Chrome Steel	3.18	247	Roll back and crease multiple impact				
3-0441	8-1-1 Ti	15.24x2.54x0.16	Edge On	0.50	45	Simple	Chrome Steel	3.18	263	Roll back with tear multiple impact				
3-0442	8-1-1 Ti	15.24x2.54x0.16	Edge On	0.50	45	Simple	Chrome Steel	3.18	257	Roll back with crease				
3-0443	8-1-1 Ti	15.24x2.54x0.16	Edge On	0.50	45	Simple	Chrome Steel	3.18	263	Roll back with tear	6.12			
3-0444	8-1-1 Ti	15.24x2.54x0.16	Edge On	0.50	45	Simple	Chrome Steel	3.18	258	Roll back with tear	6.80			
3-0445	8-1-1 Ti	15.24x2.54x0.16	Edge On	0.50	45	Simple	Chrome Steel	3.18	261	Roll back with tear	7.41			
3-0446	8-1-1 Ti	15.24x2.54x0.16	Edge On	0.50	45	Simple	Chrome Steel	3.18	256	Roll back with tear off center	8.15			
3-0447	8-1-1 Ti	15.24x2.54x0.16	Edge On	0.50	45	Simple	Chrome Steel	3.18	258	Roll back with tear off center	7.72			
3-0448	8-1-1 Ti	15.24x2.54x0.16	Edge On	0.50	45	Simple	Chrome Steel	3.18	259	Roll back with tear also mass loss	6.75			
3-0449	8-1-1 Ti	15.24x2.54x0.16	Edge On	0.50	45	Simple	Chrome Steel	3.18	286	Roll back with tear	7.34			
3-0450	8-1-1 Ti	15.24x2.54x0.16	Edge On	0.50	45	Simple	Chrome Steel	3.18	256	Roll back with tear	7.82			
3-0451	8-1-1 Ti	15.24x2.54x0.16	Edge On	0.50	45	Simple	Chrome Steel	3.18	260	Bulge				

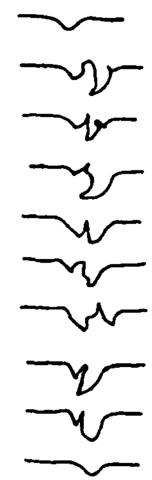

TABLE 10. IMPACT RESULTS FOR CHROME STEEL (ø3.18 mm) SPHERE IMPACTS ON 0.508 mm THICK TITANIUM (45°) (Continued)

Shot No.	Material	Size (cm)	Type of Impact	Thickness at Impact (mm)	Impact Angle (°)	Support Method	Projectile Type	Projectile Size (mm)	Velocity (m/s)	Remarks	Tear Length (mm)	Single Impact Nicks Width (mm)	Single Impact Nicks Depth (mm)	Edge On
3-0452	8-1-1 Ti	15.24x2.54x0.16	Edge On	0.50	45	Simple	Chrome Steel	3.18	254	Roll back with tear also mass loss	6.27			
3-0453	8-1-1 Ti	15.24x2.54x0.16	Edge On	0.50	45	Simple	Chrome Steel	3.18	257	Roll back with tear also mass loss	5.99			

TABLE 11. IMPACT RESULTS FOR CHROME STEEL (3.18 mm) SPHERE IMPACTS ON 1.016 mm THICK TITANIUM (30°)

Shot No.	Material	Size (cm)	Type of Impact	Thickness at Impact (mm)	Impact Angle (°)	Support Method	Projectile Type	Projectile Size (mm)	Velocity (m/s)	Remarks	Tear Length (mm)	Single Impact Width (mm)	Single Nicks Depth (mm)	Edge On
3-0357	8-1-1 Ti	15.24x2.54x0.16	Edge On	1.01	30	Simple	Chrome Steel	3.18	256	Roll back with tear		2.83	0.82	
3-0358	8-1-1 Ti	15.24x2.54x0.16	Edge On	1.01	30	Simple	Chrome Steel	3.18	244	Nick also mass loss		2.46	0.58	
3-0359	8-1-1 Ti	15.25x2.54x0.16	Edge On	1.01	30	Simple	Chrome Steel	3.18	243	Nick also mass loss		1.64	0.78	
3-0360	8-1-1 Ti	15.24x2.54x0.16	Edge On	1.01	30	Simple	Chrome Steel	3.18	243	Nick also mass loss		1.91	0.94	
3-0361	8-1-1 Ti	15.24x2.54x0.16	Edge On	1.01	30	Simple	Chrome Steel	3.18	242	Nick also mass loss		2.83	0.80	
3-0362	8-1-1 Ti	15.24x2.54x0.16	Edge On	1.01	30	Simple	Chrome Steel	3.18	242	Nick also mass loss		2.65	1.07	
3-0363	8-1-1 Ti	15.24x2.54x0.16	Edge On	1.01	30	Simple	Chrome Steel	3.18	243	Nick also mass loss		2.25	0.86	

TABLE 12. IMPACT RESULTS FOR CHROME STEEL (6.35 mm) SPHERE IMPACTS ON 1.016 mm THICK TITANIUM (30°)

Shot No.	Material	Size (cm)	Type of Impact	Thickness at Impact (mm)	Impact Angle (°)	Support Method	Projectile Type	Projectile Size (mm)	Velocity (m/s)	Remarks	Tear Length (mm)	Single Impact Nicks Width (mm)	Single Impact Nicks Depth (mm)	Edge On
3-0364	8-1-1 Ti	15.24x2.54x0.16	Edge On	1.01	30	Simple	Chrome Steel	6.35	180	Roll back with tear also mass loss	5.08			
3-0365	8-1-1 Ti	15.24x2.54x0.16	Edge On	1.01	30	Simple	Chrome Steel	6.35	155	Bulge multiple impact				
3-0366	8-1-1 Ti	15.24x2.54x0.16	Edge On	1.01	30	Simple	Chrome Steel	6.35	164	Bulge multiple impact				
3-0367	8-1-1 Ti	15.24x2.54x0.16	Edge On	1.01	30	Simple	Chrome Steel	6.35	177	Bulge multiple impact				
3-0368	8-1-1 Ti	15.24x2.54x0.16	Edge On	1.01	30	Simple	Chrome Steel	6.35	191	Bulge multiple impact				
3-0369	8-1-1 Ti	15.24x2.54x0.16	Edge On	1.01	30	Simple	Chrome Steel	6.35	203	Roll back and bulge multiple impact				
3-0370	8-1-1 Ti	15.24x2.54x0.16	Edge On	1.01	30	Simple	Chrome Steel	6.35	208	Roll back and bulge multiple impact				
3-0371	8-1-1 Ti	15.24x2.54x0.16	Edge On	1.01	30	Simple	Chrome Steel	6.35	223	Roll back and bulge multiple impact				
3-0372	8-1-1 Ti	15.24x2.54x0.16	Edge On	1.01	30	Simple	Chrome Steel	6.35	237	Roll back with tear	8.99			
3-0373	8-1-1 Ti	15.24x2.54x0.16	Edge On	1.01	30	Simple	Chrome Steel	6.35	240	Roll back with bulge				
3-0374	8-1-1 Ti	15.24x2.54x0.16	Edge On	1.01	30	Simple	Chrome Steel	6.35	263	Roll back and bulge				
3-0375	8-1-1 Ti	15.24x2.54x0.16	Edge On	1.01	30	Simple	Chrome Steel	6.35	258	Roll back with tear	9.34			
3-0376	8-1-1 Ti	15.24x2.54x0.16	Edge On	1.01	30	Simple	Chrome Steel	6.35	265	Roll back with tear	13.20			
3-0377	8-1-1 Ti	15.24x2.54x0.16	Edge On	1.01	30	Simple	Chrome Steel	6.35	293	Roll back with tear also started to plug	11.32			

TABLE 12. IMPACT RESULTS FOR CHROME STEEL (6.35 mm) SPHERE IMPACTS ON 0.254 mm THICK TITANIUM (30°) (Continued)

Shot No.	Material	Size (cm)	Type of Impact	Thickness at Impact (mm)	Impact Angle (°)	Support Method	Projectile Type	Projectile Size (mm)	Velocity (m/s)	Remarks	Tear Length (mm)	Single Impact Nicks Width (mm)	Single Impact Nicks Depth (mm)	Edge On
3-0378	8-1-1 Ti	15.24x2.54x0.16	Edge On	1.01	30	Simple	Chrome Steel	6.35	253	Roll back with tear also mass loss	10.36			
3-0379	8-1-1 Ti	15.24x2.54x0.16	Edge On	1.01	30	Simple	Chrome Steel	6.35	252	Roll back and bulge				
3-0380	8-1-1 Ti	15.24x2.54x0.16	Edge On	1.01	30	Simple	Chrome Steel	6.35	261	Roll back and bulge				
3-0381	8-1-1 Ti	15.24x2.54x0.16	Edge On	1.01	30	Simple	Chrome Steel	6.35	308	Roll back with tear	12.39			
3-0382	8-1-1 Ti	15.24x2.54x0.16	Edge On	1.01	30	Simple	Chrome Steel	6.35	337	Roll back and bulge				
3-0383	8-1-1 Ti	15.24x2.54x0.16	Edge On	1.01	30	Simple	Chrome Steel	6.35	263	Roll back and bulge				
3-0384	8-1-1 Ti	15.24x2.54x0.16	Edge On	1.01	30	Simple	Chrome Steel	6.35	316	Roll back with tear also started to plug	14.45			
3-0385	8-1-1 Ti	15.24x2.54x0.16	Edge On	1.01	30	Simple	Chrome Steel	6.35	263	Roll back with tear also plugged	11.25			
3-0386	8-1-1 Ti	15.24x2.54x0.16	Edge On	1.01	30	Simple	Chrome Steel	6.35	263	Roll back with tear also plugged	14.35			
3-0387	8-1-1 Ti	15.24x2.54x0.16	Edge On	1.01	30	Simple	Chrome Steel	6.35	303	Roll back with tear	13.76			
3-0388	8-1-1 Ti	15.24x2.54x0.16	Edge On	1.01	30	Simple	Chrome Steel	6.35	321	Roll back with tear also plugged	12.14			
3-0389	8-1-1 Ti	15.24x2.54x0.16	Edge On	1.01	30	Simple	Chrome Steel	6.35	319	Roll back with tear also plugged	12.27			
3-0390	8-1-1 Ti	15.24x2.54x0.16	Edge On	1.01	30	Simple	Chrome Steel	6.35	248	Roll back with tear	12.03			

TABLE 13. IMPACT RESULTS FOR CHROME STEEL (3.18 mm) SPHERE IMPACTS ON 0.508 mm THICK TITANIUM (5-8N SHOT PEENED) 30°

Shot No.	Material	Size (cm)	Type of Impact	Thickness at Impact (mm)	Impact Angle (°)	Support Method	Projectile Type	Projectile Size (mm)	Velocity (m/s)	Remarks	Tear Length (mm)	Single Impact Nicks Width (mm)	Single Impact Nicks Depth (mm)	Edge On
3-0515	Glass Bead Peened 8-1-1 Ti (5-8N)	15.24x2.54x0.16	Edge On	0.50	30	Simple	Chrome	3.18	255	Nick multiple impact				
3-0516	Glass Bead Peened 8-1-1 Ti (5-8N)	15.24x2.54x0.16	Edge On	0.50	30	Simple	Chrome Steel	3.18	224	Roll back with tear multiple impact				
3-0517	Glass Bead Peened 8-1-1 Ti (5-8N)	15.24x2.54x0.16	Edge On	0.50	30	Simple	Chrome Steel	3.18	226	Roll back with crease multiple impact				
3-0518	Glass Bead Peened 8-1-1 Ti (5-8N)	15.24x2.54x0.16	Edge On	0.50	30	Simple	Chrome Steel	3.18	233	Roll back with crease multiple impact				
3-0519	Glass Bead Peened 8-1-1 Ti (5-8N)	15.24x2.54x0.16	Edge On	0.50	30	Simple	Chrome Steel	3.18	250	Roll back with tear also mass loss (multiple impact)				
3-0520	Glass Bead Peened 8-1-1 Ti (5-8N)	15.24x2.54x0.16	Edge On	0.50	30	Simple	Chrome Steel	3.18	247	Roll back with tear	8.07			
3-0521	Glass Bead Peened 8-1-1 Ti (5-8N)	15.24x2.54x0.16	Edge On	0.50	30	Simple	Chrome Steel	3.18	244	Roll back with tear	5.71			
3-0522	Glass Bead Peened 8-1-1 Ti (5-8N)	15.24x2.54x0.16	Edge On	0.50	30	Simple	Chrome Steel	3.18	241	Roll back with tear also slight mass loss	3.91			
3-0523	Glass Bead Peened 8-1-1 Ti (5-8N)	15.24x2.54x0.16	Edge On	0.50	30	Simple	Chrome Steel	3.18	248	Roll back with tear also mass loss	5.81			

TABLE 13. IMPACT RESULTS FOR CHROME STEEL (3.18 mm) SPHERE IMPACTS ON 0.508 mm THICK TITANIUM (5-8N SHOT PEENED) 30° (Continued)

Shot No.	Material	Size (cm)	Type of Impact	Thickness at Impact (mm)	Impact Angle (°)	Support Method	Projectile Type	Projectile Size (mm)	Velocity (m/s)	Remarks	Tear Length (mm)	Single Impact Nicks Width (mm)	Single Impact Nicks Depth (mm)	Edge On
3-0524	Glass Bead Peened 8-1-1 Ti (5-8N)	15.24x2.54x0.16	Edge On	0.50	30	Simple	Chrome Steel	3.18	255	Roll back with tear	4.57			
3-0525	Glass Bead Peened 8-1-1 Ti (5-8N)	15.24x2.54x0.16	Edge On	0.50	30	Simple	Chrome Steel	3.18	257	Roll back with tear	6.40			
3-0526	Glass Bead Peened 8-1-1 Ti (5-8N)	15.24x2.54x0.16	Edge On	0.50	30	Simple	Chrome Steel	3.18	254	Roll back with tear also slight mass loss	6.50			

TABLE 14. IMPACT RESULTS FOR CHROME STEEL (3.18 mm) SPHERE IMPACTS ON 0.508 mm THICK TITANIUM (10-16N SHOT PEENED) (30°)

Shot No.	Material	Size (cm)	Type of Impact	Thickness at Impact (mm)	Impact Angle (°)	Support Method	Projectile Type	Projectile Size (mm)	Velocity (m/s)	Remarks	Tear Length (mm)	Single Impact Nicks Width (mm)	Single Impact Nicks Depth (mm)	Edge On
3-0527	Glass Bead Peened 8-1-1 Ti (10-16N)	15.24x2.54x0.16	Edge On	0.50	30	Simple	Chrome Steel	3.18	2[illegible]	Roll back with crease multiple impact				
3-0528	Glass Bead Peened 8-1-1 Ti (10-16N)	15.24x2.54x0.16	Edge On	0.50	30	Simple	Chrome Steel	3.18	259	Roll back with tear multiple impact				
3-0529	Glass Bead Peened 8-1-1 Ti (10-16N)	15.24x2.54x0.16	Edge On	0.50	30	Simple	Chrome Steel	3.18	292	Roll back with tear also mass loss	5.35			
3-0530	Glass Bead Peened 8-1-1 Ti (10-16N)	15.24x2.54x0.16	Edge On	0.50	30	Simple	Chrome Steel	3.18	249	Roll back with tear	7.72			
3-0531	Glass Bead Peened 8-1-1 Ti (10-16N)	15.24x2.54x0.16	Edge On	0.50	30	Simple	Chrome Steel	3.18	260	Roll back with crease multiple impact				
3-0532	Glass Bead Peened 8-1-1 Ti (10-16N)	15.24x2.54x0.16	Edge On	0.50	30	Simple	Chrome Steel	3.18	258	Roll back with tear multiple impact				
3-0533	Glass Bead Peened 8-1-1 Ti (10-16N)	15.24x2.54x0.16	Edge On	0.50	30	Simple	Chrome Steel	3.18	255	Roll back with crease multiple impact				
3-0534	Glass Bead Peened 8-1-1 Ti (10-16N)	15.24x2.54x0.16	Edge On	0.50	30	Simple	Chrome Steel	3.18	261	Roll back with tear multiple impact				
3-0535	Glass Bead Peened 8-1-1 Ti (10-16N)	15.24x2.54x0.16	Edge On	0.50	30	Simple	Chrome Steel	3.18	259	Roll back with tear also mass loss	5.63			

TABLE 14. IMPACT RESULTS FOR CHROME STEEL (3.18 mm) SPHERE IMPACTS ON 0.508 mm THICK TITANIUM (10-16N SHOT PEENED) (30°) (Continued)

Shot No.	Material	Size (cm)	Type of Impact	Thickness at Impact (mm)	Impact Angle (°)	Support Method	Projectile Type	Projectile Size (mm)	Velocity (m/s)	Remarks	Tear Length (mm)	Single Impact Nicks Width (mm)	Single Impact Nicks Depth (mm)	Edge On
3-0536	Glass Bead Peened 8-1-1 Ti (10-16N)	15.24x2.54x0.16	Edge On	0.50	30	Simple	Chrome Steel	3.18	263	Roll back with tear	7.36			
3-0537	Glass Bead Peened 8-1-1 Ti (10-16N)	15.24x2.54x0.16	Edge On	0.50	30	Simple	Chrome Steel	3.18	269	Roll back with tear also mass loss	7.95			
3-0538	Glass Bead Peened 8-1-1 Ti (10-16N)	15.24x2.54x0.16	Edge On	0.50	30	Simple	Chrome Steel	3.18	263	Roll back with tear also mass loss	6.04			
3-0539	Glass Bead Peened 8-1-1 Ti (10-16N)	15.24x2.54x0.16	Edge On	0.50	30	Simple	Chrome Steel	3.18	289	Roll back with tear also mass loss	6.83			

TABLE 15. IMPACT RESULTS FOR CHROME STEEL (3.18 mm) SPHERE IMPACTS ON 0.508 mm THICK STEEL (ANNEALED CONDITION) (30°)

Shot No.	Material	Size (cm)	Type of Impact	Thickness at Impact (mm)	Impact Angle (°)	Support Method	Projectile Type	Projectile Size (mm)	Velocity (m/s)	Remarks	Tear Length (mm)	Single Impact Nicks Width (mm)	Single Impact Nicks Depth (mm)	Edge On
3-0483	4130 Annealed	15.24x2.54x0.16	Edge On	0.50	30	Simple	Chrome Steel	3.18	250	Roll back and crease multiple impact				
3-0484	4130 Annealed	15.24x2.54x0.16	Edge On	0.50	30	Simple	Chrome Steel	3.18	269	Roll back and crease multiple impact				
3-0485	4130 Annealed	15.24x2.54x0.16	Edge On	0.50	30	Simple	Chrome Steel	3.18	302	Roll back and started to plug (multiple impact)				
3-0486	4130 Annealed	15.24x2.54x0.16	Edge On	0.50	30	Simple	Chrome Steel	3.18	274	Roll back and started to plug (multiple impact)				
3-0487	4130 Annealed	15.24x2.54x0.16	Edge On	0.50	30	Simple	Chrome Steel	3.18	281	Roll back and started to plug	2.74			
3-0488	4130 Annealed	15.24x2.54x0.16	Edge On	0.50	30	Simple	Chrome Steel	3.18	277	Roll back and started to plug	1.85			
3-0489	4130 Annealed	15.24x2.54x0.16	Edge On	0.50	30	Simple	Chrome Steel	3.18	281	Roll back and started to plug	2.33			
3-0490	4130 Annealed	15.24x2.54x0.16	Edge On	0.50	30	Simple	Chrome Steel	3.18	291	Roll back and started to plug	1.82			
3-0491	4130 Annealed	15.24x2.54x0.16	Edge On	0.50	30	Simple	Chrome Steel	3.18	317	Roll back and started to plug	2.43			
3-0492	4130 Annealed	15.24x2.54x0.16	Edge On	0.50	30	Simple	Chrome Steel	3.18	346	Roll back and started to plug	2.15			
3-0493	4130 Annealed	15.24x2.54x0.16	Edge On	0.50	30	Simple	Chrome Steel	3.18	317	Roll back and started to plug	1.75			
3-0494	4130 Annealed	15.24x2.54x0.16	Edge On	0.50	30	Simple	Chrome Steel	3.18	273	Roll back and started to plug	2.31			
3-0495	4130 Annealed	15.24x2.54x0.16	Edge On	0.50	30	Simple	Chrome Steel	3.18	281	Roll back and started to plug				
3-0496	4130 Annealed	15.24x2.54x0.16	Edge On	0.50	30	Simple	Chrome Steel	3.18	283	Roll back and started to plug	2.92			

TABLE 16. IMPACT RESULTS FOR CHROME STEEL (3.18 mm) SPHERE IMPACTS ON 0.508 mm THICK STEEL (HEAT-TREATED CONDITION) (30°)

Shot No.	Material	Size (cm)	Type of Impact	Thickness at Impact (mm)	Impact Angle (°)	Support Method	Projectile Type	Projectile Size (mm)	Velocity (m/s)	Remarks	Tear Length (mm)	Single Impact Nicks Width (mm)	Single Impact Nicks Depth (mm)	Edge On
3-0502	4130 Heat Treated	15.24x2.54x0.16	Edge On	0.50	30	Simple	Chrome Steel	3.18	252	Roll back and started to plug (multiple impact)				
3-0503	4130 Heat Treated	15.24x2.54x0.16	Edge On	0.50	30	Simple	Chrome Steel	3.18	217	Roll back and bulge multiple impact				
3-0504	4130 Heat Treated	15.24x2.54x0.16	Edge On	0.50	30	Simple	Chrome Steel	3.18	227	Roll back with tear	4.11			
3-0505	4130 Heat Treated	15.24x2.54x0.16	Edge On	0.50	30	Simple	Chrome Steel	3.18	229	Roll back and started to plug (multiple impact)				
3-0506	4130 Heat Treated	15.24x2.54x0.16	Edge On	0.50	30	Simple	Chrome Steel	3.18	236	Roll back and started to plug (multiple impact)				
3-0507	4130 Heat Treated	15.24x2.54x0.16	Edge On	0.50	30	Simple	Chrome Steel	3.18	252	Roll back with tear	2.31			
3-0508	4130 Heat Treated	15.24x2.54x0.16	Edge On	0.50	30	Simple	Chrome Steel	3.18	252	Roll back with tear	2.79			
3-0509	4130 Heat Treated	15.24x2.54x0.16	Edge On	0.50	30	Simple	Chrome Steel	3.18	241	Roll back and started to plug	0.81			
3-0510	4130 Heat Treated	15.24x2.54x0.16	Edge On	0.50	30	Simple	Chrome Steel	3.18	249	Roll back with tear	2.15			
3-0511	4130 Heat Treated	15.24x2.54x0.16	Edge On	0.50	30	Simple	Chrome Steel	3.18	262	Roll back with tear	2.94			
3-0512	4130 Heat Treated	15.24x2.54x0.16	Edge On	0.50	30	Simple	Chrome Steel	3.18	252	Roll back with tear	2.43			
3-0513	4130 Heat Treated	15.24x2.54x0.16	Edge On	0.50	30	Simple	Chrome Steel	3.18	254	Roll back with tear	2.61			

TABLE 17. IMPACT RESULTS FOR CHROME STEEL (1.60 mm) SPHERE IMPACTS ON 0.508 mm THICK ALUMINUM (30°)

Shot No.	Material	Size (cm)	Type of Impact	Thickness at Impact (mm)	Impact Angle (°)	Support Method	Projectile Type	Projectile Size (mm)	Velocity (m/s)	Remarks	Tear Length (mm)	Single Impact Nicks Width (mm)	Single Impact Nicks Depth (mm)	Edge On
3-0468	Aluminum 7075-T651	15.24x2.54x0.16	Edge On	0.50	30	Simple	Chrome Steel	1.58	326	Nick multiple impact				
3-0469	Aluminum 7075-T651	15.24x2.54x0.16	Edge On	0.50	30	Simple	Chrome Steel	1.58	305	Nick also mass loss multiple impact				
3-0470	Aluminum 7075-T651	15.24x2.54x0.16	Edge On	0.50	30	Simple	Chrome Steel	1.58	285	Nick also mass loss multiple impact				
3-0471	Aluminum 7075-T651	15.24x2.54x0.16	Edge On	0.50	30	Simple	Chrome Steel	1.58	267	Nick multiple impact				
3-0472	Aluminum 7075-T651	15.24x2.54x0.16	Edge On	0.50	30	Simple	Chrome Steel	1.58	267	Bulge multiple impact				
3-0473	Aluminum 7075-T651	15.24x2.54x0.16	Edge On	0.50	30	Simple	Chrome Steel	1.58	291	Bulge multiple impact				
3-0474	Aluminum 7075-T651	15.24x2.54x0.16	Edge On	0.50	30	Simple	Chrome Steel	1.58	310	Bulge and started to plug (multiple impact)				
3-0475	Aluminum 7075-T651	15.24x2.54x0.16	Edge On	0.50	30	Simple	Chrome Steel	1.58	328	Nick also mass loss multiple impact				
3-0476	Aluminum 7075-T651	15.24x2.54x0.16	Edge On	0.50	30	Simple	Chrome Steel	1.58	312	Nick also mass loss		2.17	0.89	
3-0477	Aluminum 7075-T651	15.24x2.54x0.16	Edge On	0.50	30	Simple	Chrome Steel	1.58	309	Nick also mass loss		1.50	1.01	
3-0478	Aluminum 7075-T651	15.24x2.54x0.16	Edge On	0.50	30	Simple	Chrome Steel	1.58	309	Nick also mass loss		1.54	0.60	
3-0479	Aluminum 7075-T651	15.24x2.54x0.16	Edge On	0.50	30	Simple	Chrome Steel	1.58	304	Nick also mass loss		1.55	0.66	

TABLE 17. IMPACT RESULTS FOR CHROME STEEL (1.60 mm) SPHERE IMPACTS ON 0.508 mm THICK ALUMINUM (30°) (Continued)

Shot No.	Material	Size (cm)	Type of Impact	Thickness at Impact (mm)	Impact Angle (°)	Support Method	Projectile Type	Projectile Size (mm)	Velocity (m/s)	Remarks	Tear Length (mm)	Single Impact Nicks Width (mm)	Single Impact Nicks Depth (mm)	Edge On
3-0480	Aluminum 7075-T651	15.24x2.54x0.16	Edge On	0.50	30	Simple	Chrome Steel	1.58	306	Nick also mass loss		1.58	0.83	
3-0481	Aluminum 7075-T651	15.24x2.54x0.16	Edge On	0.50	30	Simple	Chrome Steel	1.58	306	Nick also mass loss		1.52	0.73	
3-0482	Aluminum 7075-T651	15.24x2.54x0.16	Edge On	0.50	30	Simple	Chrome Steel	1.58	296	Nick also mass loss		1.53	0.94	

TABLE 18. IMPACT RESULTS FOR CHROME STEEL (3.18 mm) SPHERE IMPACTS ON 0.508 mm THICK ALUMINUM (30°)

Shot No.	Material	Size (cm)	Type of Impact	Thickness at Impact (mm)	Impact Angle (°)	Support Method	Projectile Type	Projectile Size (mm)	Velocity (m/s)	Remarks	Tear Length (mm)	Single Impact Nicks Width (mm)	Single Impact Nicks Depth (mm)	Edge On
3-0454	Aluminum 7075-T651	15.24x2.54x0.16	Edge On	0.50	30	Simple	Chrome Steel	3.18	146	Roll back with crease multiple impact				
3-0455	Aluminum 7075-T651	15.24x2.54x0.16	Edge On	0.50	30	Simple	Chrome Steel	3.18	185	Roll back with tear multiple impact				
3-0456	Aluminum 7075-T651	15.24x2.54x0.16	Edge On	0.50	30	Simple	Chrome Steel	3.18	185	Roll back with tear multiple impact				
3-0457	Aluminum 7075-T651	15.24x2.54x0.16	Edge On	0.50	30	Simple	Chrome Steel	3.18	188	Roll back with slight tear (multiple impact)				
3-0458	Aluminum 7075-T651	15.24x2.54x0.16	Edge On	0.50	30	Simple	Chrome Steel	3.18	208	Roll back and tear down the side of test area				
3-0459	Aluminum 7075-T651	15.24x2.54x0.16	Edge On	0.50	30	Simple	Chrome Steel	3.18	205	Roll back with tear	6.70			
3-0460	Aluminum 7075-T651	15.24x2.54x0.16	Edge On	0.50	30	Simple	Chrome Steel	3.18	201	Roll back with tear	5.61			
3-0461	Aluminum 7075-T651	15.24x2.54x0.16	Edge On	0.50	30	Simple	Chrome Steel	3.18	206	Roll back with tear	8.86			
3-0462	Aluminum 7075-T651	15.24x2.54x0.16	Edge On	0.50	30	Simple	Chrome Steel	3.18	206	Roll back with tear	4.97			
3-0463	Aluminum 7075-T651	15.24x2.54x0.16	Edge On	0.50	30	Simple	Chrome Steel	3.18	210	Roll back with tear	7.62			
3-0464	Aluminum 7075-T651	15.24x2.54x0.16	Edge On	0.50	30	Simple	Chrome Steel	3.18	207	Roll back with tear	4.67			
3-0465	Aluminum 7075-T651	15.24x2.54x0.16	Edge On	0.50	30	Simple	Chrome Steel	3.18	204	Roll back with tear	7.74			
3-0466	Aluminum 7075-T651	15.24x2.54x0.16	Edge On	0.50	30	Simple	Chrome Steel	3.18	207	Roll back with slight tear				

*U.S.Government Printing Office: 1981 — 559-006/5034

DATE

FILMED